Report No. K-TRAN: KSU-08-7 ▪ FINAL REPORT▪ July 2012

Alleviating Concrete Placement Issues Due to Congestion of Reinforcement in Post-Tensioned Haunch-Slab Bridges

Patrick Sheedy
Robert J. Peterman, Ph.D., P.E.

Kansas State University Transportation Center

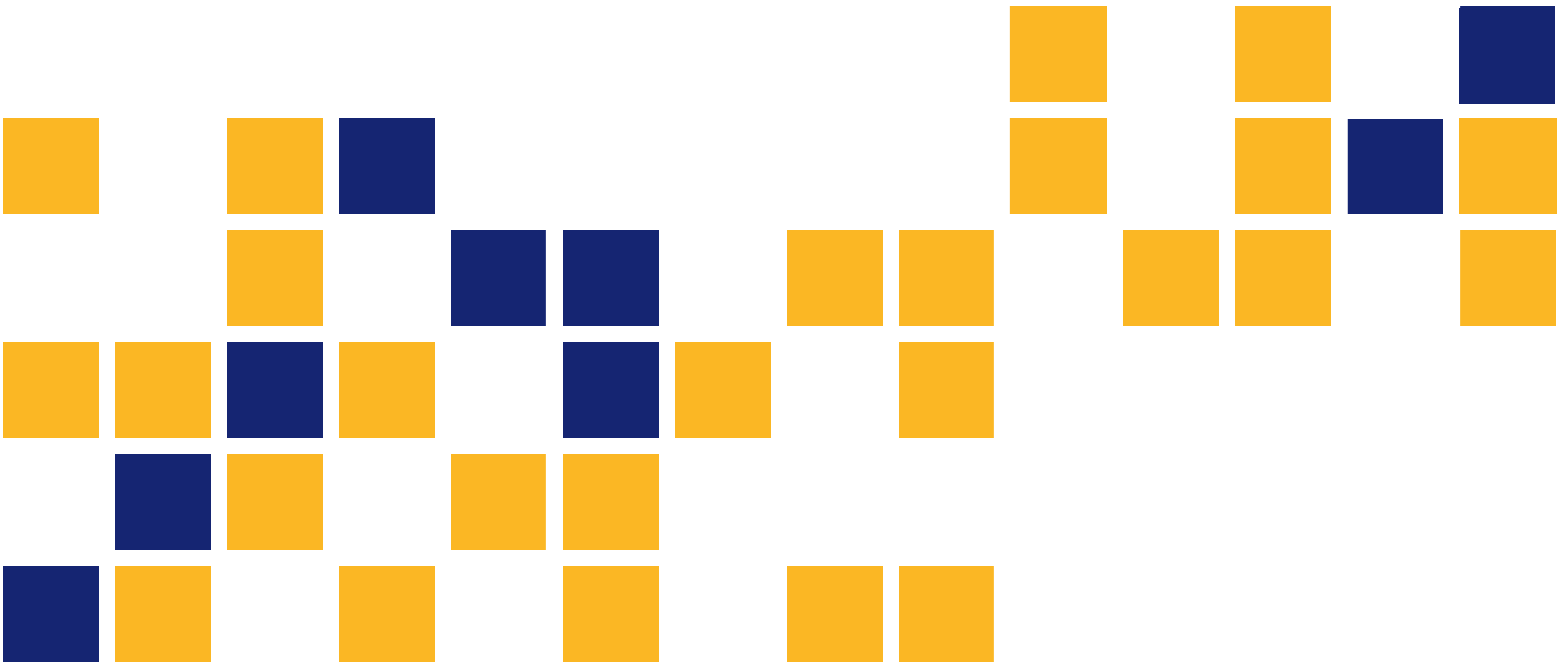

A cooperative transportation research program between
Kansas Department of Transportation,
Kansas State University Transportation Center, and
The University of Kansas

Kansas Department of Transportation

This page intentionally left blank.

1 Report No. K-TRAN: KSU-08-7	**2 Government Accession No.**	**3 Recipient Catalog No.**
4 Title and Subtitle Alleviating Concrete Placement Issues Due to Congestion of Reinforcement in Post-Tensioned Haunch-Slab Bridges		**5 Report Date** July 2012 **6 Performing Organization Code**
7 Author(s) Patrick Sheedy; Robert J. Peterman, Ph.D., P.E.		**8 Performing Organization Report No.**
9 Performing Organization Name and Address Department of Civil Engineering Kansas State University Transportation Center 2118 Fiedler Hall Manhattan, Kansas 66506		**10 Work Unit No. (TRAIS)** **11 Contract or Grant No.** C1687
12 Sponsoring Agency Name and Address Kansas Department of Transportation Bureau of Materials and Research 700 SW Harrison Street Topeka, Kansas 66603-3745		**13 Type of Report and Period Covered** Final Report May 2007–May 2012 **14 Sponsoring Agency Code** RE-0466-01
15 Supplementary Notes For more information write to address in block 9.		

16 Abstract

A flowable hybrid concrete mix with a spread of 17 to 20 inches was created with a superplasticizer to be used in post-tension haunch-slab (PTHS) bridges where rebar congestion is heaviest. The mix would allow for proper concrete consolidation. A conventional concrete mix with a slump of three to four inches was also created to be placed on top of the hybrid mix. The conventional mix would be used to create a sloping surface on the top of the concrete. The two mixes could be combined in the PTHS bridge deck and act as one monolithic specimen. Standard concrete tests such as compressive strength, tensile strength, modulus of elasticity, permeability, freeze/thaw resistance, and coefficient of thermal expansion were determined for the mixes and compared. Core blocks were cast using both mixes and composite cores were drilled. The cores were tested and their composite split-tensile strengths were compared to the split-tensile strengths of cylinders made from the respective mixes.

A third concrete mix was made by increasing the superplasticizer dosage in the hybrid concrete mix to create a self-consolidating concrete (SCC) mix with a 24-inch spread. The SCC mix was created as a worst-case scenario and used in the determination of shear friction. Eighty-four push-off shear friction specimens were cast using the SCC mix. Joint conditions for the specimens included uncracked, pre-cracked, and cold-joints. Uncracked and pre-cracked specimens used both epoxy- and non-epoxy-coated shear stirrups. Cold-joint specimens used both the SCC mix and the conventional concrete mix. Joint-conditions of the cold-joint specimens included a one-hour cast time, a seven-day joint with a clean shear interface, and a seven-day joint with an oiled shear interface. The shear friction specimens were tested using a pure shear method and their results were compared to the current American Concrete Institute code equation.

17 Key Words Bridges, SCC, Post-Tension Hardened Slab, Rebar, Flowable Concrete Mix, Self-Consolidating Concrete, Self-Compacting Concrete		**18 Distribution Statement** No restrictions. This document is available to the public through the National Technical Information Service www.ntis.gov.	
19 Security Classification (of this report) Unclassified	**20 Security Classification (of this page)** Unclassified	**21 No. of pages** 148	**22 Price**

Form DOT F 1700.7 (8-72)

Alleviating Concrete Placement Issues Due to Congestion of Reinforcement in Post-Tensioned Haunch-Slab Bridges

Final Report

Prepared by

Patrick Sheedy

Robert J. Peterman, Ph.D., P.E.

Kansas State University Transportation Center

A Report on Research Sponsored by

THE KANSAS DEPARTMENT OF TRANSPORTATION
TOPEKA, KANSAS

and

KANSAS STATE UNIVERSITY TRANSPORTATION CENTER
MANHATTAN, KANSAS

July 2012

PREFACE

The Kansas Department of Transportation's (KDOT) Kansas Transportation Research and New-Developments (K-TRAN) Research Program funded this research project. It is an ongoing, cooperative and comprehensive research program addressing transportation needs of the state of Kansas utilizing academic and research resources from KDOT, Kansas State University and the University of Kansas. Transportation professionals in KDOT and the universities jointly develop the projects included in the research program.

NOTICE

The authors and the state of Kansas do not endorse products or manufacturers. Trade and manufacturers names appear herein solely because they are considered essential to the object of this report.

This information is available in alternative accessible formats. To obtain an alternative format, contact the Office of Transportation Information, Kansas Department of Transportation, 700 SW Harrison, Topeka, Kansas 66603-3754 or phone (785) 296-3585 (Voice) (TDD).

DISCLAIMER

The contents of this report reflect the views of the authors who are responsible for the facts and accuracy of the data presented herein. The contents do not necessarily reflect the views or the policies of the state of Kansas. This report does not constitute a standard, specification or regulation.

ABSTRACT

A flowable hybrid concrete mix with a spread of 17 to 20 inches was created with a superplasticizer to be used in post-tension haunch-slab (PTHS) bridges where rebar congestion is heaviest. The mix would allow for proper concrete consolidation. A conventional concrete mix with a slump of three to four inches was also created to be placed on top of the hybrid mix. The conventional mix would be used to create a sloping surface on the top of the concrete. The two mixes could be combined in the PTHS bridge deck and act as one monolithic specimen. Standard concrete tests such as compressive strength, tensile strength, modulus of elasticity, permeability, freeze/thaw resistance, and coefficient of thermal expansion were determined for the mixes and compared. Core blocks were cast using both mixes and composite cores were drilled. The cores were tested and their composite split-tensile strengths were compared to the split-tensile strengths of cylinders made from the respective mixes.

A third concrete mix was made by increasing the superplasticizer dosage in the hybrid concrete mix to create a self-consolidating concrete (SCC) mix with a 24-inch spread. The SCC mix was created as a worst-case scenario and used in the determination of shear friction. Eighty-four push-off shear friction specimens were cast using the SCC mix. Joint conditions for the specimens included uncracked, pre-cracked, and cold-joints. Uncracked and pre-cracked specimens used both epoxy- and non-epoxy-coated shear stirrups. Cold-joint specimens used both the SCC mix and the conventional concrete mix. Joint-conditions of the cold-joint specimens included a one-hour cast time, a seven-day joint with a clean shear interface, and a seven-day joint with an oiled shear interface. The shear friction specimens were tested using a pure shear method and their results were compared to the current American Concrete Institute code equation.

TABLE OF CONTENTS

LIST OF FIGURES

LIST OF TABLES

ACKNOWLEDGMENTS

The authors would like to thank the Kansas Department of Transportation (KDOT) for funding this project. The assistance of KDOT personnel David Meggers and Jim Bernica is especially appreciated. Additionally, the authors would like to thank Dr. Brian Coon for his support and input on this project.

CHAPTER 1. INTRODUCTION

1.1 OVERVIEW

The Kansas Department of Transportation (KDOT) implements post-tension haunch-slab (PTHS) bridges for some of its state highway bridges. A PTHS bridge is a haunch-slab bridge deck cast monolithically with transverse and longitudinal ductwork. Cables are run through the ducts, and the bridge is post-tensioned in transverse and longitudinal directions.

A large amount of reinforcement is needed around the tensioning anchorage points at the abutments in order for the bridge to be post-tensioned. This requirement results in rebar congestion at those points. Figure 1 shows longitudinal and transverse anchorage points and rebar congestion at the bridge abutment. Figure 2 shows a close-up view of rebar congestion around the longitudinal anchorage point.

Figure 1. Longitudinal and transverse anchorage points and rebar congestion at bridge abutment (KDOT).

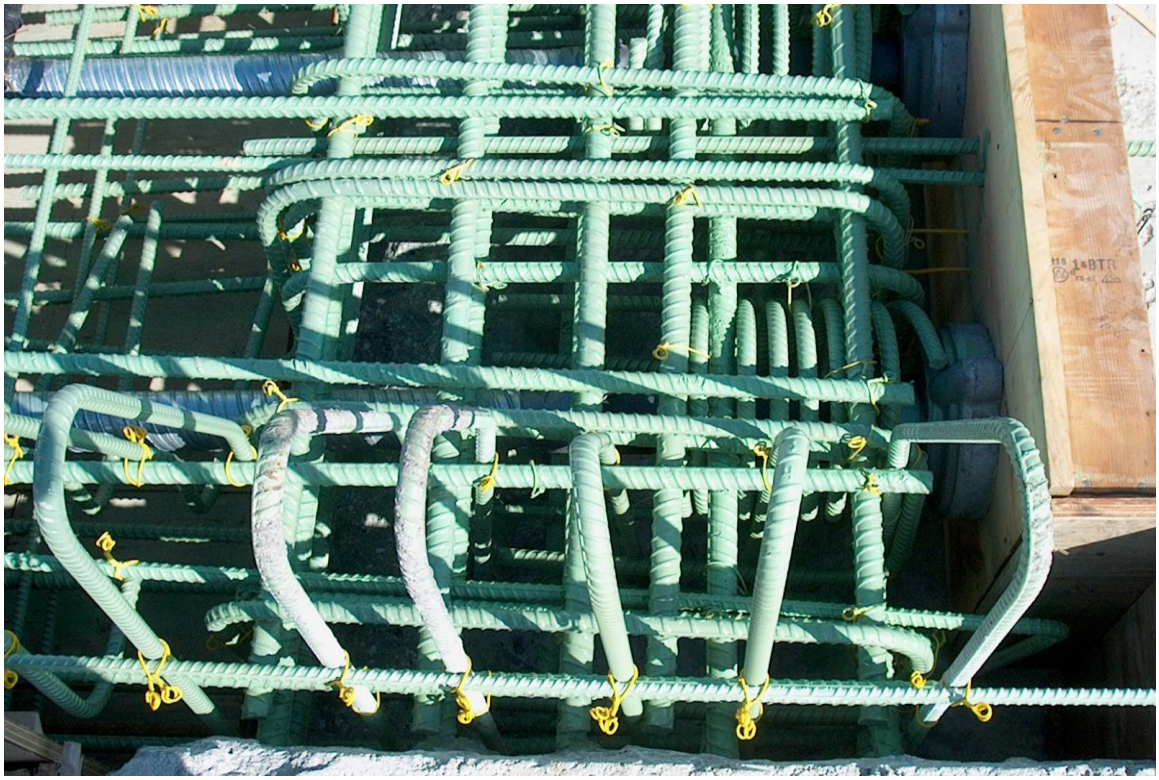

Figure 2. Close-up view of rebar congestion around longitudinal anchorage points (KDOT).

Anchorage points need to be thoroughly vibrated to ensure the concrete is properly consolidated. The rebar congestion, however, makes it difficult to properly consolidate the concrete. When post-tensioning forces are applied to the cables, it results in stresses at the anchorage points. If the anchorage points are not properly consolidated, a failure of the concrete and successive "blow-out" can occur. Figure 3 shows a failure of the longitudinal anchorage points due to poor concrete consolidation. Figure 4 shows a close-up view of the longitudinal anchorage point failure. Figure 4 also illustrates how far the anchorage point was forced into the concrete abutment.

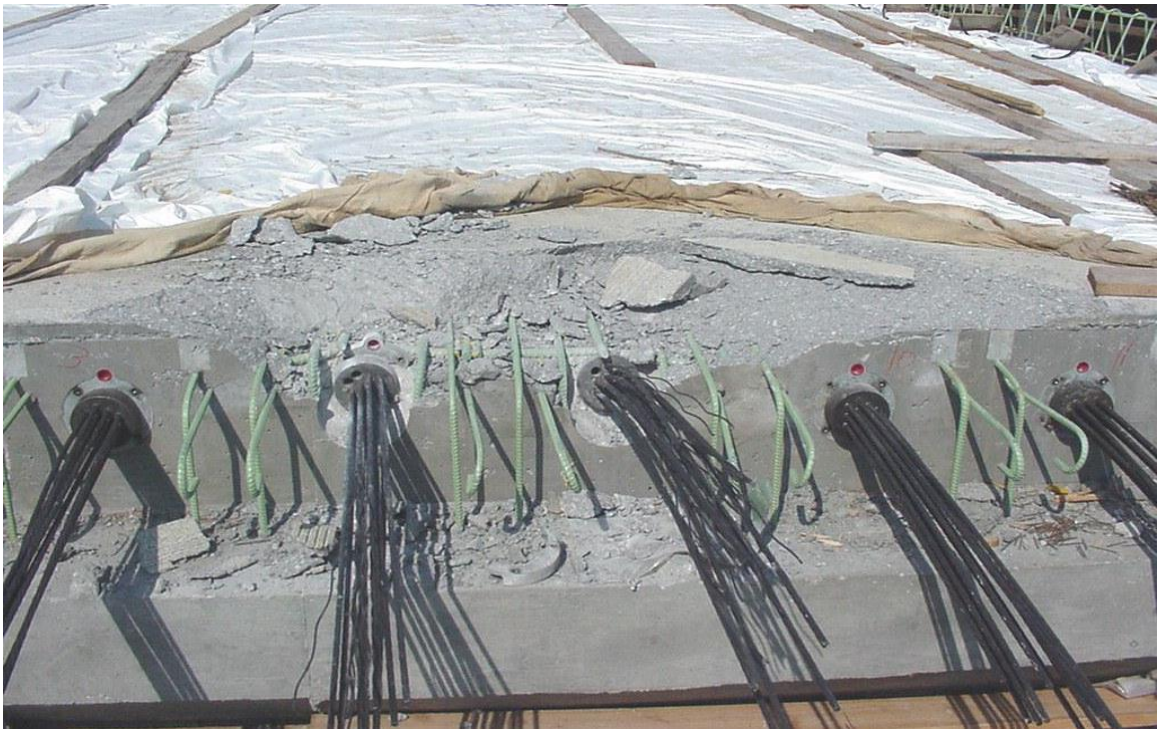

Figure 3. Failure of longitudinal anchorage points due to poor concrete consolidation (KDOT).

Figure 4. Close-up view of longitudinal anchorage point failure (KDOT).

A failure has to be fixed, which adds costs to the project budget. KDOT would like to avoid these additional costs. Development of self-consolidating concrete (SCC) mixes in recent years presents a solution to the problem. SCC is a self-leveling concrete that flows freely and needs little or no vibration. Typical SCC mixes have spreads of 24 to 28 inches. SCC may be an answer, but another problem arises. It cannot be used on a structure such as a bridge deck where a "crown" or other sloping surface is desired.

A hybrid concrete mix with a spread of 17 to 20 inches is proposed instead. The hybrid concrete mix will flow through the heavy rebar congestion and properly consolidate with minimal vibration. It would be placed in the bottom of bridge piers and abutments where reinforcement congestion is highest or other areas where proper consolidation is critical. A conventional concrete mix with a slump of three to four inches is proposed to be placed on top of the hybrid concrete mix. The "crown" or other sloping surface will be constructed using the conventional concrete mix. Both concrete mixes should be vibrated together to ensure proper consolidation and create a monolithically cast bridge deck, but excessive vibration should be avoided to avert segregation.

1.2 OBJECTIVES

There were two main phases of this research project. Phase 1 is development of a compatible hybrid mix (with a 17- to 20-inch spread) for use in KDOT bridge decks and other field-placed structural elements. Phase 2 is instrumentation and monitoring of a PTHS bridge utilizing a hybrid concrete mix; and monitoring placement conditions, hydration temperatures, prestress forces/losses, and deflections. This research paper covers only Phase 1. The following tasks were performed in Phase 1:

1. Perform a literature review to obtain state-of-the-art information about flowable concrete mixes and appropriate tests to evaluate the bond of deformed bars.
2. Develop hybrid concrete mixes using KDOT-approved aggregate and cement sources. Standard KDOT bridge deck mixes will form the basis of the initial trial mixes in terms of water-to-cement and sand-aggregate ratios.

3. Determine the amount of vibration required to properly consolidate these mixes without inducing segregation, and to blend these mixes with the three-inch slump concrete. Specimens with two different layers and various levels of vibration will be saw-cut to determine the condition of the interface between the two layers.
4. Determine potential durability of these mixes in terms of rapid chloride-ion permeability and freeze-thaw resistance. These tests will be conducted by KDOT personnel after development of promising mixes.
5. Determine strength, modulus of elasticity, and coefficient of thermal expansion of these mixes. In order for the proposed method to be successful, the modulus of elasticity and thermal expansion of both top and bottom layers need to be essentially the same.
6. Determine the effect of time vs. slump/spread loss of these mixes at different temperatures.
7. Determine the ability of these mixes to adequately bond with mild reinforcing steel. Because the bond of steel reinforcement typically decreases with increasing concrete fluidity, the ability of these high-fluidity mixes to adequately bond with epoxy-coated reinforcement will be evaluated by performing a series of standard ASTM or AASHTO bond tests. Exact specimen arrangement will be determined after performing the literature review in Task 1.

1.3 SCOPE

Chapter Two reviews previous research on shear friction specimens using conventional concrete. A brief history of use and testing methods for SCC is also discussed.

Chapter Three describes material properties of aggregates, cement, and admixtures used in the concrete mixes.

Chapter Four describes concrete mixture proportioning and design. Test methods performed on fresh and hardened concrete are also described.

Chapter Five discusses experimental concrete results from hardened concrete tests.

Chapter Six describes design and testing of a procedure to determine the bond of two concrete mixes. Results from the testing are discussed.

Chapter Seven discusses design, fabrication, and testing of shear friction specimens.

Chapter Eight reports findings from the shear friction specimen tests. Results are compared to the ACI code equation.

Chapter Nine discusses conclusions and recommendations from this project.

CHAPTER 2. LITERATURE REVIEW

This chapter reviews research done on shear friction specimens using conventional concrete. A brief history of use and testing methods for SCC is also discussed.

2.1 SCC

The Precast/Prestressed Concrete Institute (2003) defines self-consolidating concrete, or self-compacting concrete, as—

> "A highly workable concrete that can flow through densely reinforced or complex structural elements under its own weight, and adequately fill voids without segregation or excessive bleeding without the need for vibration."

Ouchi (2001) investigated use of self-compacting concrete (SCC) in Japan in an attempt to make it a standard concrete. The first prototype of SCC was developed in Japan in 1988. SCC was developed to shorten the construction period of a project, assure adequate compaction in confined zones where vibrating is difficult, and eliminate noise due to vibration. Ouchi used a superplasticizer to lower the water-to-cement ratio yet retain workability. Two testing methods were used to determine if the concrete was self-compacting and to evaluate the deformability of proper mix proportioning. The author used a project in Japan as an example of how use of SCC drastically reduced the number of concrete castings, the number of concrete workers, and overall construction time.

Khayat et al. (2004) examined the test methods used to determine the performance of SCC. These were slump, concrete rheometer, J-ring, L-box, U-box, V-funnel, pressure-bleed tests, and Visual Stability Index (VSI) rating. The authors made 16 SCC mixes with constant aggregate ratios and varying water-to-cement ratios. A high-range water reducer and a set-retarding agent were used in all of the mixes. The authors concluded the VSI rating and slump test, along with either the L-box or J-ring test, were adequate in determining deformability and passing nature of the mixes.

2.2 SHEAR FRICTION

Hanson (1960) studied horizontal shear connections in composite T-beams. His work consisted of 62 push-off tests with varying surface conditions, shear keys, and stirrups. The specimens were constructed with cold-joints. U-shaped stirrups acted as shear connections between the two cold-joint sections. The tests showed the capacity of the connection was not affected by the magnitude of the roughness and the amount of shear reinforcement was proportional to the ultimate shear strength. Shear keys were found to be unnecessary as they did not affect the connection strength.

Anderson (1960) studied effects of high-strength concrete on composite cold-joint connections. Specimens had concrete strengths of 3,000 psi and 7,500 psi, and reinforcing ratios of 0.2% to 2.48%. Specimens were tested under a pure shear load. The author found the cold-joint specimens to behave monolithically up to 75% of the ultimate strength and the ultimate strength to be proportional to the amount of reinforcement. Concrete strength and reinforcement ratio affected the ultimate strength. Shear keys were also found to be unnecessary.

Birkland and Birkland (1966) proposed the shear friction hyporeport on connections in precast construction. The modern shear friction equation is derived from their proposal. Large coefficients of friction were used in their equation. Their hyporeport was determined by graphically comparing their equation to results from Anderson (1960), Hanson (1960), and unpublished data. The authors found the data supported their proposal but further research needed to be conducted.

Basler and Witta (1966) discussed the shear friction hyporeport proposed by Birkland and Birkland (1966). The authors questioned use of large coefficients of friction. They interpreted the data differently and instead proposed use of smaller coefficients of friction.

Mast (1968) introduced a shear friction hyporeport similar to Birkland and Birkland (1966) based on data from tests conducted by Anderson (1960) and Hanson (1960). A coefficient of friction of 1.4 was recommended for cold-joint specimens with a rough shear interface. Shear friction will develop as long as the shear interface reinforcement is fully anchored. It was

discussed how shear friction works in composite beams when designing for horizontal shear. The author applied his hyporeport to corbels, composite beams, and other precast concrete applications, but noted any further research should take into account the possibility of a crack forming prior to loading.

Hofbeck et al. (1969) researched shear friction behavior between a precast concrete beam and a cast-in-place slab. Specimens were cast as monolithic specimens with 4,500 psi concrete and varying shear reinforcements. Some specimens were pre-cracked to determine strength of the connection with a crack present prior to loading as proposed by Mast (1968). A pre-cracking procedure was developed. Results of uncracked and pre-cracked specimens were compared. The monolithic specimens were found to have higher strengths than the pre-cracked specimens. The pre-cracked specimens failed with a sliding behavior as shear friction hypothesized. The data was compared to the shear friction equation proposed by Birkland and Birkland (1966) and Mast (1968). The authors concluded a coefficient of friction of 1.0 be used for pre-cracked specimens.

Mattock et al. (1975) studied the effect of a moment normal to the shear plane in shear friction. Uncracked and pre-cracked push-off specimens were used similar to previous research. The uncracked specimens were discovered to form diagonal cracks as they failed. The pre-cracked specimens showed large amounts of slip and separation along the shear plane with concrete spalling. The data was graphed and compared to previous research. The authors concluded an external normal stress should be combined with the clamping stress when a moment is applied to the shear plane.

Cowan and Cruden (1975) questioned usefulness and versatility of the shear friction hyporeport. A modified shear friction theory was proposed. Clamping stress and shear stress were normalized from previous published data and graphed on a dimensionless plot. Unpublished data from tests conducted by the authors using high-strength steel were compared to the data of Hofbeck et al. (1969). Specimens with the high-strength steel were found to have similar strengths as specimens that used mild steel when the clamping force was the same. The authors concluded their modified shear friction theory accurately predicted the strength of specimens with normal-strength concrete.

Mattock et al. (1975) studied the shear strength of connections using lightweight concrete. The authors used both uncracked and pre-cracked specimens and concretes with four different aggregates. Three of the aggregates were lightweight. Concrete strengths varied from 2,500 psi to 6,000 psi, and the area of reinforcement crossing the shear plane varied from 0.22 in^2 to 1.32 in^2. Shear friction tests were performed similarly to those of Hofbeck et al. (1969). Load-and-slip characteristics were measured up to a slip of 0.05 inches. Uncracked specimens showed diagonal cracking until a final failure crack formed along the shear plane. Pre-cracked specimens failed as the slip and load increased until a maximum load was reached.

Shear values of the uncracked specimens were larger than those of the pre-cracked specimens. Neither uncracked nor pre-cracked specimens reached a yield plateau. The residual load of both types of specimens was found to be the same. The authors concluded that joint strength is less for lightweight concrete than for normal-weight concrete. The coefficient of friction should be reduced for lightweight concrete to 75%-85% of the value used for normal-weight concrete.

Shaikh (1978) proposed revisions to the shear friction code provisions for PCI. An effective coefficient of friction was proposed, as it takes into account the parabolic relationship of shear stress and clamping stress. It also included factors for joint conditions and lightweight concrete reductions proposed by Mattock et al. (1975). The modified shear equation was compared to previous shear friction equations and found to have conservative results.

Walraven et al. (1987) researched how concrete strength affects shear capacity. Eighty-eight pre-cracked push-off specimens were made with concrete strengths ranging from 2,400 psi to 8,550 psi. The specimens were similar to those used by Hofbeck et al. (1969). A pre-cracking procedure was used that left aggregate crossing the shear plane mostly intact. An in-depth statistical analysis was performed on the results to create an equation for shear strength based on concrete strength. The resulting equation was extremely complex, so a design chart with various concrete strengths was created.

Mattock (1988) agreed with Walraven et al. (1987) that concrete strength affected shear capacity and a proper equation was needed. A better equation was proposed based on results of 6,000 psi

concrete tested by the author in previous research. The equation was found to be conservative but was the first to include concrete strength as a variable.

Hoff (1992) researched shear friction with high-strength lightweight concrete. Specimens were made similar to Mattock et al. (1975) with compressive strengths varying from 8,500 psi to 11,000 psi. The specimens were pre-cracked similar to Mattock et al. (1975) as well. The author concluded the current ACI code equation accurately predicted strength but was not conservative.

Walraven and Stroband (1994) studied shear friction with high-strength concrete. Tests were performed on nine push-off specimens consisting of plain concrete with external restraint bars of various stiffness and six push-off specimens with reinforced cracks. Concrete strength of both sets of specimens was 14,500 psi. The authors concluded the shear friction capacity of cracks in high-strength concrete was significantly reduced, often by 25% to 45% due to aggregate fracture.

Kahn and Mitchell (2002) further researched shear friction with high-strength concrete. The purpose of the study was to determine if current ACI code provisions were appropriate for concrete strengths up to 18,000 psi. Fifty push-off specimens were made with concrete strengths varying between 6,800 and 17,900 psi and reinforcement ratios of 0.37% to 1.47%. Uncracked and pre-cracked monolithic specimens and cold-joint specimens were cast. Ultimate shear stresses were determined from the ultimate shear strength of the specimens. Results were graphed and compared to current ACI code limits. Graphs were also made that compared the data from the study to data from Anderson (1960) and Hofbeck et al (1969). The authors determined the code gave conservative estimates of shear strength for high-strength concrete and recommended limiting the yield stress of transverse reinforcement to 60 ksi. They also proposed raising the upper limit of shear stress to 20% of concrete strength instead of limiting it to 800 psi.

CHAPTER 3. MATERIAL PROPERTIES

This chapter discusses materials to be used in the concrete mix design. All material property tests are included as well.

3.1 AGGREGATE GRADATION

Gradations of the fine and coarse aggregate used in this project were tested according to the American Association of State Highway and Transportation Officials (AASHTO) *Standard Specifications* (2004) test AASHTO T 27. Aggregate specifications were followed as outlined in section 1102 of the KDOT *Standard Specifications for State Road and Bridge Construction* (2007).

3.1.1 Fine Aggregate

Fine aggregate used in the study was normal-weight sand obtained from a Midwest Concrete Materials local quarry and designated as FA-A by KDOT. A sieve analysis was performed and compared to the high and low passing values permitted by KDOT under the fine aggregate specification FA-A. The sieve analysis can be seen in Table 1. The entire gradation fell within accepted KDOT ranges. Figure 5 shows the gradation curve for the fine aggregate.

Table 1. Sieve analysis of fine aggregate.

Sieve	Weight Retained (g)	Percent Retained	Percent Passing	Cumulative Percent Retained	KDOT Percent Passing - High	KDOT Percent Passing - Low
1"	0	0.0	100.0	0.0	100.0	100.0
3/4"	0	0.0	100.0	0.0	100.0	100.0
1/2"	0	0.0	100.0	0.0	100.0	100.0
3/8"	0	0.0	100.0	0.0	100.0	100.0
#4	41	2.1	97.9	2.1	100.0	90.0
#8	207	10.4	87.5	12.5	100.0	73.0
#16	417	20.9	66.6	33.4	85.0	45.0
#30	530	26.6	40.0	60.0	60.0	23.0
#50	550	27.6	12.4	87.6	30.0	7.0
#100	213	10.7	1.7	98.3	10.0	0.0
Pan	33	1.7	0.0	100.0	0.0	0.0

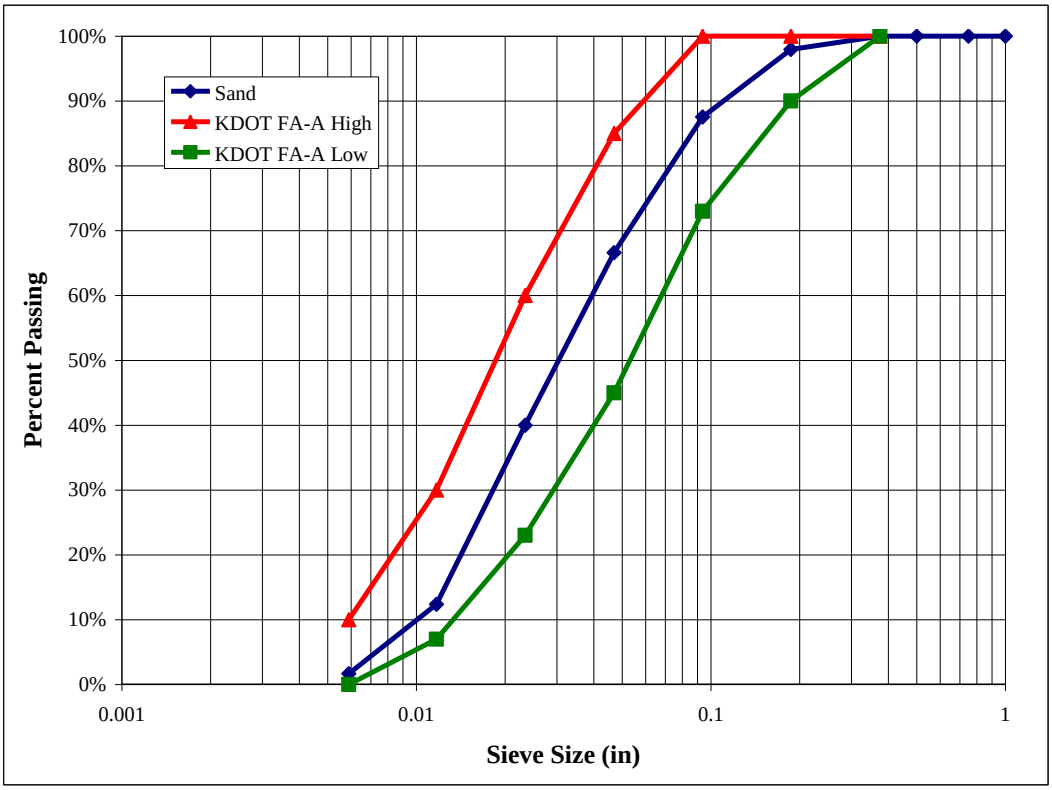

Figure 5. Gradation curve of fine aggregate.

3.1.2 Coarse Aggregate

Coarse aggregate used in this study was normal-weight siliceous gravel with a maximum aggregate size of 3/4-inch by 3/8-inch and obtained from a Midwest Concrete Materials local quarry. A sieve analysis was performed and compared to the high and low passing values permitted by KDOT under the coarse aggregate specification SCA-2. The sieve analysis can be seen in Table 2. The entire gradation fell within accepted KDOT ranges. Figure 6 shows the gradation curve for the coarse aggregate.

Table 2. Sieve analysis of coarse aggregate.

Sieve	Weight Retained (g)	Percent Retained	Percent Passing	Cumulative Percent Retained	KDOT Percent Passing - High	KDOT Percent Passing - Low
1"	0	0.0	100.0	0.0	100.0	100.0
3/4"	0	0.0	100.0	0.0	100.0	100.0
1/2"	762	12.7	87.3	12.7	100.0	65.0
3/8"	1478	24.6	62.7	37.3	70.0	30.0
#4	3324	55.4	7.2	92.8	25.0	0.0
#8	345	5.8	1.5	98.5	5.0	0.0
#16	52	0.9	0.6	99.4	0.0	0.0
#30	11	0.2	0.4	99.6	0.0	0.0
#50	5	0.1	0.4	99.6	0.0	0.0
#100	3	0.1	0.3	99.7	0.0	0.0
Pan	18	0.3	0.0	100.0	0.0	0.0

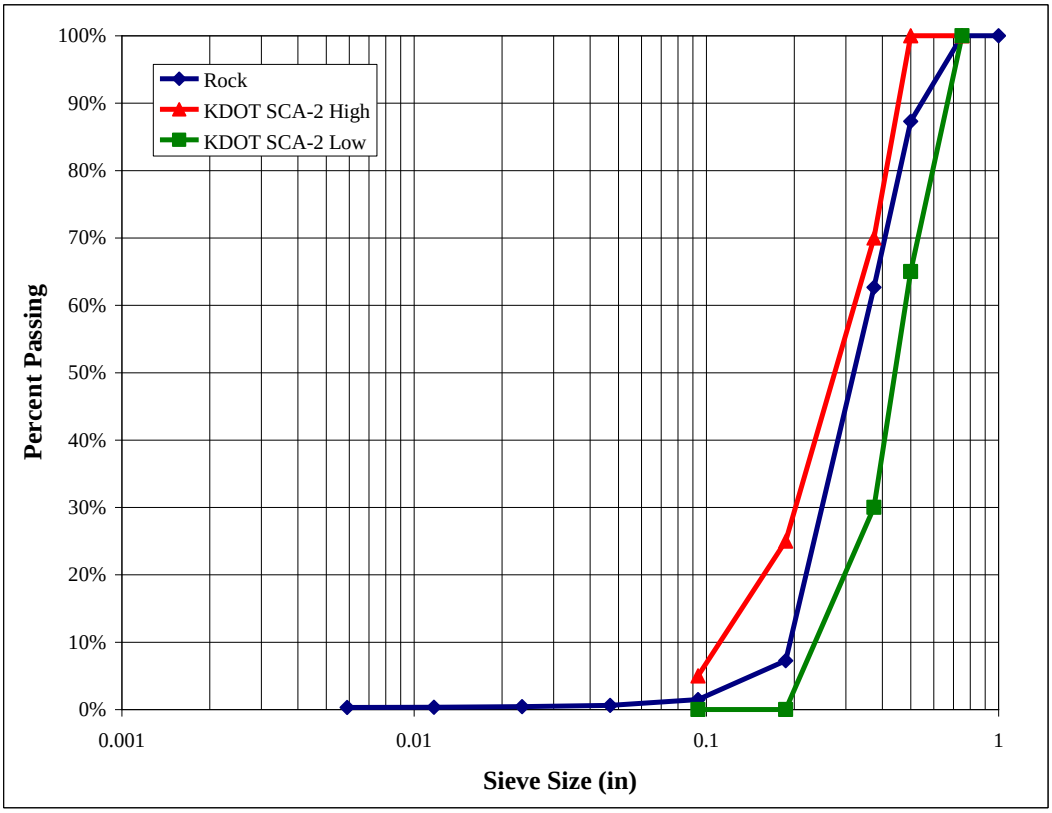

Figure 6. Gradation curve of coarse aggregate.

3.1.3 Mixed Aggregate

A mixed aggregate gradation was also performed. Trial and error was used to determine the proper ratio of fine-to-coarse aggregate. A sieve analysis was performed on the mixed aggregate and compared to the passing high and low values permitted by KDOT under the mixed aggregate specification MA-2. A final blend ratio of 50% fine aggregate by weight to 50% coarse aggregate by weight was used and fell within the parameters of the KDOT values. The sieve analysis for the mixed aggregate can be seen in Table 3, and the gradation curve for the mixed aggregate can be seen in Figure 7.

Table 3. Sieve analysis of mixed aggregate.

Sieve	Weight Retained (g)	Percent Retained	Percent Passing	Cumulative Percent Retained	KDOT Percent Passing - High	KDOT Percent Passing - Low
1"	0	0.0	100.0	0.0	100.0	100.0
3/4"	0	0.0	100.0	0.0	100.0	100.0
1/2"	635	6.4	93.6	6.4	97.0	85.0
3/8"	1232	12.3	81.3	18.7	85.0	70.0
#4	2874	28.7	52.6	47.4	67.0	50.0
#8	807	8.1	44.5	55.5	55.0	34.0
#16	1091	10.9	33.6	66.4	36.0	20.0
#30	1340	13.4	20.2	79.8	22.0	10.0
#50	1385	13.9	6.4	93.6	13.0	4.0
#100	537	5.4	1.0	99.0	5.0	0.0
Pan	98	1.0	0.0	100.0	0.0	0.0

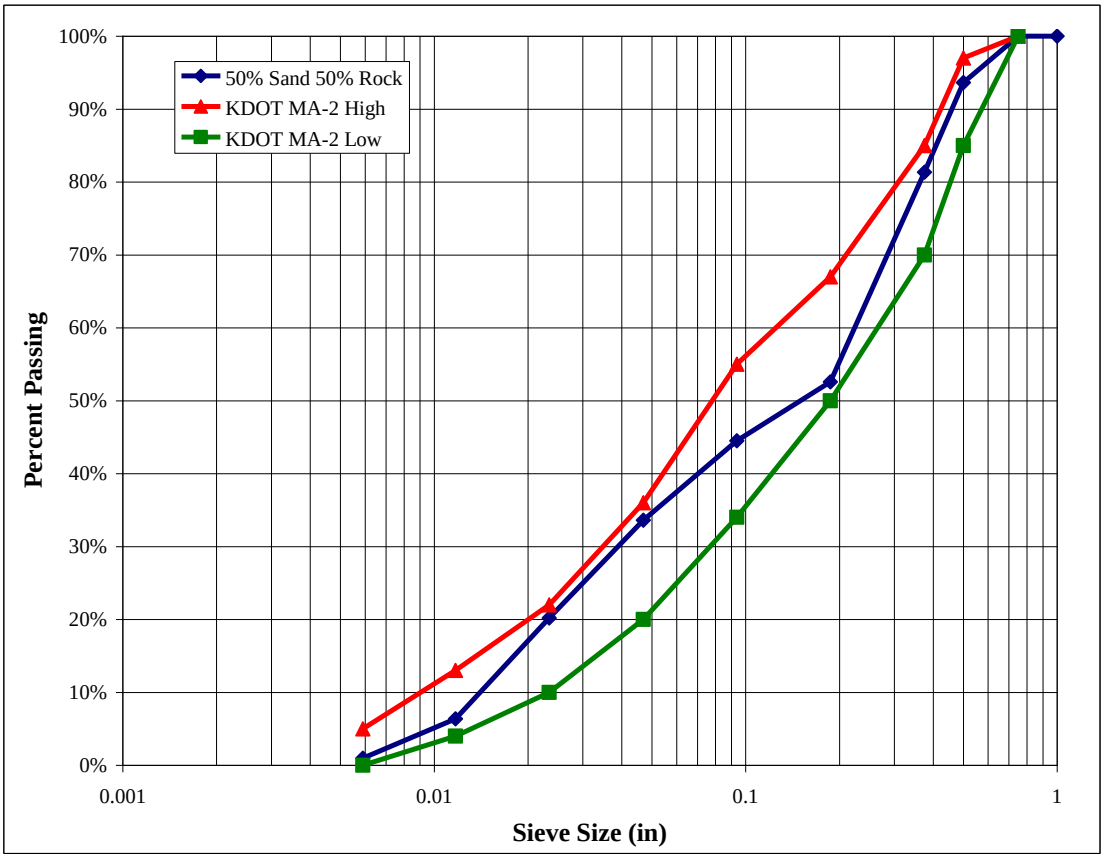

Figure 7. Gradation curve of mixed aggregate.

3.2 ABSORPTION, SPECIFIC GRAVITY, AND MOISTURE CONTENT

Absorption and specific gravity of the fine aggregate were determined using AASHTO T 84. Apparent specific gravity was found to be 2.62 and absorption was found to be 0.44%. In order to control moisture content, the fine aggregate was completely dried in a convection oven, resulting in a moisture content of 0.0%.

Absorption and specific gravity of the coarse aggregate were determined using AASHTO T 85. Apparent specific gravity was found to be 2.65 and absorption was found to be 1.50%. Just like the fine aggregate, moisture content of the coarse aggregate was controlled. The coarse aggregate was completely submerged in water and allowed to soak for two days. This allowed it to not only reach full absorption but also determine the amount of water present on the outer surface of the aggregate. Surface water determination was critical as it is used by the cement for hydration during mixing and placement.

Several samples of submerged aggregate were removed and strained, and their wet weights were measured. Samples were then placed in a convection oven, completely dried, and then reweighed. Moisture content of the coarse aggregate was calculated for each sample and then averaged. This resulted in a two-day moisture content of 4.25%. Moisture content calculated consisted of both surface water and absorbed water.

3.3 CEMENT

Type I/II blend cement was used for all trial mixes and test specimens. Two shipments were used throughout the research, both produced by Ash Grove Cement Company. There were no noticeable differences between the two shipments. A specific gravity of 3.15 was used in the concrete mix design.

3.4 ADMIXTURES

Two different admixtures were used throughout the project. The first was an air-entrainer, Daravair 1000, produced by W. R. Grace. The second was a high-range water-reducer, or Type F

polycarboxylate-based superplasticizer, Adva Cast 530, also produced by W. R. Grace. The superplasticizer was chosen because of its ability to produce a wide range of concrete fluidity.

CHAPTER 4. CONCRETE MIXTURE PROPORTIONING AND DESIGN

This chapter discusses the concrete mix design process of the trial mixes. Test methods performed on the fresh and hardened concrete are also included.

4.1 ABSOLUTE VOLUME METHOD

The absolute volume method of proportioning concrete was used to determine the mix designs for the project. It is the most common method used in concrete mix design. The basis of this method is to design a cubic yard of concrete based on the volume of the materials used in the concrete. An air content of 6.5% was used in the mix design. Batch weights of the concrete materials are determined by using the final volume measurements and the materials' respective specific gravities. A sample mix design sheet is shown in Figure 8.

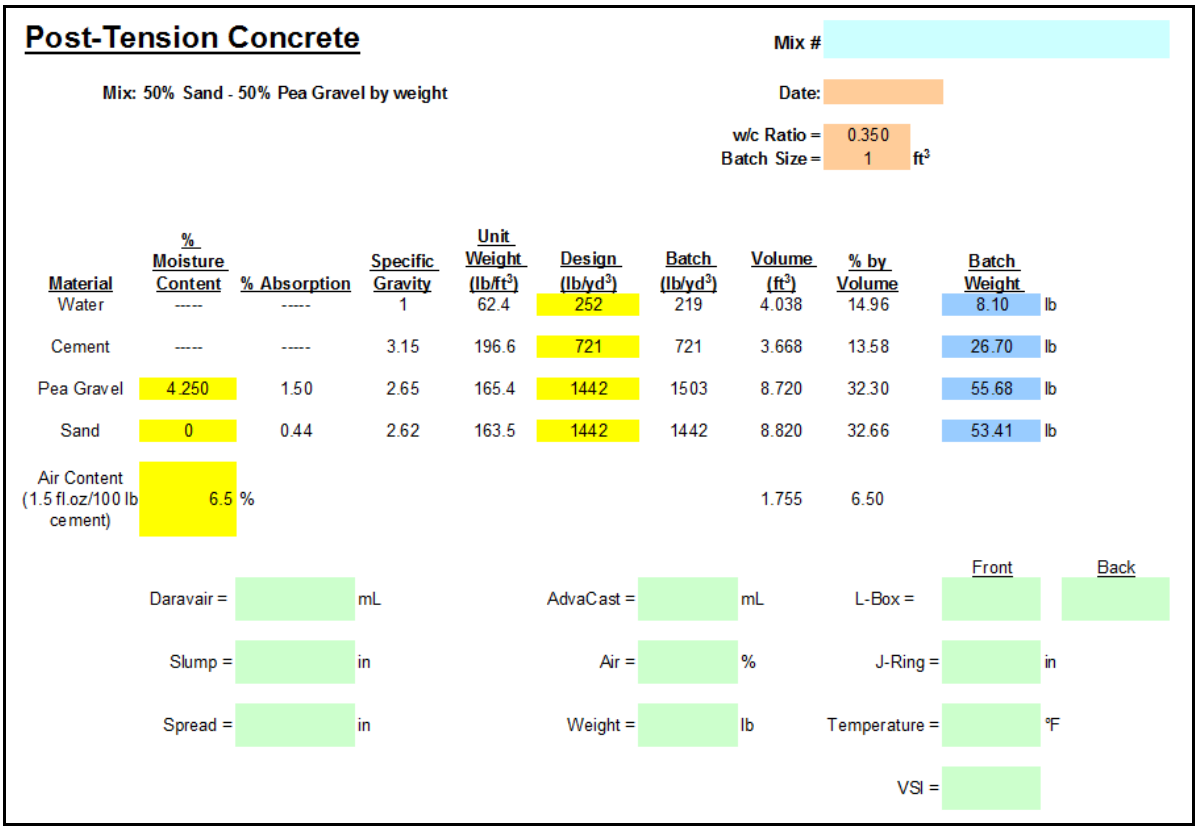

Post-Tension Concrete

Mix #

Mix: 50% Sand - 50% Pea Gravel by weight

Date:

w/c Ratio = 0.350

Batch Size = 1 ft^3

Material	% Moisture Content	% Absorption	Specific Gravity	Unit Weight (lb/ft^3)	Design (lb/yd^3)	Batch (lb/yd^3)	Volume (ft^3)	% by Volume	Batch Weight	
Water	-----	-----	1	62.4	252	219	4.038	14.96	8.10	lb
Cement	-----	-----	3.15	196.6	721	721	3.668	13.58	26.70	lb
Pea Gravel	4.250	1.50	2.65	165.4	1442	1503	8.720	32.30	55.68	lb
Sand	0	0.44	2.62	163.5	1442	1442	8.820	32.66	53.41	lb
Air Content (1.5 fl.oz/100 lb cement)	6.5	%					1.755	6.50		

Daravair = mL

Slump = in

Spread = in

AdvaCast = mL

Air = %

Weight = lb

L-Box = Front Back

J-Ring = in

Temperature = °F

VSI =

Figure 8. Sample mix design sheet.

4.2 TRIAL MIX DESIGN

The purpose of a trial mix design is to determine optimized mixture proportions. This includes water-to-cement ratio, minimum cement content, aggregate ratio, and admixture dosages. KDOT specification 401 provides values for the minimum amount of cement and water/cement ratio that can be used in designing air-entrained concrete for structures.

A mix design approved and used by KDOT on another PTHS bridge deck was used for this project and can be seen in Figure A1 in Appendix A. The KDOT mix design was used on KDOT Project K-3433-03, which was a local bridge replacement, and was classified as using Grade 3.5 (AE)(SA) designed concrete. This meant the mix was a structural concrete air-entrained with select coarse aggregate for wear and absorption. Materials and proportions were kept the same for this project, except for the admixtures. To verify the KDOT mix and determine proper admixture dosages, one-cubic-foot trial mixes were batched in a 2.5-cubic-foot pan mixer as shown in Figure 9.

Figure 9. Pan mixer.

Materials used in the trial mixes were weighed in five-gallon buckets. Coarse aggregate was soaked in buckets for two days, drained, and then weighed. This allowed the two-day moisture content to be used.

For larger batches bigger than what the pan mixer could hold, a 1.25-cubic-yard drum-mixer trailer was used as seen in Figure 10. Coarse aggregate for these larger batches was soaked in 55-gallon drums and drained prior to mixing. Figure 11 shows water being drained for a large concrete batch.

Figure 10. Drum-mixer trailer.

Figure 11. Water being drained for large concrete batch.

A total of three final mixes were made from all the trial mixes. The first was a conventional concrete mix with a three- to four-inch slump. The second was a hybrid flowable concrete mix with an 18- to 20-inch spread. The third was a fully flowable SCC mix with a 24-inch spread. Conventional and hybrid mixes would be used as the main focus of the research project, while the SCC mix was used only for the shear friction specimens.

A constant problem with batching the concrete mixes was not being able to consistently achieve the target slump/spread. Many times the mixes would result in a slump/spread lower than the target slump/spread. It was found to be easier to slightly overdose the concrete mixes with superplasticizer and allow them to drop to the target slump/spread.

4.3 FRESH CONCRETE TEST METHODS

Several tests were performed to determine the rheological properties of the fresh concrete mixes. Typical fresh concrete properties measured were slump, unit weight, and volumetric air content. SCC undergoes typical fresh concrete test methods as well as additional tests including spread, J-

ring, L-box, and VSI. Concrete cylinders for testing compressive strength of the trial mixes were made for each mix. Specific tests performed on each mix are listed below:

1. Conventional concrete mixes were subjected to slump, unit weight, and volumetric air content tests.
2. Hybrid concrete mixes were subjected to spread, unit weight, and volumetric air content tests.
3. SCC mixes were subjected to spread, unit weight, volumetric air content, J-ring, L-box, and VSI tests.

4.3.1 Slump

The slump test was performed according to AASHTO T 119. The slump cone was filled in three layers of equal volume and rodded 25 times after each layer. The cone was then slowly lifted, which allowed the concrete to sink down, inverted, and placed back on the base. The slump was recorded as the distance from the top of the cone to the center of the concrete. The slump test is shown in Figure 12.

Figure 12. Slump test.

4.3.2 Unit Weight

Unit weight of the concrete was determined according to AASHTO T 121. A rigid container of known volume and weight was filled with concrete in layers by volume, rodded 25 times after each layer, struck off at the top, and weighed. Unit weight was calculated by subtracting the base weight from the total weight, and then dividing by the known volume. The base of an airmeter pot was the rigid container used for this test. A picture of the airmeter base on the scale can be seen in Figure 13.

Figure 13. Airmeter base on scale.

Figure 14. Airmeter pot.

4.3.3 Volumetric Air Content

An airmeter pot, commonly called a rollometer, was used to determine the percentage of air in the concrete according to AASHTO T 196 and KDOT specification KT-19. The airmeter pot is shown in Figure 14. After the unit weight test had been performed, the concrete was left in the base and the top of the airmeter pot was attached. A liter of isopropyl alcohol was poured into the pot via a funnel. Water was then added until the fluid line was filled up to a calibration mark. A lid was attached and the airmeter was shaken and inverted in order to break up the concrete mix. The airmeter was then placed on the ground at a 45° angle and rolled back and forth while being hit with a rubber mallet. After several minutes, the airmeter was placed on a level surface which allowed the air to settle out. The final fluid line was recorded as the air content percent. KDOT specification 401 allows air-entrained concrete to have 6.5±1.5% air.

4.3.4 Spread

The spread test was performed according to the American Society for Testing and Materials (ASTM) *Standard Specifications* (2008) test ASTM C1611. The slump cone was inverted, placed on a large flat surface, filled in three layers of equal volume, and rodded 25 times after each layer. The cone was then slowly lifted and the concrete was allowed to flow out and form a patty. The diameter of the concrete patty was measured and recorded as the spread. Figure 15 shows a picture of the spread test.

Figure 15. Spread test.

4.3.5 J-Ring

The J-ring test was performed according to ASTM C1621. It measured the lateral flow of the concrete patty through rebar. A ring with steel rebar attached was placed around the inverted slump cone. The cone was filled according to the spread test, lifted, and the concrete was allowed to flow through the rebar. The diameter of the resulting concrete patty was measured. A picture of the J-ring test can be seen in Figure 16.

Figure 16. J-ring test.

4.3.6 L-Box

The L-box test measured the filling and passing ability of the concrete through rebar in an L-shaped rigid box. The vertical end of the L-box was filled with concrete, a door at the bottom was opened, and the concrete was allowed to flow out through rebar into the horizontal end of the L-box. A picture of the L-box test is illustrated in Figure 17. Vertical distance was measured from the top of the horizontal end of the box down to the concrete at both the front and back of the box. Theoretically, the height measurements should be equal, which meant the concrete was truly self-leveling.

Figure 17. L-box test.

4.3.7 VSI Rating

The Visual Stability Index (VSI) rating measured stability and segregation of the concrete mix through visual observation. The VSI rating was performed on the concrete patty after the spread test and given a rating on a scale of 0-3. A “0” meant the concrete was completely stable with no signs of water bleeding or mix segregation, while a “3” meant the concrete was completely unstable with several signs of water bleeding and/or mix segregation.

4.3.8 Concrete Cylinders

Concrete cylinders were made according to AASHTO T 126. Concrete cylinder molds were filled in three layers by volume and rodded 25 times after each layer. The tops of the cylinders were smoothed out using a concrete float, covered with plastic sacks to prevent moisture loss, and carefully placed in a moist room. After 24 hours, the molds were removed and the cylinders were placed back in the moist room. The concrete cylinder molds were either 4-inch diameter by 8-inch height or 6-inch diameter by 12-inch height. Figure 18 shows 4-inch by 8-inch cylinders being made.

Figure 18. Making concrete cylinders.

4.4 HARDENED CONCRETE TEST METHODS

Several tests were performed on the hardened concrete mixes to determine if they were acceptable for structural applications. The compressive strength test was performed on all trial

mixes, while the rest of the tests were performed on only the final conventional and hybrid concrete mixes.

4.4.1 Compressive Strength

Concrete cylinders were tested according to AASHTO T 22. Three, 4-inch by 8-inch cylinders were used for this test. The cylinders were removed from the moist room and their average diameter was measured. Each cylinder was placed between neoprene pads that were inside steel end caps and loosely wrapped with a canvas cover as shown in Figure 19. Then it was placed vertically in a hydraulic testing machine and loaded until failure. Compressive strength was calculated by dividing the maximum load by the cross-sectional area of the cylinder. Average compressive strength of the three cylinders was recorded.

Figure 19. Compressive strength test.

4.4.2 Tensile Strength

The split-tensile test was performed according to AASHTO T 198. Three, 6-inch by 12-inch cylinders were used for this test. The cylinders were removed from the moist room and their average diameter and length were measured. Each cylinder was placed horizontally in a split-tensile load fixture and loaded until failure using a hydraulic testing machine. Equation 1 was used to determine the split-tensile strength. Average split-tensile strength of the three cylinders was recorded. Figure 20 shows the split-tensile test.

$$T = \frac{2P}{\pi l d} \qquad \text{(Equation 1)}$$

$T =$ Tensile Strength (psi)

$P =$ Maximum Load (lbs)

$l =$ Length of Specimen (in)

$d =$ Diameter of Specimen (in)

Figure 20. Split-tensile test.

4.4.3 Modulus of Elasticity

The modulus of elasticity test was performed according to ASTM C 469. The diameter of three, 4-inch by 8-inch cylinders was measured. The cylinders were then capped with sulfur, mounted with a digital compressometer, and placed in an MTS-controlled hydraulic testing machine. Figure 21 shows a cylinder mounted with the compressometer. The cylinders underwent three load cycles not exceeding 40% of their compressive strength. The first cycle seated the compressometer and cylinder, while the other two cycles were used to calculate the modulus of elasticity. The MTS system recorded load and displacement of the compressometer. This data was graphed in Microsoft Excel and the average modulus of elasticity (E_{graph}) was calculated. The chord modulus of elasticity (E_{chord}) was calculated using Equation 2.

$$E_{chord} = \frac{(S_2 - S_1)}{(\varepsilon_2 - 0.000050)} \qquad \text{(Equation 2)}$$

E_{chord} = Chord Modulus of Elasticity (psi)

S_2 = Stress Corresponding to Maximum Load (psi)

S_1 = Stress Corresponding to Strain of 0.000050 (psi)

ε_2 = Longitudinal Strain Produced by S_2 (in/in)

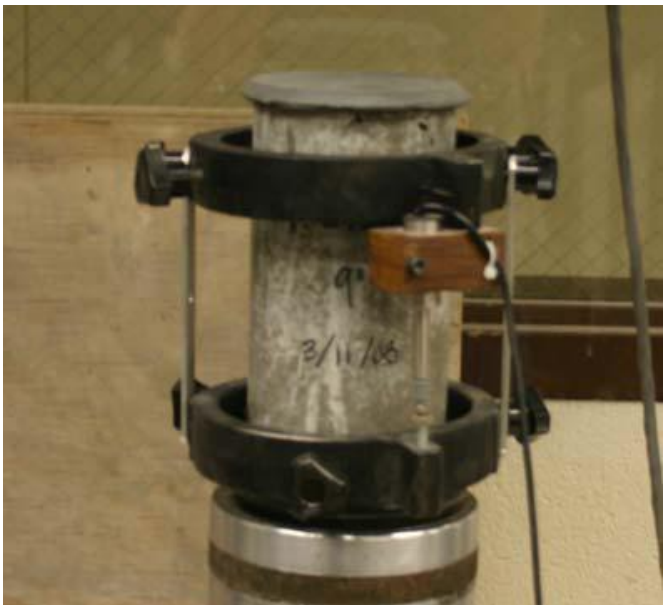

Figure 21. Cylinder mounted with compressometer.

4.4.4 Permeability

The *Electrical Indication of Concrete's Ability to Resist Chloride-Ion Penetration* test was used to determine permeability of the final concrete mixes. The test was performed according to AASHTO T 277 and involved taking 2-inch slices of a 4-inch by 8-inch cylinder and passing current through them during a six-hour period. The slices were submerged in a sodium-chloride solution on one end and a sodium-hydroxide solution on the other end. The test was performed at the KDOT materials lab by KDOT personnel. Volume of permeable voids was measured at 28 days and permeability was measured at 56 days. Correlation of chloride-ion permeability based on charge passed in this test is shown in Table 4.

Table 4. Chloride-ion permeability.

Charge Passed (coulombs)	Chloride-Ion Penetrability
> 4000	High
> 2000 - 4000	Moderate
> 1000 - 2000	Low
100 - 1000	Very Low
< 100	Negligible

4.4.5 Freeze-Thaw Resistance

The *Resistance of Concrete to Rapid Freezing and Thawing* test was performed according to AASHTO T 161 and KDOT specification KTMR-22. The purpose of the test was to determine resistance of the concrete mixes when subjected to freezing and thawing cycles. Procedure B was used for this project. Six, 4-inch by 3-inch by 16-inch beams were made from finalized conventional and hybrid concrete mixes. The beams were brought to the KDOT materials lab where they were tested by KDOT personnel. Figure 22 shows the freeze-thaw chamber used by KDOT for the test. According to KDOT specification 1102, acceptable values for free-thaw resistance is a durability factor of 95 or higher and an expansion not greater than 0.025%. Relative dynamic modulus of elasticity was calculated using Equation 3. The durability factor was calculated using Equation 4.

$$P_c = \left(\frac{n_1^{\,2}}{n^2} \right) * 100 \qquad \text{(Equation 3)}$$

$P_c =$ Relative Dynamic Modulus of Elasticity after c cycles of freezing and thawing (%)

$n_1^{\,2} =$ Fundamental Transverse Frequency at 0 cycles of freezing and thawing

$n^2 =$ Fundamental Transverse Frequency after c cycles of freezing and thawing

$$DF = \frac{PN}{M} \qquad \text{(Equation 4)}$$

$DF =$ Durability Factor

$P =$ Relative Dynamic Modulus of Elasticity at N cycles (%)

$N =$ Number of cycles at which P reaches the specified minimum value for discontinuing the test or the specified number of cycles at which the exposure is to be terminated, whichever is less

$M =$ Specified number of cycles at which the exposure is to be terminated

Figure 22. Freeze-thaw chamber.

4.4.5 Coefficient of Thermal Expansion

The coefficient of thermal expansion (CTE) was determined for the concrete mixes. Six, 4-inch by 3-inch by 16-inch beams were cast with Geokon vibrating wire strain gages (VWSG). The VWSG were placed horizontally on bar chairs inside the beam molds as shown in Figure 23. The VWSG were aligned with the longitudinal orientation of the mold prior to casting. Concrete was placed inside the mold and carefully rodded around the VWSG to ensure proper consolidation. The beams were cured for 28 days inside a moist room and then submerged in a lime-water bath for another 28 days. The lime-water bath ensured the beams would not undergo length deformation due to swelling.

Figure 23. Beam mold with VWSG.

An initial reading of the beams was taken at room temperature (approximately 72°) while submerged in the lime-water bath inside the moist room. The beams were then removed from the moist room and submerged in water in an insulated tank. Temperature of the water in the tank

was lowered to 33° using ice. Temperature and strain was measured using a Geokon VWSG reader every hour until the readings had stabilized. The beams were then removed and placed back in the lime-water bath inside the moist room where they were left to stabilize overnight, and then the process was repeated the next day. Temperature of the bath on the second day was raised to 133° using a heating element.

Strain values measured were of the VWSG, so the actual strain values of the concrete had to be calculated. This was done using equations provided by Geokon. The CTE values were then calculated from the actual strains and averaged for the mixes.

4.5 SLUMP/SPREAD LOSS TEST

The SCC mix was chosen to be studied for effects of slump/spread loss vs. time. It was determined the SCC mix would represent a worst-case scenario where the hybrid flowable mix was overdosed with a superplasticizer admixture. During the hydration process, concrete loses slump/spread as time passes. Temperature of the mix was measured to determine exactly how fast the mix lost slump/spread. The starting goal of the mixtures would be a 24-inch spread and the end goal would be a 3-inch slump.

A SCC mix was made, and after the mixing process was completed, an initial slump and spread test was performed. Data was recorded along with temperature of the mix. A stopwatch was used to time the mix from the start of the tests to the finish. It took roughly two minutes to properly conduct a spread and slump test. The concrete was then allowed to mix for two additional minutes, which created a four-minute testing cycle.

After each test was performed, the concrete was placed back into the mixer and the mixer was turned on. Slump and spread boards were wetted and excess water was removed so as not to introduce it into the concrete mix. Temperature, slump, and spread were measured until the end goal was reached. The spread test was stopped when the concrete reached a 10-inch spread, and the slump test was stopped when the concrete reached below a 4-inch slump.

The concrete mix was made at three different temperatures: hot, room, and cold. The hot mix used warm fine aggregate from the oven, hot water, and room-temperature coarse aggregate. The cold mix used room-temperature fine aggregate, cold water, and coarse aggregate soaked in ice water. All materials were kept at room temperature before mixing for the room-temperature mix.

CHAPTER 5. CONCRETE EXPERIMENTAL RESULTS

This chapter gives experimental results of the final concrete mix designs. This includes conventional, hybrid, and SCC mixes. Hardened concrete test results and slump/spread loss results are included.

5.1 CONCRETE MIX DESIGNS

All three mix designs used a water-to-cement ratio of 0.35, cement content of 721 lb/yd^3, and a 50%-50% fine-to-coarse aggregate ratio. The conventional concrete mix used an air-entrainer dosage rate of 0.19 oz/100 lb of cement and a superplasticizer dosage rate of 4.43 oz/100 lb of cement. The hybrid concrete mix used an air-entrainer dosage rate of 0.18 oz/100 lb of cement and a superplasticizer dosage rate of 6.33 oz/100 lb of cement. The SCC mix used an air-entrainer dosage rate of 0.16 oz/100 lb of cement and a superplasticizer dosage rate of 7.60 oz/100 lb of cement.

Dosage rates for the above mix designs are for concrete batches of one cubic foot. It was discovered dosage rates for the admixtures did not scale up properly. Larger concrete batches had dosage rates adjusted accordingly. It was also discovered superplasticizer increased the air content of the concrete mix. Smaller dosage rates of air-entrainer were used when larger dosage rates of superplasticizer were used.

5.2 HARDENED CONCRETE TEST RESULTS

This section gives experimental results of the hardened concrete tests as discussed in Chapter 4. These results only represent the conventional and hybrid concrete mixes.

5.2.1 Compressive Strength

Compressive strengths were determined at 1, 3, 7, 14, 21, and 28 days. Specimens for the compressive strength, split-tensile strength, permeability, and modulus of elasticity were made

from the same mixes. Procedure details and test setups are outlined in Chapter 4. Fresh concrete properties of the final mixes are shown in Table 5. Average compressive strength results are shown in Table 6.

Table 5. Fresh concrete properties of final mixes (Set 1).

	Slump (in)	Spread (in)	Unit Weight (pcf)	Volumetric Air Content (%)
Conventional	4	---	137.8	6
Hybrid	---	19	135.5	6.75

Table 6. Average compressive strengths of final mixes.

	Compressive Strength (psi)	
Day	**Conventional**	**Hybrid**
1	3120	3850
3	4520	4900
7	4950	5720
14	5220	6220
21	5730	6580
28	6170	6800

5.2.2 Tensile Strength

Split-tensile strengths were determined at 1, 3, 7, 14, 21, and 28 days. Specimens for compressive strength, split-tensile strength, modulus of elasticity, and permeability tests were made from the same concrete batches. Fresh concrete properties are given in Table 5. Procedure details and test setups are outlined in Chapter 4. Average split-tensile strengths are given in Table 7.

Table 7. Average split-tensile strength of final mixes.

Day	Tensile Strength (psi)	
	Conventional	Hybrid
1	356	351
3	398	410
7	456	468
14	459	479
21	484	502
28	497	518

5.2.3 Modulus of Elasticity

The modulus of elasticity was determined at 1, 3, 7, 14, 21, and 28 days. Specimens for compressive strength, split-tensile strength, modulus of elasticity, and permeability tests were made from the same concrete batches. Fresh concrete properties are given in Table 5. Procedure details and test setups are outlined in Chapter 4. Average modulus of elasticity values are given in Table 8.

Table 8. Average modulus of elasticity of final mixes.

Day	Modulus of Elasticity (ksi)			
	Conventional E_{chord}	Conventional E_{graph}	Hybrid E_{chord}	Hybrid E_{graph}
1	2160	2140	2320	2310
3	2800	2810	2970	2990
7	2960	2980	3010	3010
14	2950	2930	3170	3200
21	3240	3290	3460	3500
28	3570	3440	3680	3700

For these mixes to be used in a composite bridge deck, the modulus of elasticity for each mix needs to be similar. As shown in the table, values of E_{chord} and E_{graph} are not only similar to each other within each mix, but similar across mixes as well. Medium-strength concrete has a 28-day modulus of elasticity value of 3600 ksi according to Beer et al. (2001).

5.2.4 Permeability

The *Electrical Indication of Concrete's Ability to Resist Chloride-Ion Penetration* test was conducted to determine permeability of the final mixes. Specimens for compressive strength, split-tensile strength, modulus of elasticity, and permeability tests were made from the same concrete batches. Fresh concrete properties are given in Table 5. Procedure details and test setups are outlined in Chapter 4. Permeability values are given in Table 9.

Table 9. Permeability of final mixes.

	Permeability (coulombs)	**Permeability Voids (%)**
Conventional	3317	12.6
Hybrid	3315	12.3

The correlation of chloride-ion permeability based on charge passed is shown in Table 4. Values from Table 9 show both mixes are within the moderate range (>2000 – 4000 Coulombs) of Table 4. According to KDOT specification 401, either a maximum volume of permeability voids of 12.5% or a maximum rapid chloride permeability of 3500 coulombs is allowed. Results of Table 9 show the values are not only similar to each other, but most fall under KDOT maximum values as well. Permeability voids of the conventional mix are slightly over the maximum value.

5.2.5 Freeze-Thaw Resistance

The *Resistance of Concrete to Rapid Freezing and Thawing* test was conducted on the final mixes. Specimens for freeze-thaw resistance and coefficient of thermal expansion tests were made from the same concrete batches. Fresh concrete properties are given in Table 10. Procedure details and test setups are outlined in Chapter 4. Durability factors and percent expansion for the final mixes are given in Table 11.

Table 10. Fresh concrete properties of final mixes (set 2).

	Slump (in)	Spread (in)	Unit Weight (pcf)	Volumetric Air Content (%)
Conventional	3.5	---	142.8	---
Hybrid	---	20	140.6	5

Table 11. Durability factor and percent expansion of final mixes.

	Durability Factor	Percent Expansion
Conventional	67	0.125
Hybrid	99	0.004

According to KDOT specification 1102, acceptable values for freeze-thaw resistance are a durability factor of 95 or higher and an expansion not greater than 0.025%. The hybrid mix showed acceptable passing levels, while the conventional mix did not. One of the reasons the conventional mix failed is that during the casting process, a problem occurred while determining volumetric air content. The airmeter leaked and there was not enough concrete to redo the test. Based on unit weights in Table 10, volumetric air content can be estimated as being lower than 5%, which is below the acceptable KDOT threshold. Another possible reason for failure could be the beams were not properly consolidated during the casting process. Replacement beams were not recast for the conventional mix.

5.2.6 Coefficient of Thermal Expansion

The coefficient of thermal expansion (CTE) was determined for the final mixes. Specimens for the freeze-thaw resistance and coefficient of thermal expansion tests were made from the same concrete batches. Fresh concrete properties are given in Table 10. Procedure details and test setups are outlined in Chapter 4. CTE values for the final mixes are given in Table 12.

Table 12. Coefficient of thermal expansion of final mixes.

	Coefficient of Thermal Expansion (με/°F)
Conventional	5.6
Hybrid	5.5

CTE values were initially calculated in Celsius and then converted to Fahrenheit. For these mixes to be used in a composite bridge deck, CTE values for each mix needs to be similar. According to Beer et al. (2001), the CTE of medium-strength concrete is 5.5 με/°F.

5.3 SLUMP/SREAD LOSS RESULTS

The slump/spread loss was conducted on the SCC mix at three different temperatures. Procedure details are discussed in Chapter 4. There was a hot, room temperature, and cold mix. The hot mix was measured at 90°F, room temperature mix was measured at 74°F, and cold mix was measured at 56°F. Figure 24 shows slump loss over time and Figure 25 shows spread loss over time. Figure 26 illustrates spread vs. slump at various temperatures.

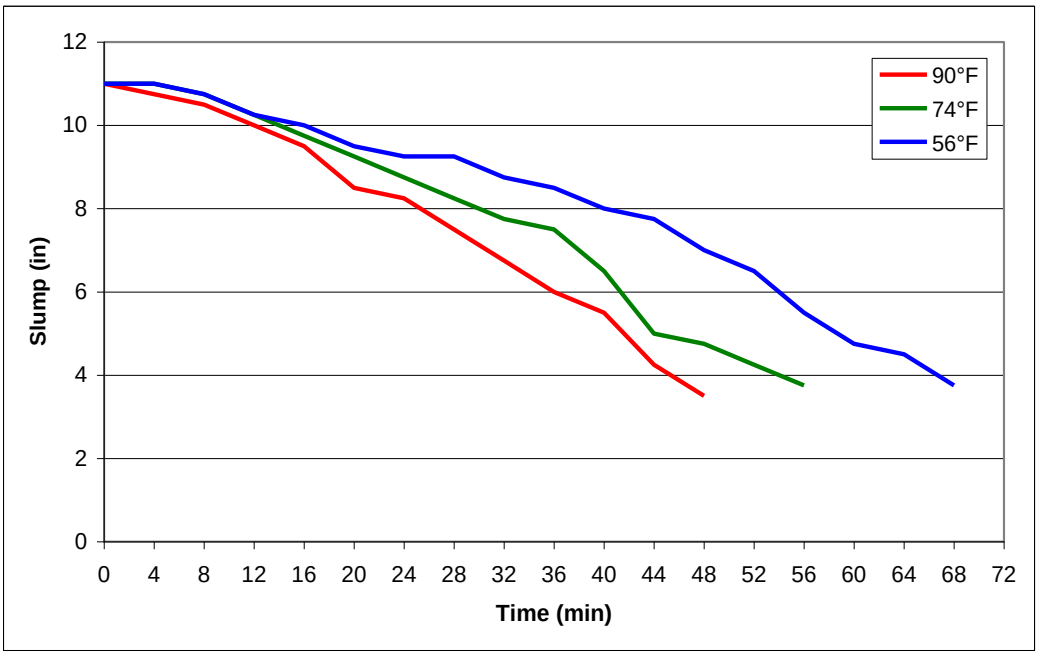

Figure 24. Slump loss over time.

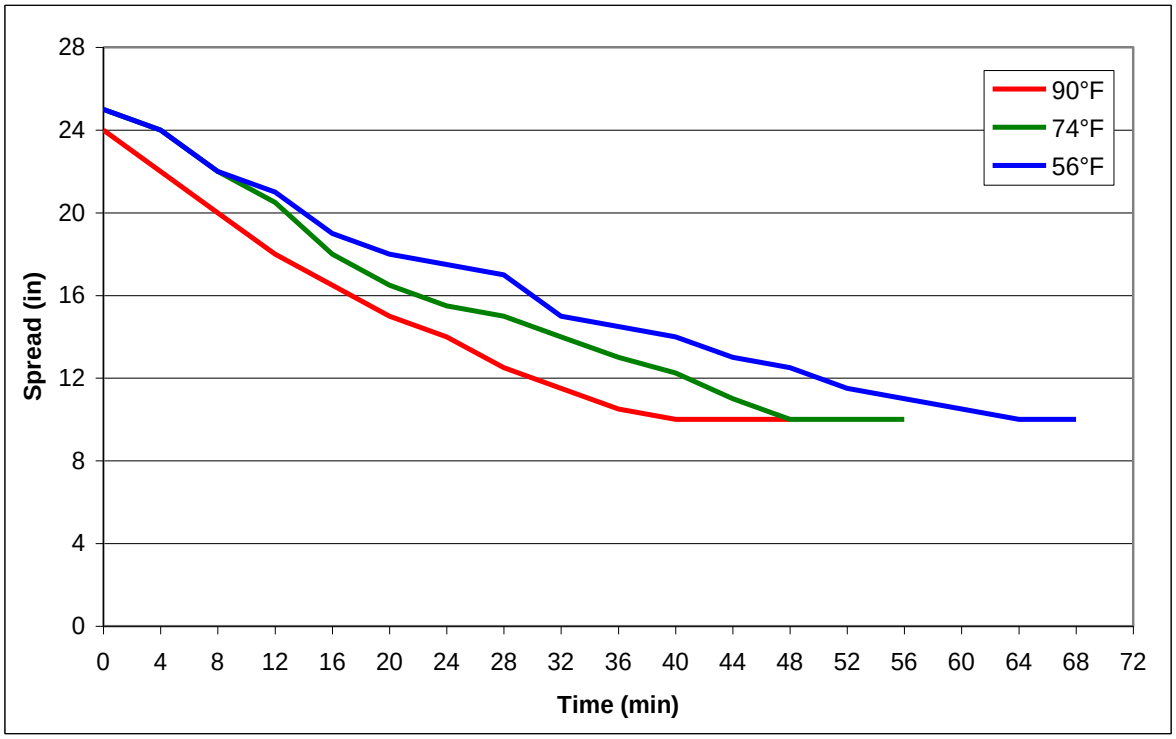

Figure 25. Spread loss over time.

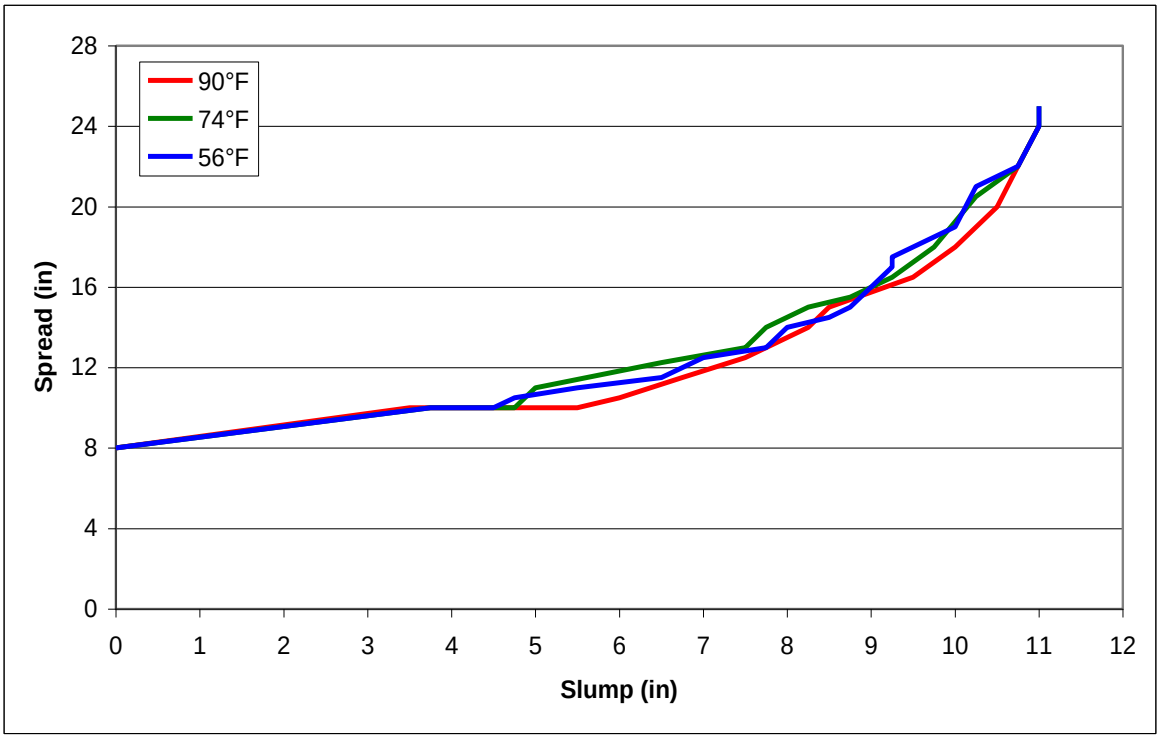

Figure 26. Spread versus slump at various temperatures.

According to KDOT specification 401, temperature of mixed concrete shall be between 50° and 90°F when being placed. All three mixes fell within the acceptable temperature range. Maximum slump that could be recorded was height of the slump cone minus the maximum coarse aggregate size. Conversely, the minimum spread that could be recorded was the diameter of the base of the slump cone.

Figures 24 and 25 show slump/spread loss over time, at different temperatures, follows the same basic trend pattern. The figures also show the higher the concrete temperature, the faster it loses slump/spread, while the colder the concrete temperature, the slower it loses slump/spread. This is because heat increases the hydration process. Figure 26 shows the curves of all three mixes mostly fall on top of each other. Although the spread was stopped at 10 inches and the slump at 3 inches, the curves of Figure 26 were projected to the minimum possible spread and slump readings.

The graphs also show that an 18- to 20-inch spread is equivalent to a 9.5- to 10.5-inch slump. KDOT specification 401 states the maximum allowable slump for concrete with plasticizing admixture is 7 inches. Equation 5 was developed from data in Figure 26 to determine spread based on a given slump.

$$Spread = 0.0025x^4 - 0.0311x^3 + 0.1482x^2 + 0.2273x + 8 \qquad \text{(Equation 5)}$$

$x =$ Slump

CHAPTER 6. CONCRETE-TO-CONCRETE BOND

This chapter outlines the design, fabrication, and coring of concrete core blocks. Results of the core breaks are also included.

6.1 BACKGROUND

The split-tensile test uses a shear force to determine the approximate tensile strength of concrete. In order for a split-tensile test to be performed on concrete made from two different mixes, a core block was constructed and cores were extracted from it. The cores were then tested as split-tensile specimens and the results of the two concrete mixes were compared.

6.2 CORE BLOCK DESIGN

The first step in determining the bond of two concrete layers was to design a core block. A large core block was designed with a height of 30 inches, a width of 30 inches, and a depth of 12 inches. The bottom half of the block would be cast with hybrid concrete mix, while the top half would be cast with conventional concrete mix. Size of the block would allow for nine separate specimens to be cored. There would be three each from the hybrid and conventional mixes, and three that were composite. Each cored specimen was 6 inches in diameter and 12 inches in height, or the same as the split-tensile specimens discussed in Chapter 4. Figure 27 shows the large core block dimensions.

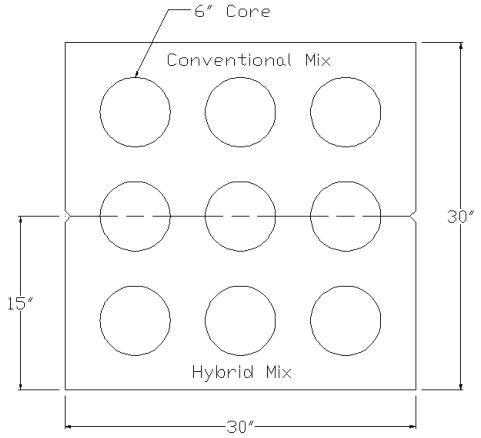

Figure 27. Large core block dimensions.

A sample large core block was made to compare cores from conventional and hybrid mixes to cylinders made from the same mixes. This was done to see if tensile strength of the cores and cylinders were similar. If the case is true, then size of the core block can be reduced and only three core samples will be needed instead of the original nine. Results of the sample big core block found the cylinders had higher tensile strengths than their respective cores, but the difference in tensile strength was 3% or less. Figure 28 shows the coring of the large core block.

Figure 28. Coring of a large core block.

Size of the big core block was reduced. A small core block was designed with a height of 12 inches, a width of 30 inches, and a depth of 12 inches. Only three composite cores would be extracted from the small core block along the interface of the two concrete mixes. Cylinders would be made to determine tensile strength of each concrete mix. The small core block dimensions are shown in Figure 29.

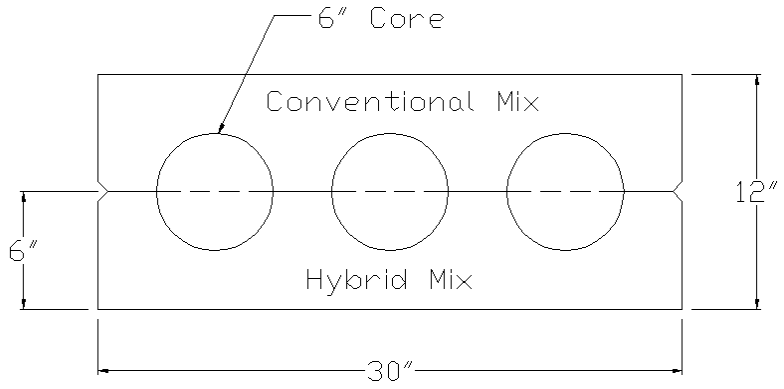

Figure 29. Small core block dimensions.

6.3 CORE BLOCK CASTING

Wooden forms were designed and built to be reused for several castings. Additional pieces of wood were attached to the inside of the forms as midpoint markers. The forms were coated with form-release agent before casting, and silicone sealant was used to fill any cracks or voids in the forms.

Conventional and hybrid concrete mix designs are discussed in Chapter 5. The hybrid concrete was mixed in the drum-mixer trailer and discharged into wheelbarrows. The concrete was then placed into the forms by hand and filled up to the midpoint markers. Any excess concrete was removed. A concrete vibrator was used to ensure proper consolidation and the concrete surface was left as-cast. The forms were then covered with wet burlap and a layer of polyethylene plastic to prevent moisture loss. The mixer was cleaned and the conventional concrete was then mixed. The conventional concrete had a concrete dye mixed in to help differentiate between the two concrete layers. The conventional concrete was mixed in the drum-mixer trailer and discharged into wheelbarrows. The forms were uncovered and the conventional concrete was placed on top the hybrid concrete by hand. The time between concrete placements varied from 47 to 63 minutes. Figure 30 shows placement of the concrete for a small core block.

Figure 30. Concrete placement for small core block.

The conventional concrete was vibrated in two ways. The first method was to just vibrate the top layer of conventional concrete without disturbing the bottom layer. This would provide concrete cores that were not vibrated between layers. The second method was to vibrate the top layer while dipping the vibrator into the bottom layer. This would provide concrete cores that had blending occur between the layers. Theoretically, the cores that had no vibration between layers should have lower tensile strengths than those that had vibration between layers, as the blending process creates a more homogenous core.

After the cores had been vibrated, the tops were finished with a wood float and steel inserts were placed into the concrete to aid with lifting. When the concrete reached initial set, the forms were recovered with wet burlap and polyethylene plastic. Three, 6-inch by 12-inch split-tensile specimens and several 4-inch by 8-inch compressive strength specimens were made for each mix. The next day the core blocks were removed from their forms and placed in the moist room with the split-tensile and compressive strength cylinders.

A total of four small core blocks were cast. The first and second blocks were cast at separate times. The third and fourth blocks were cast at the same time. Only one set of cylinders was made for the third and fourth core blocks. The first and third blocks had no vibration between concrete layers. The second and fourth blocks had vibration between concrete layers.

The concrete casting did not always go to plan. One of the persistent problems was not hitting the target spread/slump. In the end, it was discovered to be easier to slightly overdose the concrete with superplasticizer and overshoot the target spread/slump. The concrete was allowed to mix until the target spread/slump was achieved. Only then was the concrete discharged and placed into the forms.

6.4 CORING

The blocks were cored after 28 days. They were laid on their sides and a core drill with a 6-inch core bit was used for extracting the cores. Special care was taken during the coring process to insure the cores were drilled directly down the middle of the two concrete layers. Figure 31 shows the coring of a small core block. The core blocks were kept wet to prevent the concrete from drying.

Cores were marked after they were removed from the block. They were then immediately placed in the moist room. Three cores were removed from each block. Several core bits were used during the coring process to ensure the cutting teeth remained sharp and created cores with smooth sides for the split-tensile test.

Figure 31. Coring of a small core block.

6.5 CORE SPLIT-TENSILE RESULTS

The cores were removed from the moist room and tested using the split-tensile test. Procedure details of the test are outlined in Chapter 4. Fresh concrete properties of the mixes are given in Table 13. Cylinders made from each respective mix were also tested. Average tensile-strengths of the cylinders and cores are given in Table 14. Figure 32 shows a core after the split-tensile test.

Table 13. Fresh concrete properties of core blocks.

		Slump (in)	Spread (in)	Unit Weight (pcf)	Volumetric Air Content (%)
Block 1 (No Vibration Between Layers)	**Conventional**	3	---	136.5	7.25
	Hybrid	---	19	138.4	6.5
Block 2 (Vibration Between Layers)	**Conventional**	3.5	---	137.8	7
	Hybrid	---	20	139.1	5.5
Block 3 (No Vibration Between Layers)	**Conventional**	3.25	---	140.6	5
	Hybrid	---	18.5	138.4	6.75
Block 4 (Vibration Between Layers)	**Conventional**	3.25	---	140.6	5
	Hybrid	---	18.5	138.4	6.75

Table 14. Average tensile strength of cylinders and cores.

		Average Tensile Strength (psi)
Block 1 (No Vibration Between Layers)	**Conventional**	495
	Hybrid	521
	Composite	358
Block 2 (Vibration Between Layers)	**Conventional**	501
	Hybrid	510
	Composite	417
Block 3 (No Vibration Between Layers)	**Conventional**	488
	Hybrid	500
	Composite	320
Block 4 (Vibration Between Layers)	**Conventional**	488
	Hybrid	500
	Composite	424

Figure 32. Core after split-tensile test.

According to results in Table 14, tensile strength of the composite cores was lower than the strength of the cylinders made from the parent mixes. Tensile strength of the composite cores is increased when vibration between layers is introduced. Blocks 1 and 3 had no vibration between concrete layers and strength of the composite cores was found to be 64-72% the strength of the cylinders made from each mix. Blocks 2 and 4 had vibration between concrete layers and strength of the composite cores was found to be 82-87% the strength of the cylinders made from each mix.

The time between concrete placements restricted the casting and coring of more blocks. The approximate one-hour time frame could not be reduced. The first layer of concrete was beginning to stiffen as the second layer was placed. If the time between concrete placements could have been reduced, then the two layers may have blended better. This would likely result in higher tensile strengths for the composite cores.

CHAPTER 7. SHEAR FRICTION SPECIMENS

This chapter outlines procedures followed for design, fabrication, and testing of the shear friction specimens.

7.1 BACKGROUND

Shear friction was first recognized and presented more than 40 years ago (Birkeland and Birkeland, 1966). It was originally hypothesized based on research of shear connections in composite concrete beams. The research states that shear is transferred across the joint of a composite beam only by friction between the two concrete surfaces.

Slip occurs when a shear force is applied to a slip plane. Steel reinforcement crossing the slip plane yields in tension at an ultimate load and produces a clamping force, $A_v f_y$. Shear friction is calculated using Equation 6 (ACI 318-08). Dividing the shear friction equation by the area of concrete gets the shear stress. Shear stress allows for flexibility in the data interpolation (Kahn and Mitchell, 2002). Shear stress is calculated using Equation 7.

$$V_n = \mu A_v f_y \qquad \text{(Equation 6)}$$

V_n = Nominal shear strength

μ = Coefficient of friction: 1.4λ for concrete placed monolithically; 0.6λ for concrete placed against hardened concrete not intentionally roughened; $\lambda = 1.0$ for normal-weight concrete

A_v = Area of shear reinforcement across shear plane

f_y = Yield stress of reinforcement ($\leq$ 60 ksi)

$$v_n = \mu \rho_v f_y \qquad \text{(Equation 7)}$$

v_n = Nominal shear stress, V_n / A_c ($\leq$ 800 psi)

A_c = Area of concrete interface

ρ_v = Shear friction reinforcement ratio, A_v / A_c

Shear stress shall not be greater than the following limits:

1. $0.2 f'_c$
2. $480 + 0.08 f'_c$
3. 1600

f'_c = Compressive strength of concrete at time of testing; when two concrete layers are cast together, f'$_c$ is the smaller of the two

AASHTO code equations were not used for shear friction. The American Concrete Institute (ACI) code included newer limits for the shear friction equations.

Push-off tests have been the primary test specimen used to evaluate shear friction. The main advantage of using push-off tests over composite beam tests is the ability to clearly control the forces as well as the failure mechanism. This is because the shear plane can be tested not only in pure shear, but can be combined with external normal forces or a moment. Shear capacity can be evaluated by changing the surface condition. A monolithic specimen can be tested in either an uncracked or pre-cracked state. The pre-cracked state represents the worst-case scenario situation where a crack would exist as purposed by Mast (1968). A composite cold-joint can be used to simulate the interface between two different layers of cast-in-place concrete.

7.2 PUSH-OFF SPECIMEN DESIGN

The push-off specimens were chosen as the best representation of the behavior of a shear interface between two different layers of concrete, which would occur in the deck of a PTHS bridge as outlined in this project. The specimens were designed identically to the specimens from previous research (Kahn and Mitchell, 2002), except for the gap spacing. They were tested with three different joint conditions at the shear plane: pre-cracked, uncracked, and cold-joint. The

uncracked monolithic specimens would provide an upper bound of shear capacity, while the pre-cracked monolithic specimens would provide a lower bound of shear capacity. The cold-joint composite specimens were used because they best represented the interface of the composite concrete bridge deck. The cold-joint surface condition would be left as-cast and unaltered, which would result in a roughness amplitude of ¼ inch.

Design of the push-off specimens is shown in Figures 33 and 34. The shear plane was a rectangle with dimensions 5 inches wide by 12 inches long. This created a shear plane, A_c, of 60 in^2. Stirrup reinforcement crossing the shear plane was varied between a single #3 stirrup to four #3 stirrups. This allowed the reinforcement ratio to vary from 0.37% to 1.47%. The shear stirrups were equally distributed across the shear plane.

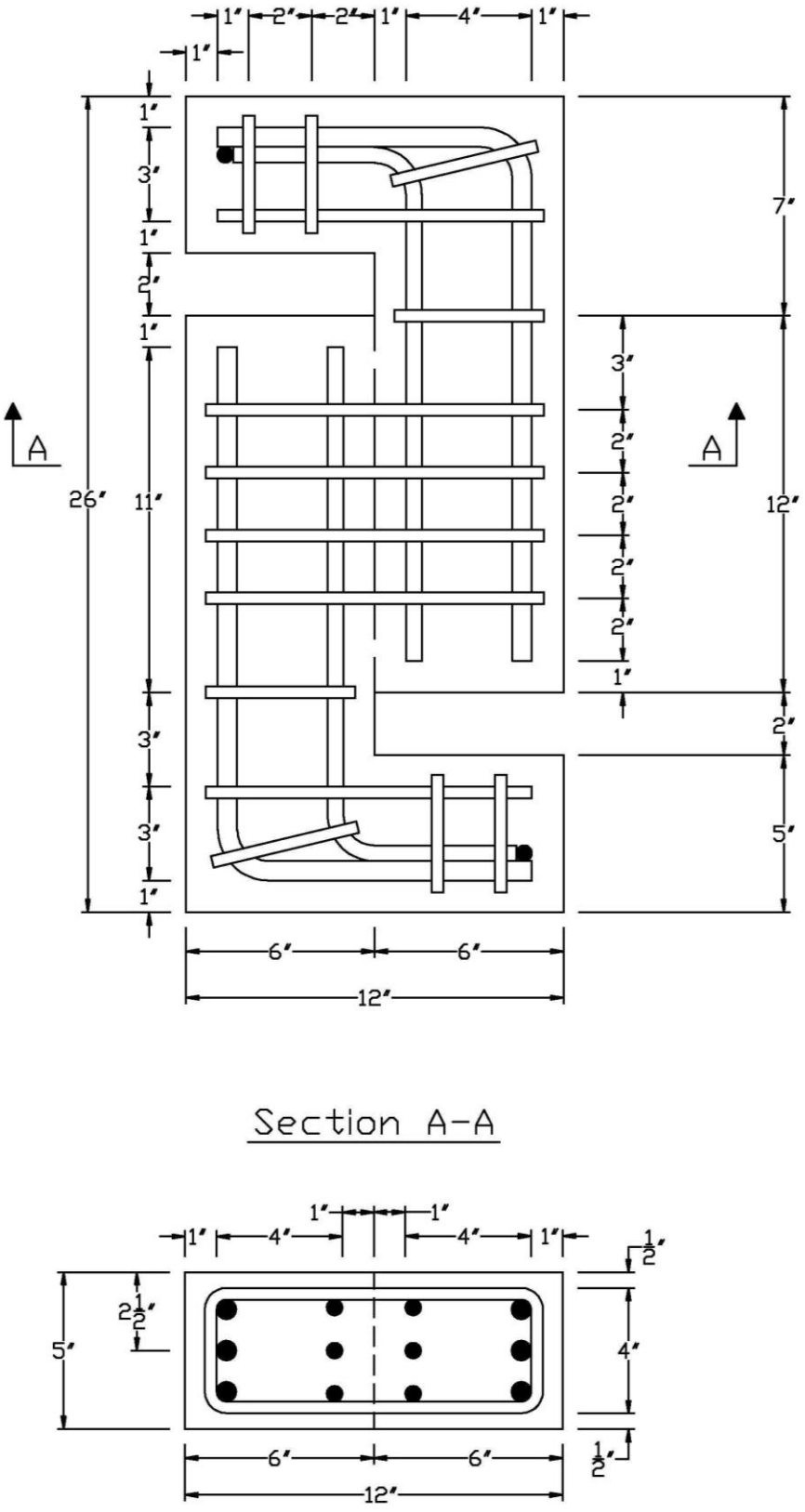

Figure 33. Design of push-off specimen spacing.

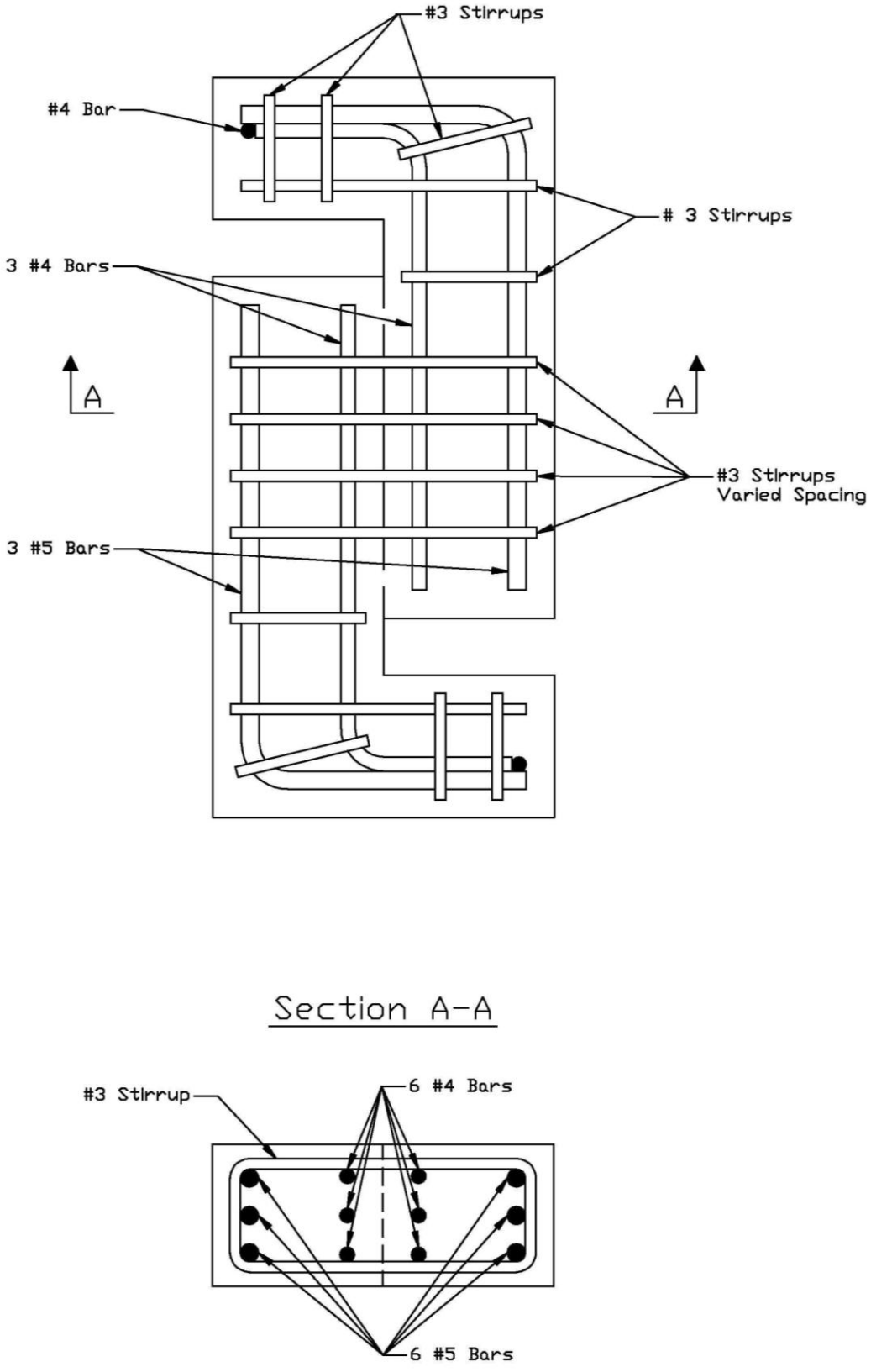

Figure 34. Design of push-off specimen rebar.

Pre-cracked and uncracked monolithic specimens used both epoxy- and non-epoxy-coated stirrups. This would allow for data to be compared for specimens with similar reinforcement ratios but different stirrup coatings. The cold-joint composite specimens would use only epoxy-coated stirrups and have three different shear-face conditions. A total of seven different sets of push-off specimens, with 12 specimens per set, were tested. Overall design data of the 84 push-off specimens is illustrated in Tables 15 and 16. The table shows the area of the reinforcement crossing the shear plane and the joint condition of each specimen.

The letter “B” indicates the specimen used a non-epoxy-coated (black) stirrup, while the letter “E” indicates the specimen used an epoxy-coated stirrup. The letter “P” indicates the specimen had a pre-cracked shear plane, while the letter “U” indicates the specimen had an uncracked shear plane. The letters “OH” indicate the specimen had a one-hour cold-joint between castings. The letters “CJC” indicate the specimen had a seven-day cold-joint with a clean shear-face surface condition, while the letters “CJO” indicate the specimens had a seven-day cold-joint with an oiled shear-face surface condition. Numbers “1” through “4” represent the number of stirrups crossing the shear plane. Finally, letters “A” through “C” indicate specimens constructed with identical characteristics.

Table 15. Shear friction design data of monolithic specimens.

	Area of Shear Stirrups, A_v (in^2)	Joint Condition
BP-1A	0.22	Pre-cracked
BP-1B	0.22	Pre-cracked
BP-1C	0.22	Pre-cracked
BP-2A	0.44	Pre-cracked
BP-2B	0.44	Pre-cracked
BP-2C	0.44	Pre-cracked
BP-3A	0.66	Pre-cracked
BP-3B	0.66	Pre-cracked
BP-3C	0.66	Pre-cracked
BP-4A	0.88	Pre-cracked
BP-4B	0.88	Pre-cracked
BP-4C	0.88	Pre-cracked
EP-1A	0.22	Pre-cracked
EP-1B	0.22	Pre-cracked
EP-1C	0.22	Pre-cracked
EP-2A	0.44	Pre-cracked
EP-2B	0.44	Pre-cracked
EP-2C	0.44	Pre-cracked
EP-3A	0.66	Pre-cracked
EP-3B	0.66	Pre-cracked
EP-3C	0.66	Pre-cracked
EP-4A	0.88	Pre-cracked
EP-4B	0.88	Pre-cracked
EP-4C	0.88	Pre-cracked

	Area of Shear Stirrups, A_v (in^2)	Joint Condition
BU-1A	0.22	Uncracked
BU-1B	0.22	Uncracked
BU-1C	0.22	Uncracked
BU-2A	0.44	Uncracked
BU-2B	0.44	Uncracked
BU-2C	0.44	Uncracked
BU-3A	0.66	Uncracked
BU-3B	0.66	Uncracked
BU-3C	0.66	Uncracked
BU-4A	0.88	Uncracked
BU-4B	0.88	Uncracked
BU-4C	0.88	Uncracked
EU-1A	0.22	Uncracked
EU-1B	0.22	Uncracked
EU-1C	0.22	Uncracked
EU-2A	0.44	Uncracked
EU-2B	0.44	Uncracked
EU-2C	0.44	Uncracked
EU-3A	0.66	Uncracked
EU-3B	0.66	Uncracked
EU-3C	0.66	Uncracked
EU-4A	0.88	Uncracked
EU-4B	0.88	Uncracked
EU-4C	0.88	Uncracked

Table 16. Shear friction design data of composite specimens.

	Area of Shear Stirrups, A_v (in^2)	Joint Condition
OH-1A	0.22	One-Hour Cold-Joint
OH-1B	0.22	One-Hour Cold-Joint
OH-1C	0.22	One-Hour Cold-Joint
OH-2A	0.44	One-Hour Cold-Joint
OH-2B	0.44	One-Hour Cold-Joint
OH-2C	0.44	One-Hour Cold-Joint
OH-3A	0.66	One-Hour Cold-Joint
OH-3B	0.66	One-Hour Cold-Joint
OH-3C	0.66	One-Hour Cold-Joint
OH-4A	0.88	One-Hour Cold-Joint
OH-4B	0.88	One-Hour Cold-Joint
OH-4C	0.88	One-Hour Cold-Joint
CJC-1A	0.22	7-Day Cold-Joint (Clean)
CJC-1B	0.22	7-Day Cold-Joint (Clean)
CJC-1C	0.22	7-Day Cold-Joint (Clean)
CJC-2A	0.44	7-Day Cold-Joint (Clean)
CJC-2B	0.44	7-Day Cold-Joint (Clean)
CJC-2C	0.44	7-Day Cold-Joint (Clean)
CJC-3A	0.66	7-Day Cold-Joint (Clean)
CJC-3B	0.66	7-Day Cold-Joint (Clean)
CJC-3C	0.66	7-Day Cold-Joint (Clean)
CJC-4A	0.88	7-Day Cold-Joint (Clean)
CJC-4B	0.88	7-Day Cold-Joint (Clean)
CJC-4C	0.88	7-Day Cold-Joint (Clean)
CJO-1A	0.22	7-Day Cold-Joint (Oiled)
CJO-1B	0.22	7-Day Cold-Joint (Oiled)
CJO-1C	0.22	7-Day Cold-Joint (Oiled)
CJO-2A	0.44	7-Day Cold-Joint (Oiled)
CJO-2B	0.44	7-Day Cold-Joint (Oiled)
CJO-2C	0.44	7-Day Cold-Joint (Oiled)
CJO-3A	0.66	7-Day Cold-Joint (Oiled)
CJO-3B	0.66	7-Day Cold-Joint (Oiled)
CJO-3C	0.66	7-Day Cold-Joint (Oiled)
CJO-4A	0.88	7-Day Cold-Joint (Oiled)
CJO-4B	0.88	7-Day Cold-Joint (Oiled)
CJO-4C	0.88	7-Day Cold-Joint (Oiled)

7.3 MATERIALS

This section describes materials used in the shear friction push-off specimens. It includes steel reinforcement and concrete mix designs.

7.3.1 Steel Reinforcement

Steel reinforcement used in the push-off specimens was ordered as Grade 60. All steel was requested to be of the same heat batch, but two different batches were delivered. The non-epoxy-coated reinforcement and stirrups were made from one heat batch, and the epoxy-coated stirrups were made from another. A tensile test was performed to determine the average yield stress of the epoxy- and non-epoxy-coated stirrups.

Three stirrups from each type were randomly chosen. Each stirrup was cut into two straight tensile specimens and mounted with a strain gage. Load and strain were recorded from each test, and stress-strain curves were made from the recorded data. An example of a stress-strain curve can be seen in Figure 35. All stress-strain curves can be found in Appendix B. Average yield stress was determined by using the 0.2% offset method outlined by ASTM 370. Average yield stress for the non-epoxy-coated stirrups was 80.1 ksi. Average yield stress for the epoxy-coated stirrups was 65.3 ksi. Both yield stresses were higher than the maximum allowed limit of 60 ksi.

Thickness of the epoxy coating was also determined. Three, random epoxy-coated stirrups were chosen and tested using a non-destructive handheld device. Several measurements were taken on each stirrup and averaged. Average overall epoxy thickness was 8.79 mils.

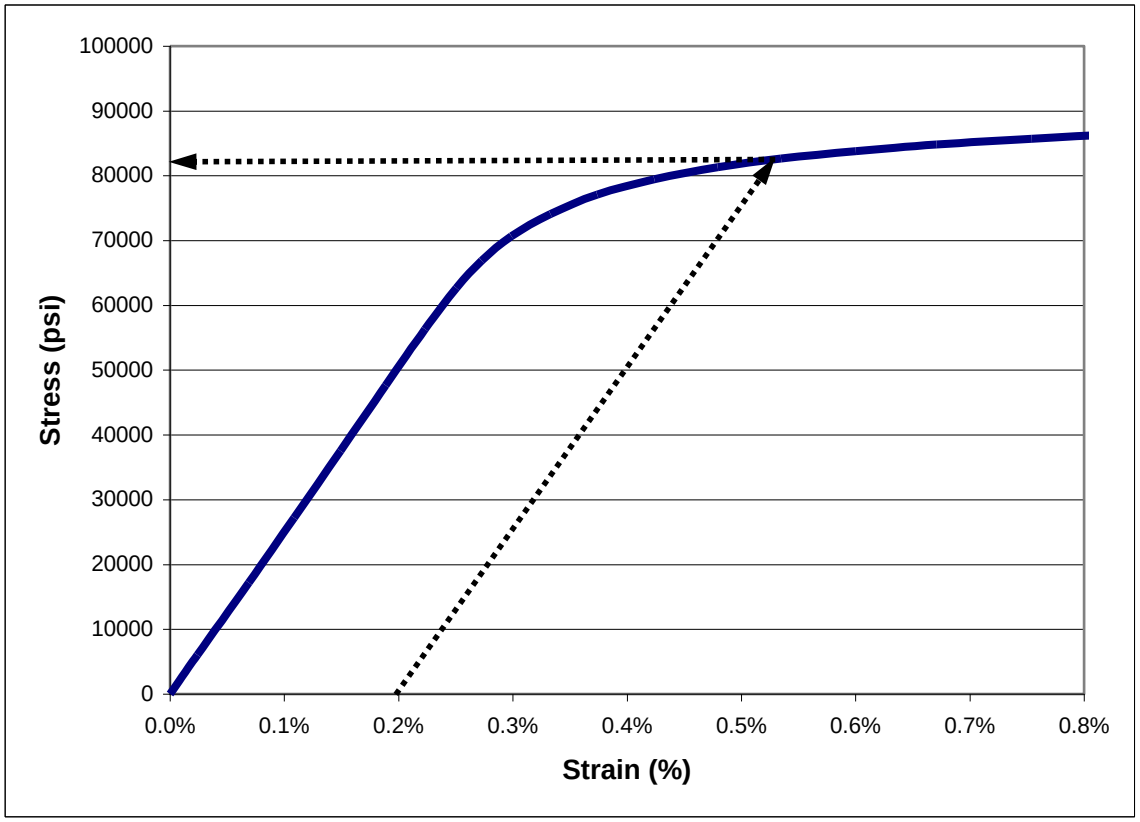

Figure 35. Stress-strain curve (B-1A).

7.3.2 Concrete

Since most of the previous shear friction research had not been conducted with SCC, a true SCC mix with a target spread of 24 inches was used for the push-off specimens. Another reason for use of the true SCC mix was as a worst-case scenario in which the concrete had been overdosed with superplasticizer and placed in the bridge superstructure. Uncracked and pre-cracked monolithic specimens were fully cast with the SCC mix. For the cold-joint composite specimens, the bottom half of the specimens used the SCC mix, and the top half used the conventional concrete mix. Both concrete mix designs were the same, as discussed earlier in Chapter 5.

7.4 FABRICATION AND CASTING

Reinforcing cages of the push-off specimens were assembled according to the designs. The cage was assembled and rigidly held together using wire ties. Jigs were made to ensure proper bar spacing and assist in the fabrication. Figure 36 shows a completed steel cage.

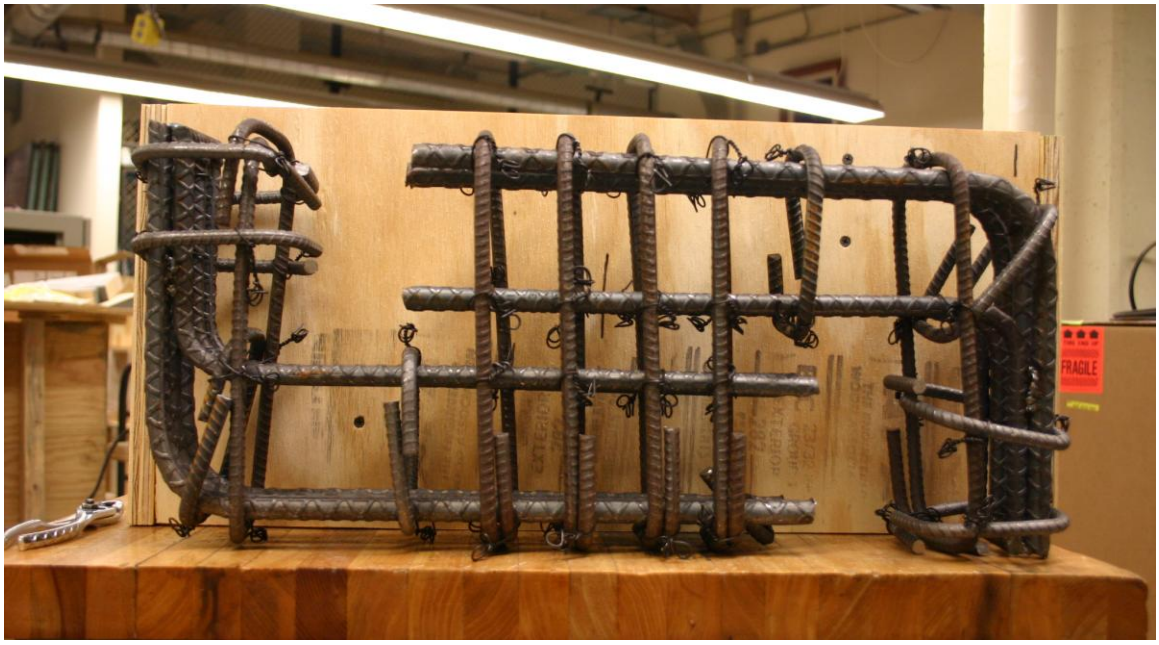

Figure 36. Completed rebar cage.

Two types of wood forms were designed and built to be reused throughout the entire casting process. The first set was used for casting pre-cracked and uncracked specimens monolithically on their sides, and can be seen in Figure 37. The second set was used for casting cold-joint specimens in an upright position, and can be seen in Figure 38. The forms were coated with a form-release agent before casting, with care taken not to get any on the reinforcing cages. The cages were set on rebar chairs to maintain proper clear cover and placement inside the forms. Wood inserts covered with Styrofoam were placed in the forms to define the shear plane. They were attached to the forms to prevent movement during the casting process. Silicone sealant was used to fill any cracks or voids in the forms.

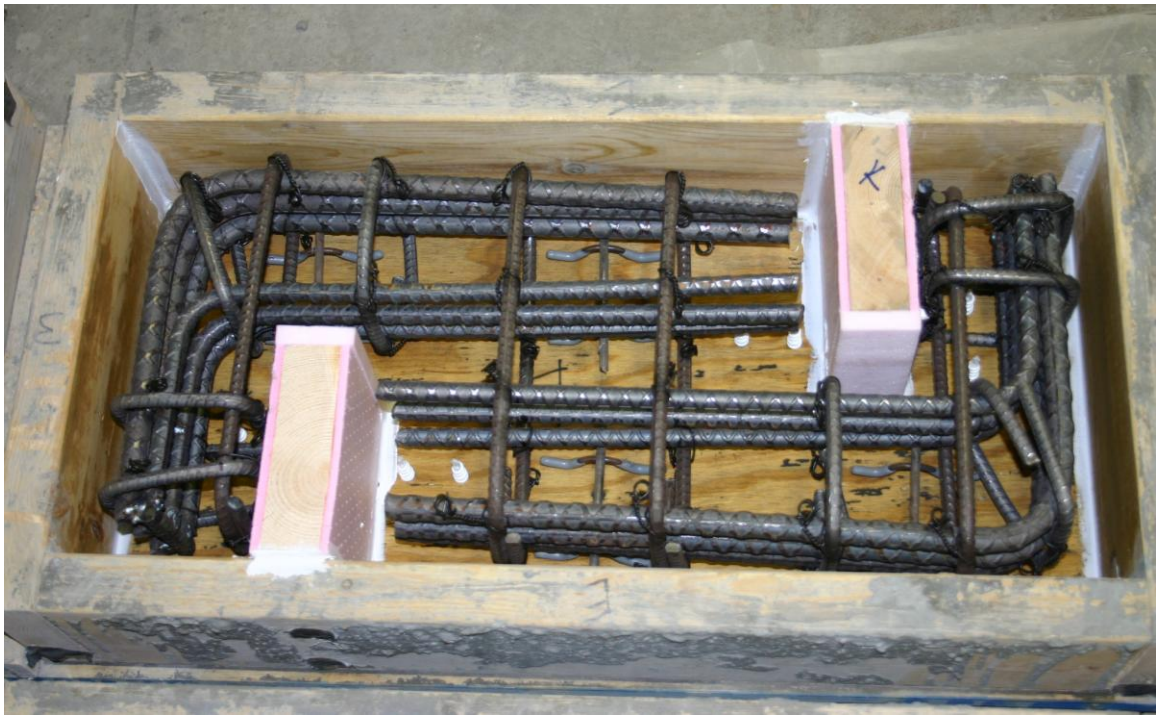

Figure 37. Monolithic specimen prior to casting.

Figure 38. Cold-joint specimen prior to casting.

Concrete was mixed in the drum-mixer trailer and when the proper spread/slump was achieved, it was discharged into wheelbarrows and placed into the forms by hand. The monolithic specimens were cast using SCC and were lightly rodded to ensure proper concrete consolidation.

A wood float was then used to finish the specimens. Several concrete cylinders were made to test the compressive strength.

After the specimens reached initial set, wet burlap and polyethylene plastic were placed over the tops of the forms. The next day, the forms and wood inserts were removed. The specimens were then placed in the moist room along with their cylinders.

The cold-joint specimens were cast differently using the vertical forms. The OH specimens were first cast with only SCC on the bottom half. Then the conventional concrete was mixed and poured for the top half of the specimens. The time between concrete placements took approximately one hour. This time frame was established during the casting of the core blocks in Chapter 6. The specimens were then finished in the same manner as the monolithic specimens. Concrete cylinders were made for both mixes as well.

For the other cold-joint specimens (CJC and CJO), half of the rebar cage with stirrups was tied and placed into the vertical forms. The bottom half of the specimens were cast using SCC. The shear surface was left as-cast and not floated. Wet burlap and polyethylene plastic were placed over the forms and the burlap was kept wet during the next seven days. Figure 39 shows a specimen after the bottom half has been poured.

Figure 39. Bottom half of cold-joint specimen.

After seven days, the shear surface of the specimens was cleaned to remove any foreign materials and impurities such as laitance. For the CJC specimens, a thin layer of form-release agent was applied to the shear surface to act as a bond breaker. Care was taken to avoid getting the form-release agent on the rebar cage or stirrups. The top half of the cage was then slid into the form and tied into place. Conventional concrete mix was poured for the upper half of the specimens and vibrated to ensure consolidation. After casting, the specimens were floated and finished just like the monolithic specimens.

The concrete casting did not always go to plan. One of the persistent problems was not hitting the target spread/slump. In the end, it was discovered to be easier to slightly overdose the concrete with superplasticizer and overshoot the target spread/slump. The concrete was allowed to mix until the target spread/slump was achieved. It was only then that the concrete was discharged and placed into the forms. Another problem was minor honeycombing on the surface of the cold-joint specimens where conventional concrete was used.

7.5 SPECIMEN TESTING

According to KDOT specification 716, the deck of a PTHS bridge is tensioned between three and seven days of the slab pour. However, the push-off specimens were tested at 28-day compressive strength. The reason being the bridge deck would not experience normal loading caused by traffic until at least 28 days.

Monolithic and OH cold-joint specimens were tested at 28 days. The CJC and CJO cold-joint specimens were tested at 35 days from first pour. This was done to allow the second casting to reach the 28-day compressive strength.

To pre-crack the specimens, the procedure was followed as outlined by Hofbeck et al. (1969). Two knife-edge apparatus' were constructed for this procedure. The specimens were placed on their sides in between the knife-edge apparatus' in a hydraulic testing machine. A load was applied to the specimens until a visible crack had appeared along the entire shear plane. A load popping noise could be heard as the specimens with a lower reinforcement ratio cracked. Wooden blocks were used to stabilize each specimen until a sufficient load was applied. Figure 40 shows the pre-cracking procedure.

Figure 40. Pre-cracking procedure.

Instrumentation and setup of the specimens was identical. Two, linear variable differential transformers (LVDTs) were used to measure the slip across the shear interface on the specimen. Two LVDTs were used in case one recorded incorrectly. The LVDTs were mounted to inserts attached to the forms during the casting process. Each LVDT was mounted across the gap at either the top or bottom of each specimen. A third LVDT was mounted to the load table. The LVDTs were attached to a Keithley Data Acquisition (DAQ) Device. The LVDTs were all 10-volt Schaevitz DC-EC-2000 LVDTs.

The specimens were placed vertically in the same testing machine used in the pre-cracking procedure. A pin connection was used at both ends of the specimen to eliminate outside moments and ensure a pure shear failure. A pin-plate was attached to the bottom and a steel plate was attached to the top of each specimen, using hydrocal cement. The reason for using the steel plate at the top, instead of another pin-plate, was because the testing machine had a swiveled loading head which acted like a pin connection. Wood blocks were used to stabilize the specimen until a sufficient load was applied. Figure 41 shows a push-off specimen instrumented and ready for loading.

Figure 41. Specimen prior to loading.

A load was applied to the specimens at a rate of 5 to 10 kips/min. Specimens with a lower reinforcement ratio were loaded at the lower rate, and specimens with a higher reinforcement ratio were loaded at the higher rate. The slip from the LVDTs and load from the testing machine's load cell were measured and recorded every second by the DAQ. The testing machine had an independent load readout which was used to verify the load cell data being recorded by the DAQ. Testing was stopped after the specimens had reached plastic yielding at the joint. This occurred after roughly 0.3 inches of slip at the shear plane.

CHAPTER 8. SHEAR FRICTION RESULTS

This chapter gives results from the shear friction tests performed in Chapter 7. Load-slip curves were graphed and shear stresses were calculated and compared to the ACI code.

8.1 CONCRETE PROPERTIES

Fresh concrete properties of the mixes used for the shear friction specimens are given in Table 17. Cold-joint composite specimens using the designation "a" means the SCC mix was used, while the designation "b" means the conventional concrete mix was used. The J-ring test found the SCC mixes to pass with minimal blocking.

Table 17. Fresh concrete properties of shear friction mixes.

	Slump (in)	Spread (in)	Unit Weight (pcf)	Volumetric Air Content (%)	VSI
BP	---	24	140.1	5.00	1
EP	---	23.5	141.3	4.50	1
BU	---	24	134.0	8.25	1
EU	---	23	144.0	2.00	2
OH (a)	---	24.5	140.9	4.50	0
OH (b)	3.5	---	137.8	6.00	---
CJC (a)	---	24	137.4	6.00	0
CJC (b)	3	---	139.1	5.50	---
CJO (a)	---	24	136.6	6.50	1
CJO (b)	3.5	---	133.0	8.50	---

Results of Table 17 are acceptable except for the mix used for the epoxy uncracked specimens. That specific concrete batch started to segregate and air bubbles were forced from the mix because the air entrainer and superplasticizer were added at the same time. That is the reason for the low air content and high VSI reading. The air entrainer was normally added first to the mix, and then the superplasticizer was added, as the concrete seemed to accept and mix the admixtures better that way.

Cylinders for the shear friction specimens were tested according to the compressive strength test. Three cylinders were tested for each concrete batch and their strengths were averaged. All monolithic specimen cylinders were tested at 28 days. Cold-joint composite specimen cylinders with the designation "a" were tested at 35 days, while cylinders with the designation "b" were tested at 28 days. Average compressive strength of the shear friction specimens are given in Table 18.

Table 18. Average compressive strength of shear friction specimens.

	Compressive Strength (psi)
BP	6560
EP	6660
BU	6380
EU	6730
OH (a)	6450
OH (b)	6000
CJC (a)	6660
CJC (b)	6030
CJO (a)	6580
CJO (b)	6090

Values of Table 18 can be compared to those from Table 6. Compressive strengths of the conventional mixes are similar to the values from Table 6. Compressive strengths of the SCC mixes are also comparable to those of the hybrid mixes from Table 6.

8.2 OBSERVED FAILURE

The crack on the pre-cracked specimens began to slowly widen until the specimen reached maximum shear load. Uncracked specimens began to show a crack along the shear plane and then a popping noise could be heard as the specimen surpassed maximum shear load. Cold-joint specimens behaved similarly to the uncracked specimens. Concrete spalling occurred on all specimens as they underwent plastic yielding. Specimens with higher reinforcement ratios had more severe concrete spalling than specimens with lower reinforcement ratios. Several smaller diagonal cracks propagated from the shear plane at angles up to 45 degrees. Figure 42 shows a

specimen after the testing procedure was complete. Steel reinforcement is visible at points where the concrete spalled.

Figure 42. Specimen after testing.

8.3 LOAD-SLIP CURVES

Load and slip recorded by the DAQ was graphed in load-slip curves. Slip measured by the two LVDTs mounted to the specimens was averaged. Slip measured by the LVDT mounted to the loading table was included in the graphs as a backup for maximum shear load and determination

of plastic yielding. Figure 43 shows an example of a typical load-slip curve. All load-slip curves can be found in Appendix C. The difference in the curves of the average LVDT and table LVDT is due to slack in the load table. After the specimens reached plastic yielding the slack in the load table disappeared and the curves overlapped.

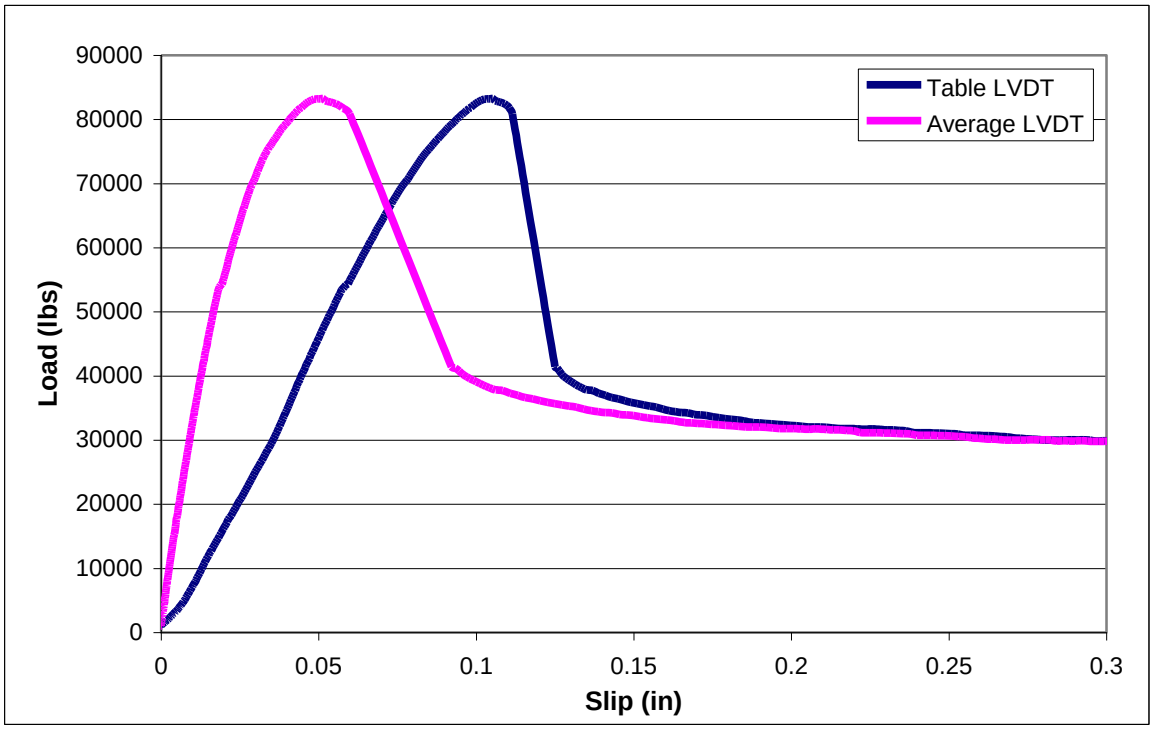

Figure 43. Typical load-slip curve (BU-2A).

Load slip curves for the pre-cracked and uncracked monolithic specimens follow the same trend pattern. The load is slowly increased until a peak or maximum shear is obtained and then the curve drops to a constant residual load. Specimens with higher reinforcement ratios had a smoother peak than specimens with lower reinforcement ratios. Maximum shear and residual load increased as the reinforcement ratio increased. Specimens with non-epoxy-coated stirrups showed higher shear loads when compared to their respective specimens using epoxy-coated stirrups. All monolithic specimens reached maximum shear before 0.06 inches of slip occurred.

Curves for the OH cold-joint specimens behaved similarly to the monolithic specimens. Curves for the CJC specimens were somewhat similar to the monolithic specimens, except each time the maximum shear was obtained, the curve reached a sharp peak. Even as the reinforcement ratio

increased, the curves still maintained the sharp peak and did not soften. Drop-off from maximum shear to the residual load was less dramatic as compared to the monolithic specimens.

Several CJC curves showed minor fluctuations on the pre-failure load slope. The load would slightly drop and then increase again. This could be the result of minor slipping occurring due to the cold-joint surface condition. Both OH and CJC cold-joint composite specimens reached maximum shear before 0.05 inches of slip occurred. The cold-joint composite specimens reached maximum shear faster than the monolithic specimens.

A majority of the CJO specimens behaved completely different than their CJC cold-joint counterparts. The curves increased until a distinct yield point was reached. At that point, the loading did not drop and a yield plateau occurred during the residual load. This is most likely due to use of the bond-breaker along the shear plane. A few of the CJO specimens did show a small but sharp peak at maximum shear. All CJO cold-joint composite specimens reached maximum shear before 0.05 inches of slip occurred.

8.4 SPECIMEN RESULTS

Maximum shear loads were determined using the load-slip graphs. They were compared as a redundancy check to values from the independent load readout attached to the testing machine. Maximum shear loads were divided by the area of concrete to get the maximum shear stresses. The clamping force provided by the shear reinforcement was divided by the area of concrete to get the clamping stress. The clamping force and clamping stress used the maximum yield stress allowed for the reinforcement which was 60 ksi. Results for the pre-cracked and uncracked monolithic specimens are given in Tables 19 and 20, respectively. Results for the cold-joint composite specimens are given in Table 21. Average shear stress for the shear friction specimens is provided in Table 22.

Table 19. Pre-cracked monolithic specimen results.

	Maximum Shear Load V_u (kips)	Maximum Shear Stress v_u (psi)	Clamping Force $A_v f_y$ (kips)	Clamping Stress $\rho_v f_y$ (psi)
BP-1A	39.2	654	13.2	220
BP-1B	40.8	681	13.2	220
BP-1C	45.1	752	13.2	220
BP-2A	66.3	1105	26.4	440
BP-2B	68.8	1146	26.4	440
BP-2C	47.4	790	26.4	440
BP-3A	83.0	1384	39.6	660
BP-3B	80.1	1335	39.6	660
BP-3C	88.3	1472	39.6	660
BP-4A	95.4	1589	52.8	880
BP-4B	93.9	1565	52.8	880
BP-4C	94.9	1582	52.8	880
EP-1A	29.9	499	13.2	220
EP-1B	44.5	742	13.2	220
EP-1C	28.6	476	13.2	220
EP-2A	52.5	876	26.4	440
EP-2B	55.5	926	26.4	440
EP-2C	55.3	922	26.4	440
EP-3A	69.3	1154	39.6	660
EP-3B	66.9	1115	39.6	660
EP-3C	71.4	1190	39.6	660
EP-4A	83.5	1391	52.8	880
EP-4B	78.4	1307	52.8	880
EP-4C	76.4	1274	52.8	880

Table 20. Uncracked monolithic specimen results.

	Maximum Shear Load V_u (kips)	Maximum Shear Stress v_u (psi)	Clamping Force $A_v f_y$ (kips)	Clamping Stress $\rho_v f_y$ (psi)
BU-1A	62.7	1046	13.2	220
BU-1B	56.9	949	13.2	220
BU-1C	63.3	1055	13.2	220
BU-2A	83.3	1388	26.4	440
BU-2B	76.4	1273	26.4	440
BU-2C	81.0	1351	26.4	440
BU-3A	86.7	1445	39.6	660
BU-3B	91.5	1524	39.6	660
BU-3C	89.1	1486	39.6	660
BU-4A	109.6	1827	52.8	880
BU-4B	108.4	1807	52.8	880
BU-4C	98.3	1639	52.8	880
EU-1A	68.1	1134	13.2	220
EU-1B	65.4	1090	13.2	220
EU-1C	72.6	1210	13.2	220
EU-2A	76.8	1280	26.4	440
EU-2B	86.8	1447	26.4	440
EU-2C	83.5	1392	26.4	440
EU-3A	86.3	1438	39.6	660
EU-3B	89.1	1484	39.6	660
EU-3C	89.6	1493	39.6	660
EU-4A	95.4	1591	52.8	880
EU-4B	93.0	1550	52.8	880
EU-4C	92.9	1548	52.8	880

Table 21. Cold-joint composite specimen results.

	Maximum Shear Load V_u (kips)	Maximum Shear Stress v_u (psi)	Clamping Force $A_v f_y$ (kips)	Clamping Stress $\rho_v f_y$ (psi)
OH-1A	63.8	1064	13.2	220
OH-1B	62.8	1047	13.2	220
OH-1C	60.2	1004	13.2	220
OH-2A	74.6	1243	26.4	440
OH-2B	75.1	1252	26.4	440
OH-2C	73.8	1231	26.4	440
OH-3A	86.5	1442	39.6	660
OH-3B	87.1	1452	39.6	660
OH-3C	91.5	1525	39.6	660
OH-4A	95.3	1588	52.8	880
OH-4B	99.5	1658	52.8	880
OH-4C	98.8	1647	52.8	880
CJC-1A	36.4	607	13.2	220
CJC-1B	35.6	594	13.2	220
CJC-1C	36.5	608	13.2	220
CJC-2A	42.6	710	26.4	440
CJC-2B	45.3	754	26.4	440
CJC-2C	43.6	726	26.4	440
CJC-3A	48.1	801	39.6	660
CJC-3B	48.3	805	39.6	660
CJC-3C	47.5	791	39.6	660
CJC-4A	54.4	906	52.8	880
CJC-4B	58.0	967	52.8	880
CJC-4C	60.1	1001	52.8	880
CJO-1A	9.3	154	13.2	220
CJO-1B	12.7	211	13.2	220
CJO-1C	16.9	282	13.2	220
CJO-2A	22.4	374	26.4	440
CJO-2B	21.2	354	26.4	440
CJO-2C	19.8	330	26.4	440
CJO-3A	23.6	393	39.6	660
CJO-3B	27.1	451	39.6	660
CJO-3C	27.1	452	39.6	660
CJO-4A	28.8	479	52.8	880
CJO-4B	36.3	605	52.8	880
CJO-4C	33.1	551	52.8	880

Table 22. Average shear stress of shear friction specimens.

	Average Shear Stress (psi)			
	A_v = 0.22 in^2	A_v = 0.44 in^2	A_v = 0.66 in^2	A_v = 0.88 in^2
BP	695	1013	1397	1579
EP	572	908	1153	1324
BU	1016	1337	1485	1758
EU	1145	1373	1472	1563
OH	1038	1242	1473	1631
CJC	603	730	799	958
CJO	216	352	432	545

Ultimate shear stress vs. clamping stress of the monolithic specimens is illustrated in Figure 44. Figure 44 shows shear stresses for uncracked specimens were higher than shear stresses of their comparable pre-cracked counterparts. The uncracked non-epoxy specimens initially had slightly lower shear stresses than those of the uncracked epoxy specimens. When the reinforcement ratio increased, the uncracked non-epoxy specimens resulted in higher shear stresses than those of the uncracked epoxy specimens. This was to be expected as epoxy coating reduces bond strength. The non-epoxy pre-cracked specimens were all higher than their counterpart epoxy pre-cracked specimens.

All shear stresses for similar specimens were grouped together except for two outliers. The first outlier was specimen BP-2C, which had a lower shear stress than the other two specimens of the same type. The reason for this could be the pre-cracking procedure was taken too far, which resulted in a much larger crack. The second outlier was specimen EP-1B, which had a higher shear stress than the other two specimens of the same type. The reason for this could be the pre-cracking procedure was not fully completed, which resulted in a partial crack forming through the shear plane instead of a full crack.

Equation 7 is graphed in Figure 44 along with the shear stresses. A coefficient of friction of 1.4 was used as all specimens were monolithically cast. All monolithic specimens exceeded the minimum limit of Equation 7. This means if the hybrid concrete mix was overdosed with superplasticizer and a full SCC mix was poured into the bridge deck, the limits set forth by the ACI code equation for shear friction would be passed.

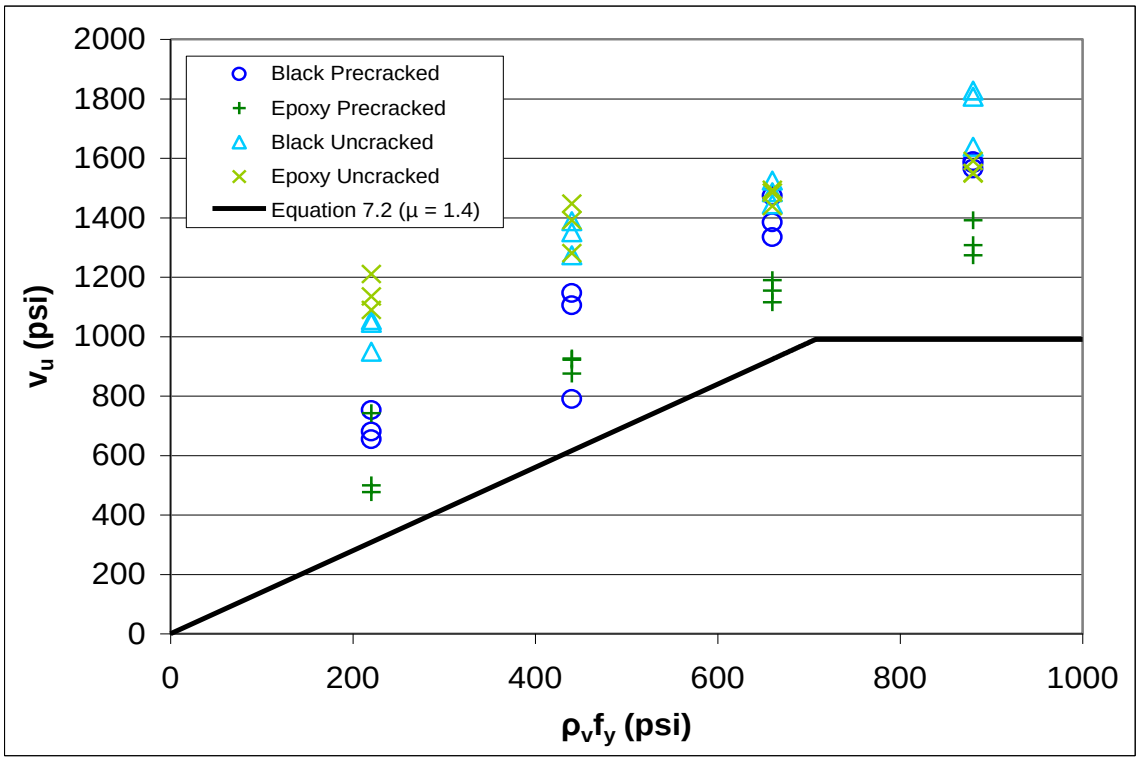

Figure 44. Ultimate shear stress versus clamping stress for monolithic specimens.

Ultimate shear stress vs. clamping stress of the cold-joint composite specimens is illustrated in Figure 45. Figure 45 shows the shear stresses for specimens with a one-hour cold-joint were higher than the specimens with a seven-day cold-joint. All shear stresses for similar specimens were grouped together with no outliers.

The one-hour cold-joint specimens were thought to be similar in nature to the uncracked monolithic specimens, as the two concrete layers seemed to bond together monolithically without a crack. Shear stresses of the one-hour cold joints in Figure 45 were higher than both the shear stresses of the monolithic pre-cracked epoxy and non-epoxy specimens of Figure 44, but lower than the shear stresses of the monolithic uncracked epoxy and non-epoxy specimens in Figure 44. The uncracked monolithic specimens provided an upper range for the shear capacity while the pre-cracked monolithic specimens provided a lower range for the shear capacity.
The seven-day cold-joint specimens with a clean shear interface had higher shear stresses than the seven-day cold-joint specimens with an oiled shear interface. This was expected, as the oil on the shear interface acted as a bond breaker between the two concrete layers.

Equation 7 is graphed in Figure 45 along with the shear stresses. A coefficient of friction of 1.4 was used for the one-hour cold-joint specimens and a coefficient of friction of 0.6 was used for the seven-day cold-joint specimens. All one-hour cold-joint specimens surpassed the minimum limit of Equation 7.

The seven-day cold-joint specimens with a clean shear interface also exceeded the minimum limit of Equation 7. The 7-day cold-joint specimens with an oiled shear interface hovered above the minimum limit of Equation 7. Only two of the specimens fell below the limit. Even though specimens had a seven-day cold-joint between concrete castings and the shear interface was coated with a bond breaker, the resulting average ultimate shear stresses still passed the minimum limits for shear friction of the ACI code equation.

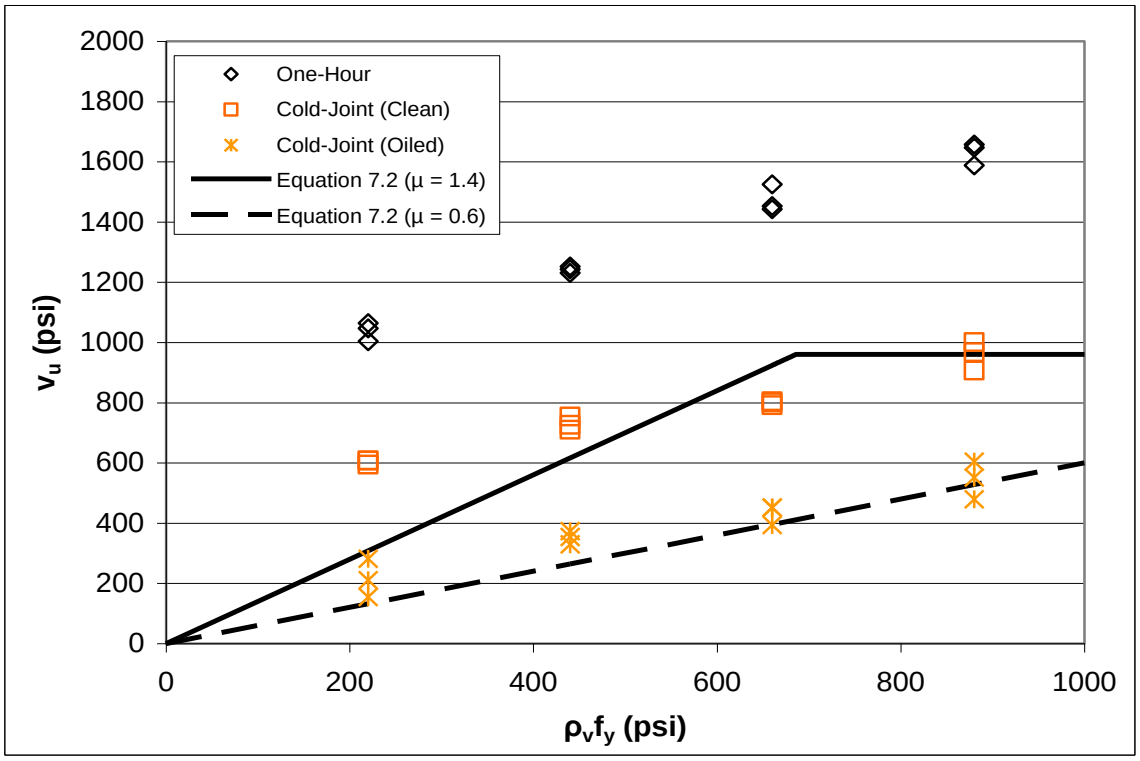

Figure 45. Ultimate shear stress versus clamping stress for cold-joint composite specimens.

CHAPTER 9. CONCLUSIONS, RECOMMENDATIONS, AND IMPLEMENTATIONS

9.1 SUMMARY AND CONCLUSIONS

The following conclusions can be made based on data obtained in this project:

1. A bridge deck using conventional and hybrid concrete mixes should be considered a monolithic piece. Therefore, hardened concrete properties should either be the same or very similar. Since the conventional and hybrid mixes in this study differed only in the amount of superplasticizer dosage, the hardened concrete properties of both mixes were found to be essentially the same. This satisfies some of the requirements of this project.
2. Conventional and hybrid concrete bridge deck mix designs containing a 0.35 water-to-cement ratio, 721 lb/yd^3 Type I/II cement, and a 50%-50% fine-to-coarse aggregate ratio both meet requirements of the project.
3. An air-entrainer dosage rate of 0.19 oz/100 lb of cement and a superplasticizer dosage rate of 4.43 oz/100 lb of cement for the conventional concrete bridge deck mix; an air-entrainer dosage rate of 0.18 oz/100 lb of cement and a superplasticizer dosage rate of 6.33 oz/100 lb of cement for the hybrid concrete bridge deck mix meet requirements of the project.
4. Fresh concrete properties show conventional and hybrid concrete mixes to have values that satisfy requirements of this project and KDOT. This includes slump, spread, air content, and workability.
5. Hardened concrete properties show conventional and hybrid concrete mixes have values that satisfy KDOT requirements. This includes compressive strength, tensile strength, modulus of elasticity, permeability, freeze/thaw resistance, and coefficient of thermal expansion.
6. Core testing showed bonding of the two concrete layers to be more successful with vibration between the two concrete layers. However, adequate bonding between both mixes was obtained even when no vibration between the layers occurred.

7. Monolithic shear friction tests revealed the worst-case scenario mix of using an SCC to pass shear friction limits of the ACI code equation. Cold-joint shear friction tests using the SCC and conventional concrete mix also passed shear friction limits of the ACI code equation. This included specimens with a one-hour cold-joint, a seven-day cold-joint with a clean shear interface, and a seven-day cold-joint with an oiled (bond breaker) shear interface.

9.2 RECOMMENDATIONS

The following are recommendations to KDOT:

1. The concept of using two different concrete mixes during a bridge deck pour has been found to be plausible and should greatly improve placements with congested reinforcement.
2. The authors recommend that the superplasticizer should be added to the concrete mixes after the air-entrainer has been added. It was found to be easier to slightly overdose the concrete mixes with superplasticizer and overshoot the target slump/spread than it was to precisely hit the target slump/spread each time a concrete batch was made.

9.3 IMPLEMENTATION

This report summarizes Phase 1 of the two-phase project. Based on the findings from this work, the authors recommend that KDOT should move forward with Phase 2, where a bridge deck is placed using both a hybrid and standard mixture. For Phase 2, the authors recommend additional instrumenting and testing of the field-placed concrete in order to evaluate the performance of both mixes.

REFERENCES

1. American Association of State Highway and Transportation Officials. *Standard Specifications,* American Association of State Highway and Transportation Officials, 2004.
2. American Concrete Institute. *ACI Manual of Concrete Practice, Part I and II,* American Concrete Institute, 2006.
3. ACI Committee 318. *Building Code Requirements for Structural Concrete,* 318-08, American Concrete Institute, 2008.
4. American Society for Testing and Materials. *Standard Specifications,* American Society for Testing and Materials, 2008.
5. Anderson, A. R. "Composite Designs in Precast and Cast-in-Place Concrete." *Progressive Architecture* 41.9, 1960: 172–179.
6. Basler, E., Witta, E. Discussion of "Connections in Precast Concrete Construction." *Journal of the American Concrete Institute*, 1966: 1027.
7. Beer, F. P., Johnston Jr., E. R., DeWolfe, J. T. *Mechanics of Materials 3rd Edition,* McGraw-Hill, 2001: 748.
8. Birkland, P. W., Birkland, H. W. "Connections in Precast Concrete Construction." *Journal of the American Concrete Institute* 63.3, 1966: 345–368.
9. Cowen, J., Cruden, A. F. "Second Thoughts on Shear Friction." *Concrete* 9.8, 1975: 31–32.
10. Hanson, N. W. "Precast-Prestressed Concrete Bridges: 2. Horizontal Shear Connections." *Journal of the Portland Cement Association Research and Development Laboratories* 2.2, 1960: 38–58.
11. Hofbeck, J. A., Ibrahim, I. O., Mattock, A. H. "Shear Transfer in Reinforced Concrete." *Journal of the American Concrete Institute* 66.2, 1969: 119–128.
12. Hoff, G. C. "High-Strength Lightweight Aggregate Concrete for Arctic Applications – Part 3." *American Concrete Institute Publication* SP 136-3, 1992: 175–245.
13. *Interim Guidelines for the Use of Self-Consolidating Concrete in Precast/Prestressed Concrete Institute Member Plants,* First Edition, 2003.

14. Kahn, L., Mitchell, A. “Shear Friction Tests with High-Strength Concrete.” *ACI Structural Journal* 99.1, 2002: 98–103.
15. Kahyat, K. H., Assaad, J., Daczko, J. “Comparison of Field-Oriented Test Methods to Assess Dynamic Stability of Self-Consolidating Concrete.” *ACI Materials Journal* 101.2, 2004: 168–176.
16. Kansas Department of Transportation. *Standard Specifications for State Road and Bridge Construction,* Kansas Department of Transportation, 2007.
17. Mast, R. F. “Auxiliary Reinforcement in Concrete Connections.” *Proceedings,* ASCE, 94.ST6, 1968: 1485–1504.
18. Mattock, A. H. Discussion of “Influence of Concrete Strength and Load History on the Shear Friction Capacity of Concrete Members.” *PCI Journal,* 1988: 165–166.
19. Mattock, A. H., Johal, L., Chow, H. C. “Shear Transfer in Reinforced Concrete with Moment or Tension Acting Across the Shear Plane.” *PCI Journal* 20.4, 1975: 76–93.
20. Mattock, A. H., Li, W. K., Wang, T. C. “Shear Transfer in Lightweight Reinforced Concrete.” *PCI Journal* 21.1, 1976: 20–39.
21. Ouchi, M. “Self-Compacting Concrete Development, Applications and Investigations.” *Proceedings of the Fourth International Conference on Materials Engineering for Resources*, 2001: 53–58.
22. Shaikh, A. F. “Proposed Revisions to Shear Friction Provisions.” *PCI Journal* 23.2, 1978: 12–21.
23. Walraven, J., Frenay, J., Pruijssers, A. “Influence of Concrete Strength and Load History on the Shear Friction Capacity of Concrete Members.” *PCI Journal* 32.1, 1987: 66–84.
24. Walraven, J., Stroband, J. “Shear Friction in High-Strength Concrete.” *American Concrete Institute Publication* SP 149–17, 1994: 311–330.

Appendix A. KDOT Data

DTMT252 Kansas Department Of Transportation PAGE - 1
Run Date: 06 07 07 PCC Design Mix
Run Time: 11:57 AM

PC Mix #: 1PWD040A E Matrl Code: PCC000059 Name: CONC (CF/GR35/AE/SA) W/C Max: 0.35
Spec Min CF: 602 Design CF: 721 % Air: 6.5 Design Slump: 2.95 Design: 0.35
Water Source: PRIVATE WELL Eff Date: 07 18 05 Term Date: 01 01 10

Material	Name	Prod #	Prod Name	spg	% Blend
001110008	FA-A NATURAL SAND	00817104	MIDWEST CONC CO(081)	2.59	50.0
001030013	CA-4 GRAVEL	00817104	MIDWEST CONC CO(081)	2.58	50.0

Cement	Name	Prod #	Prod Name	spg	% Blend
161060100	CEMENT TY 1/2 BL/BAG	00003001	ASH GROVE (CHANUTE)	3.15	100.0

Lbs Per Cubic Yard			Material	Name	Prod #	oz/cy
Agg1= 1,409	Water= 253	AEA	041000000	AIR-ENTRAINING AGENT	00000201	3.1
Agg2= 1,409	Cmnt1: 721	ADMIX1	04201000A	TYPE A (WATER REDUCE	00000201	48.3
Agg3=	Cmnt2:	ADMIX2	04203000D	TYPE-D ADMIXTURE	00000201	48.3
Agg4=	Cmnt3:	ADMIX3	04204000F	TYPE-F ADMIXTURE	00000201	40.1

Total: 3,791 Conc Unit Wt: 140.41 Air Free Unit Wt: 150.17

Remarks: MCM PLANT #5 : 00601903, AIRPORT

Figure A1. KDOT project K-3433-03 bridge mix design.

Appendix B. Shear Friction Stirrup Stress-Strain Curves

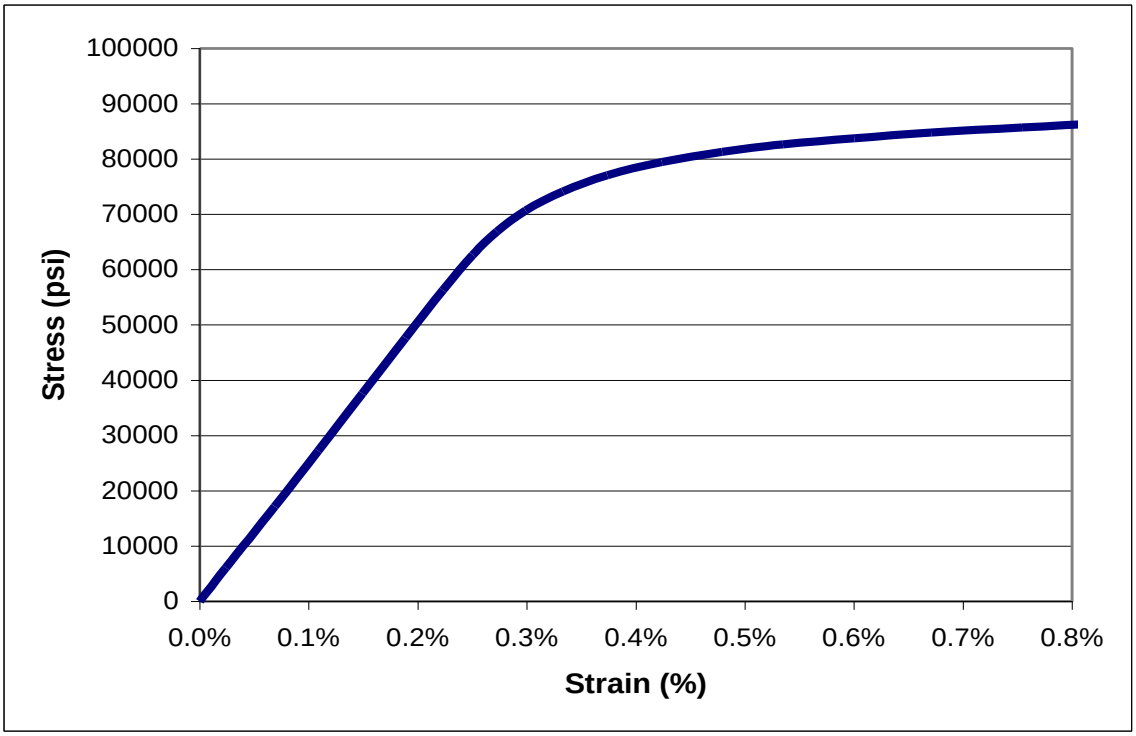

Figure B2. B-1A.

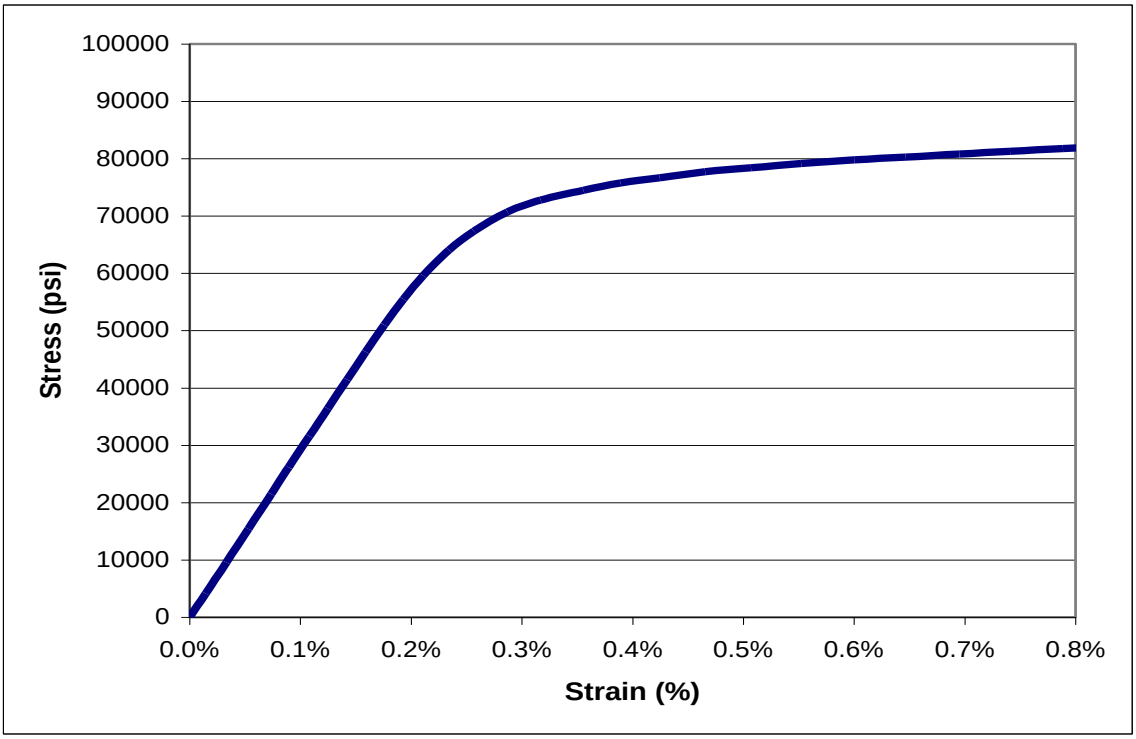

Figure B3. B-1B.

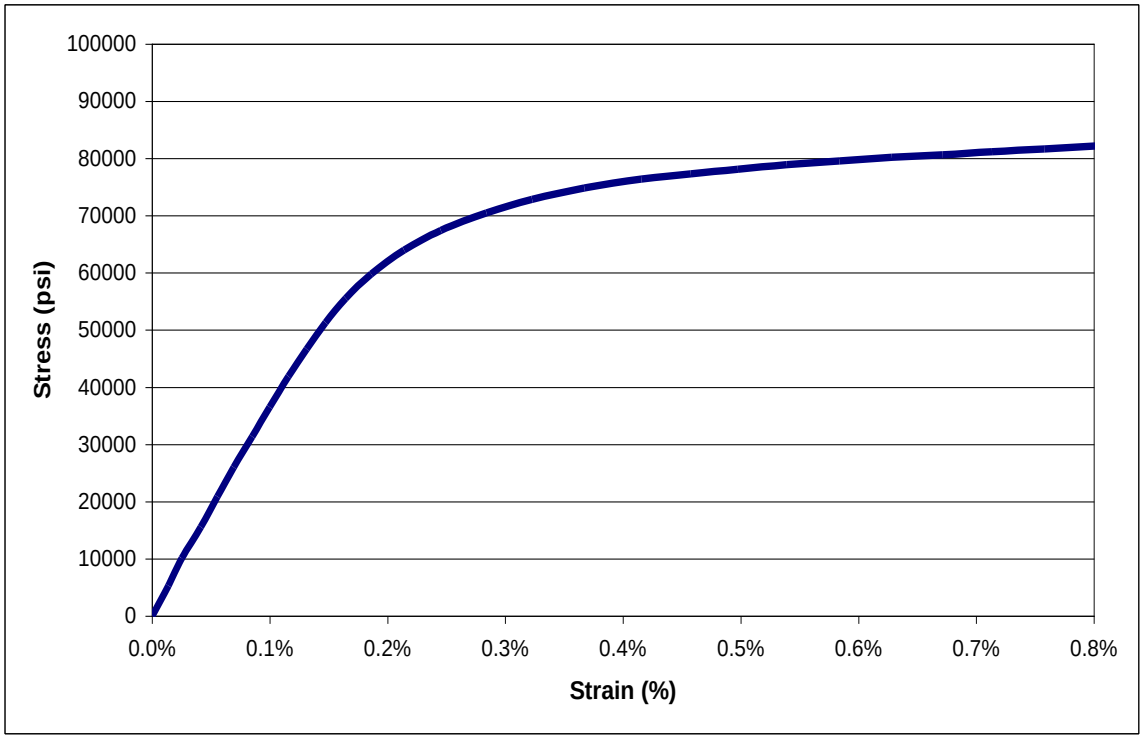

Figure B4. B-2A.

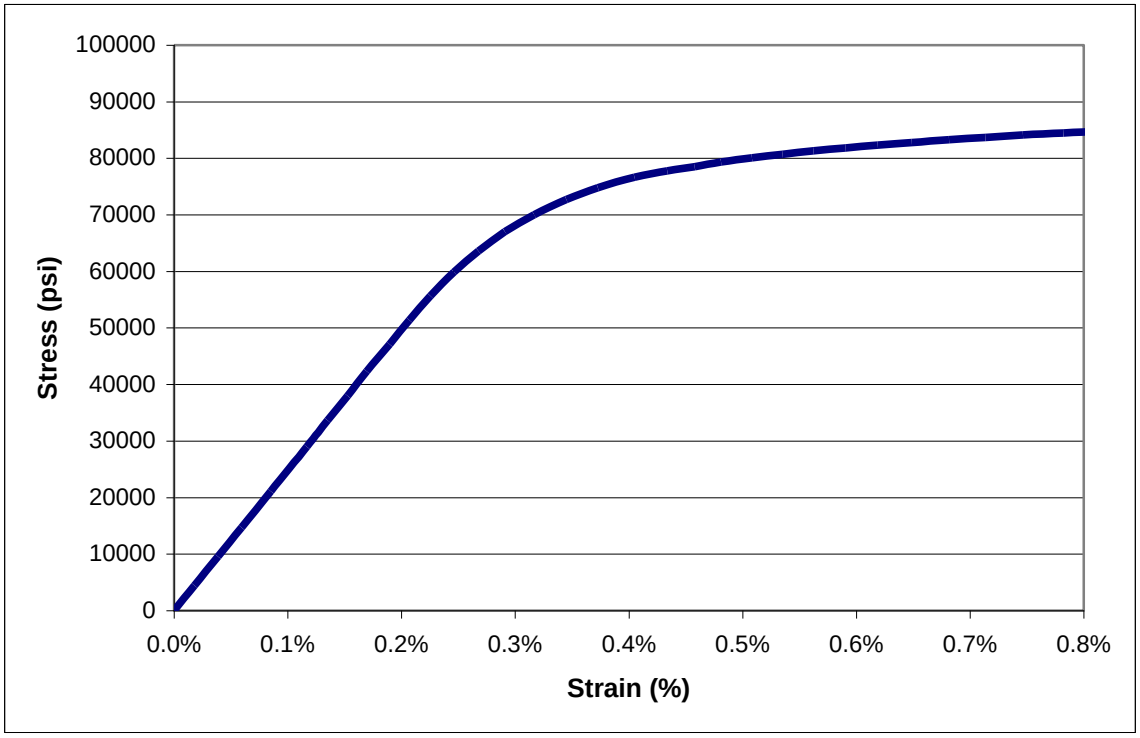

Figure B5. B-2B.

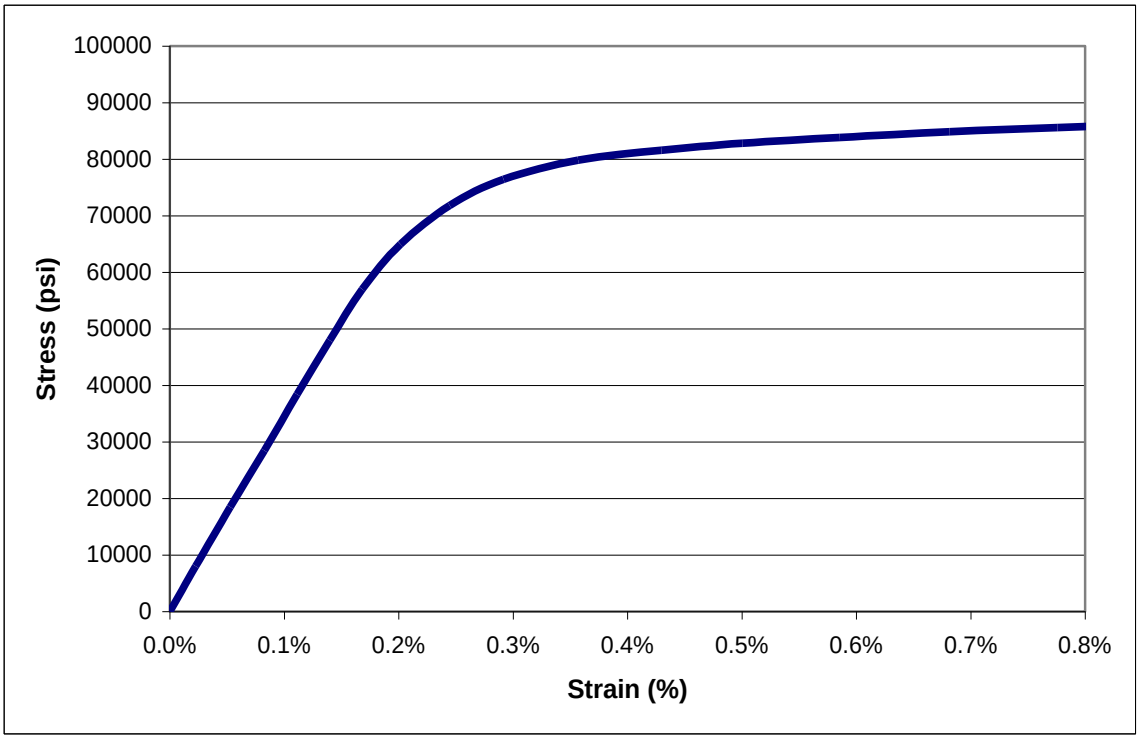

Figure B6. B-3A.

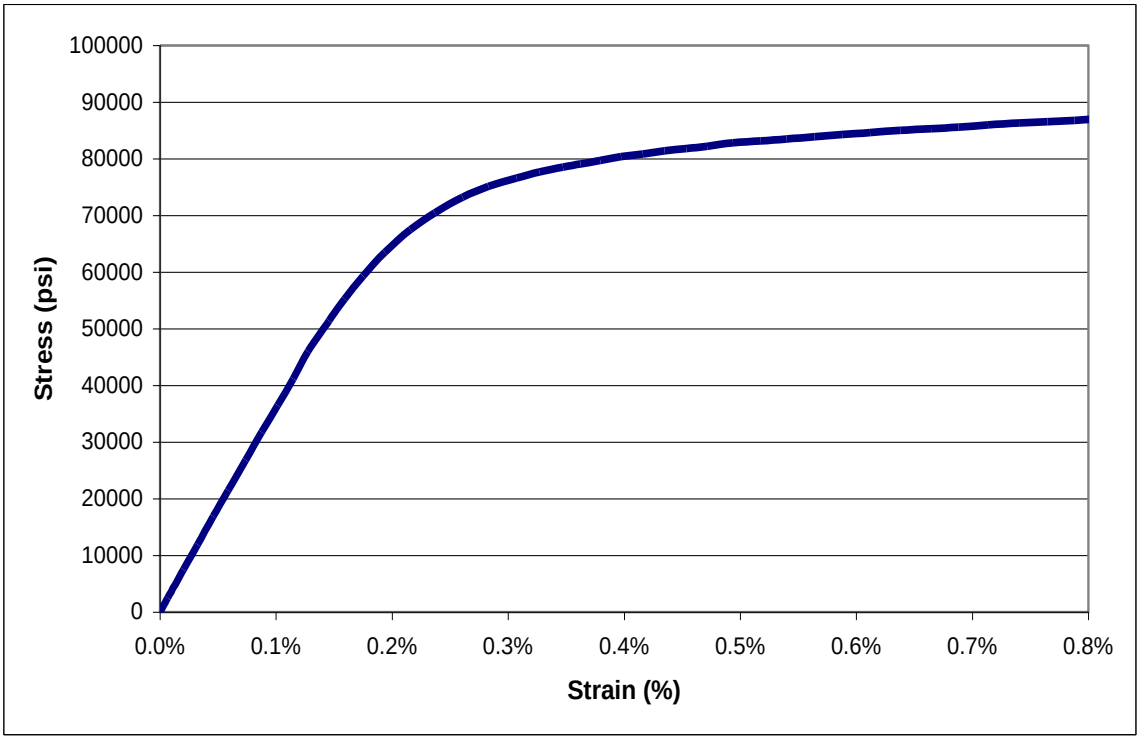

Figure B7. B-3B.

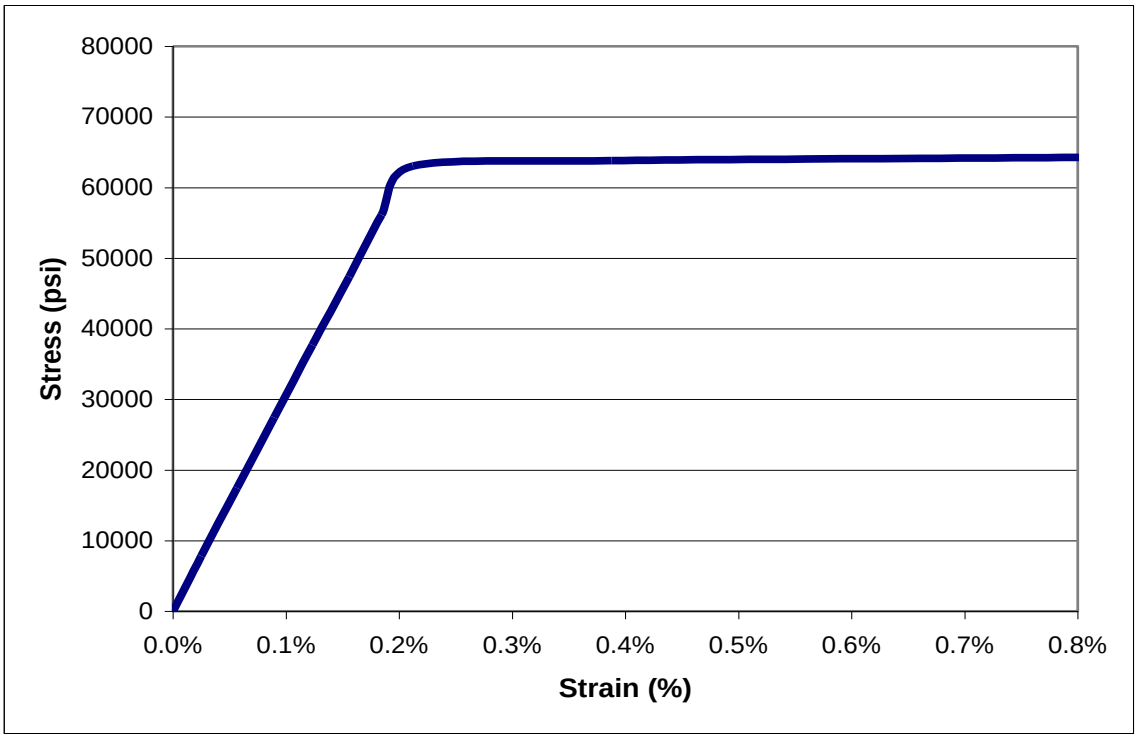

Figure B8. E-1A.

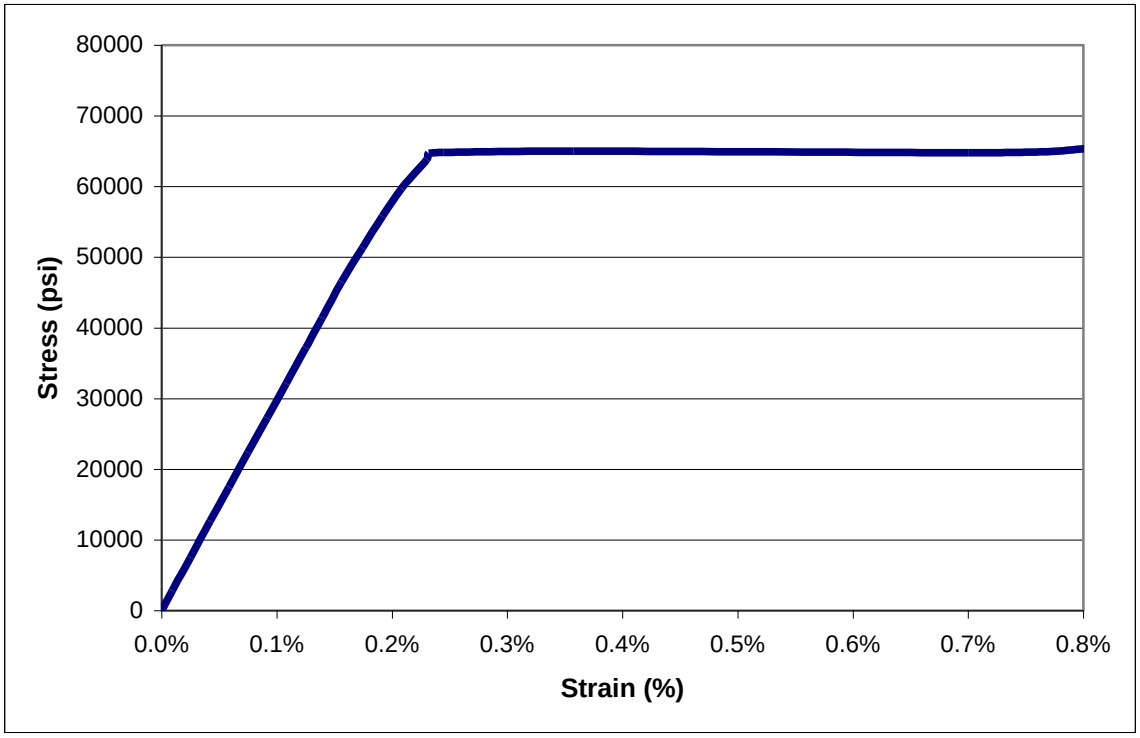

Figure B9. E-1B.

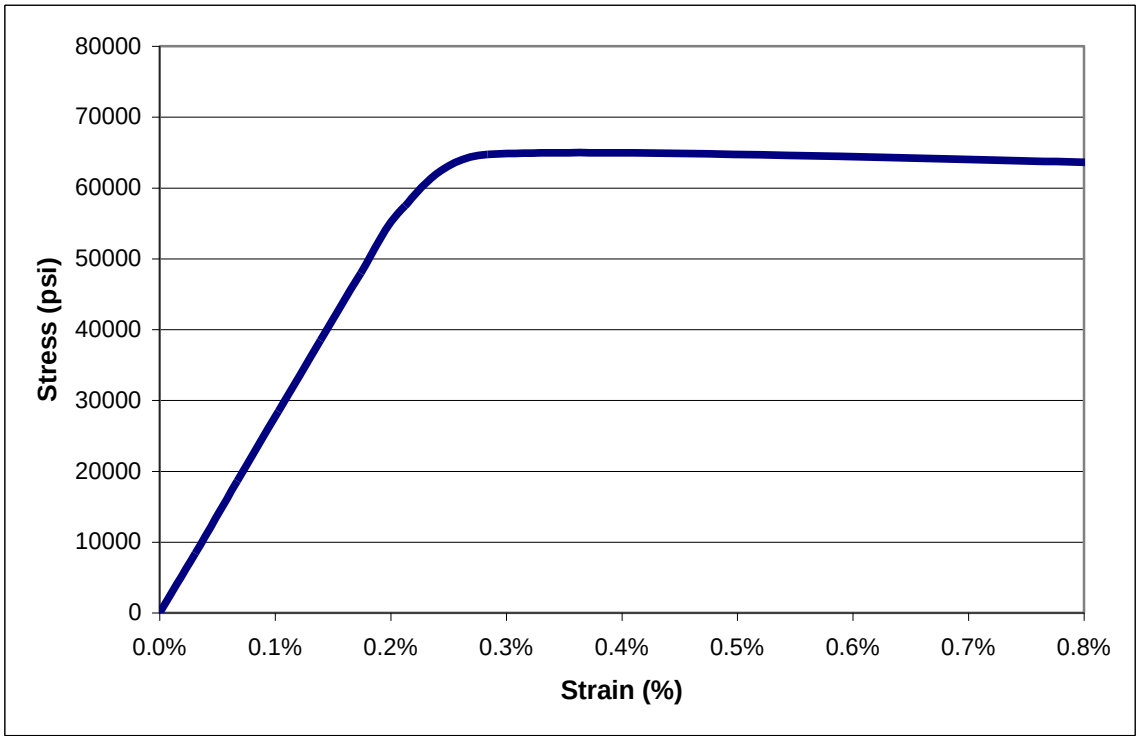

Figure B10. E-2A.

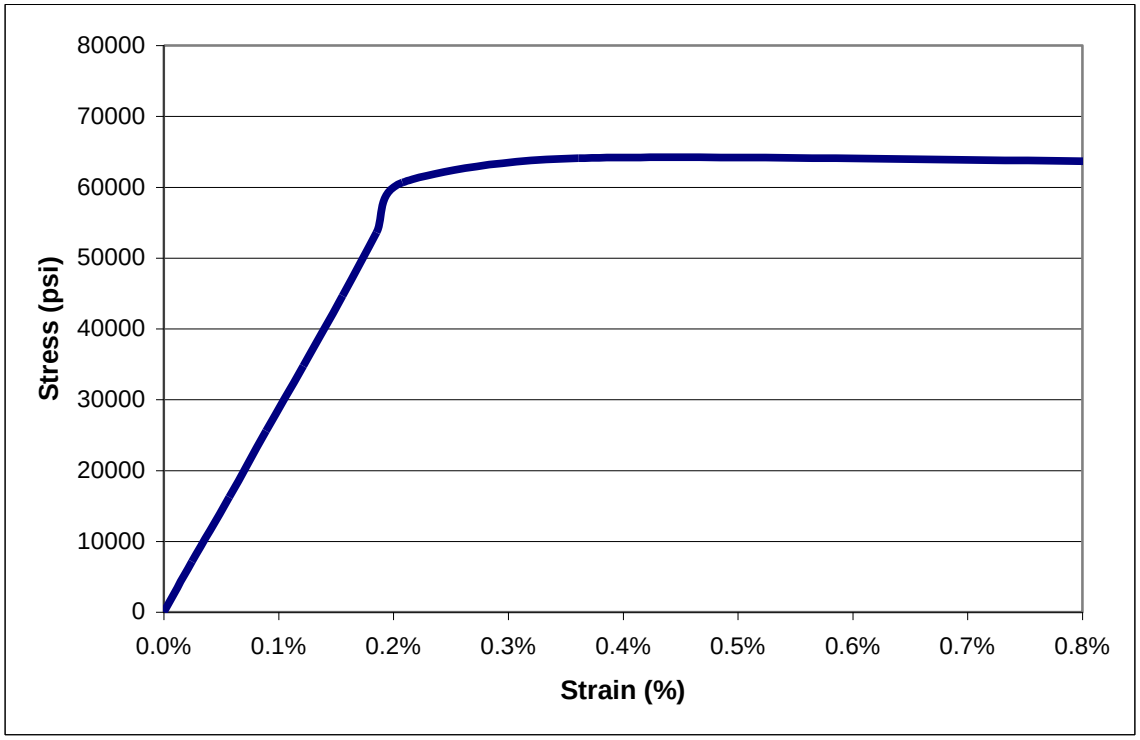

Figure B11. E-2B.

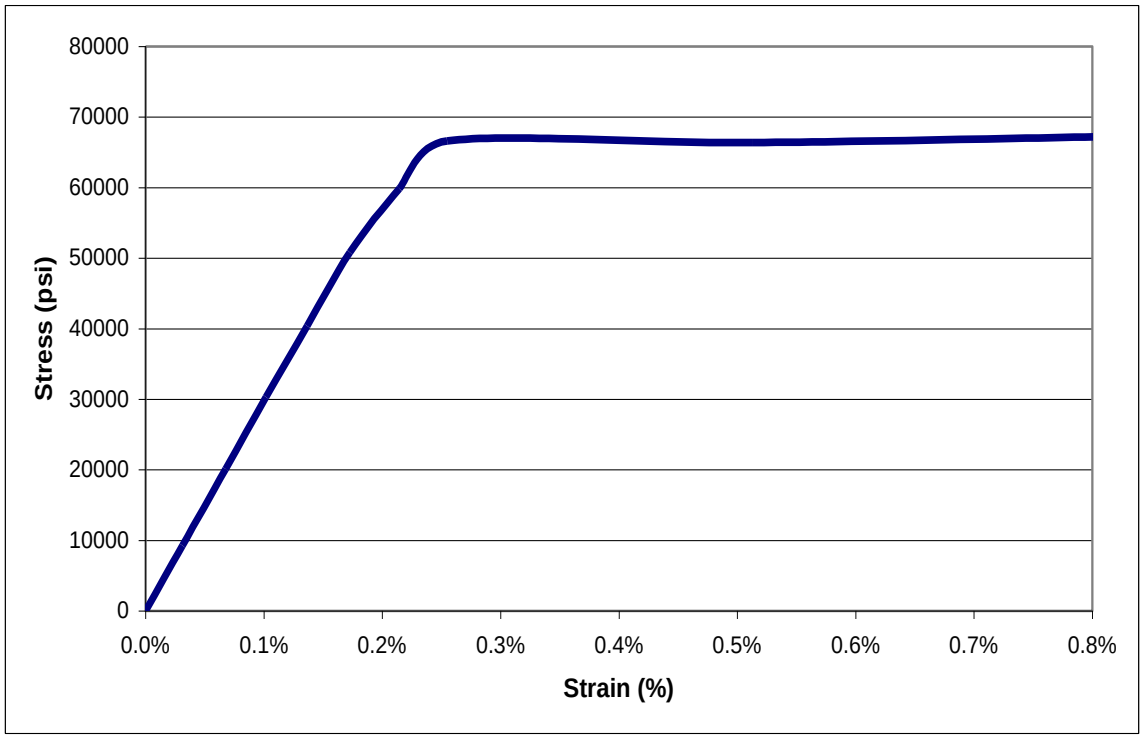

Figure B12. E-3A.

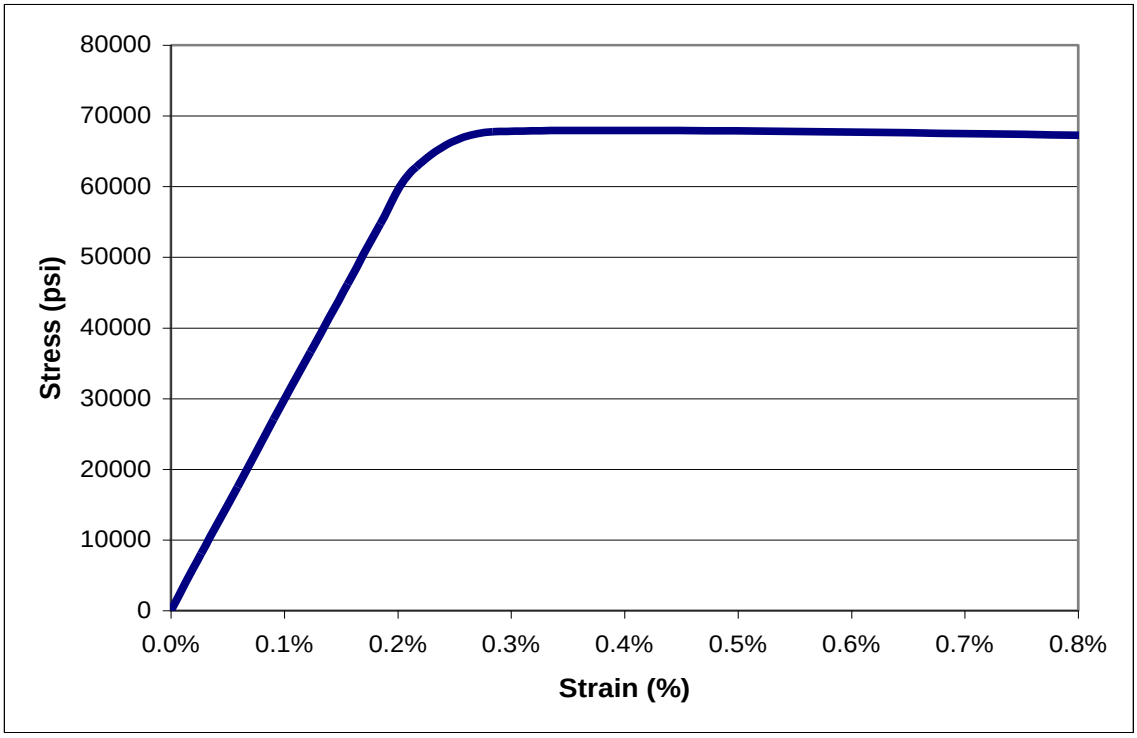

Figure B13. E-3B.

Appendix C. Shear Friction Specimen Load-Slip Curves

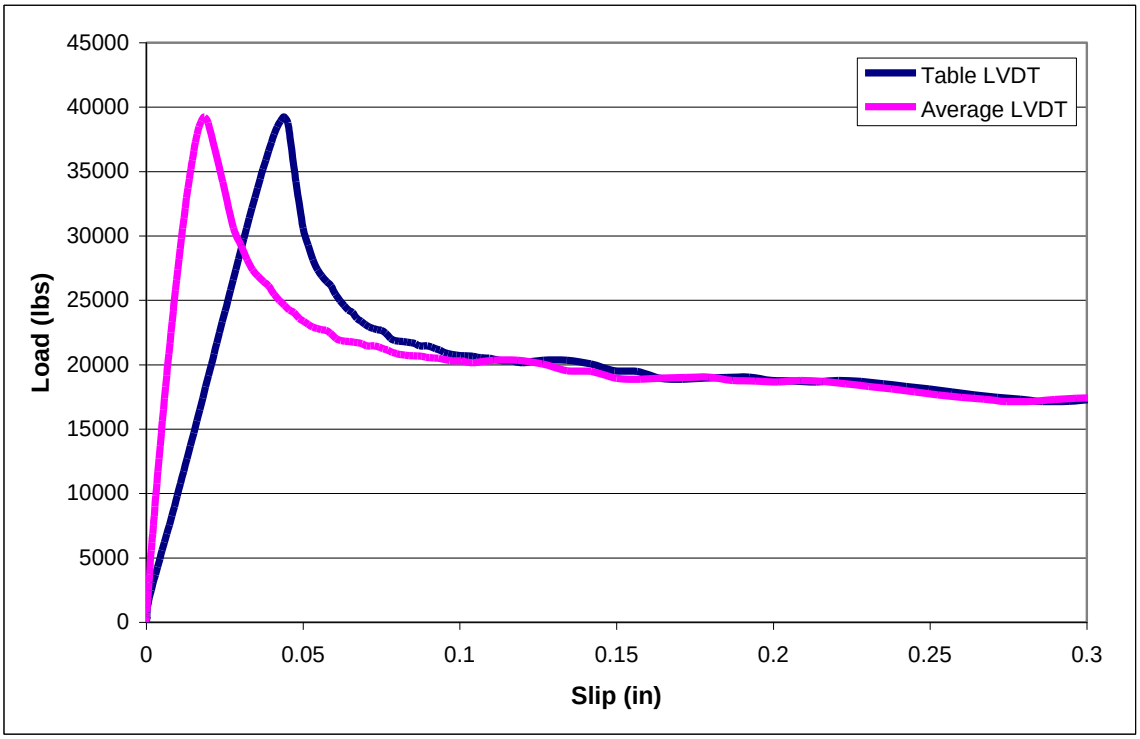

Figure C14. BP-1A.

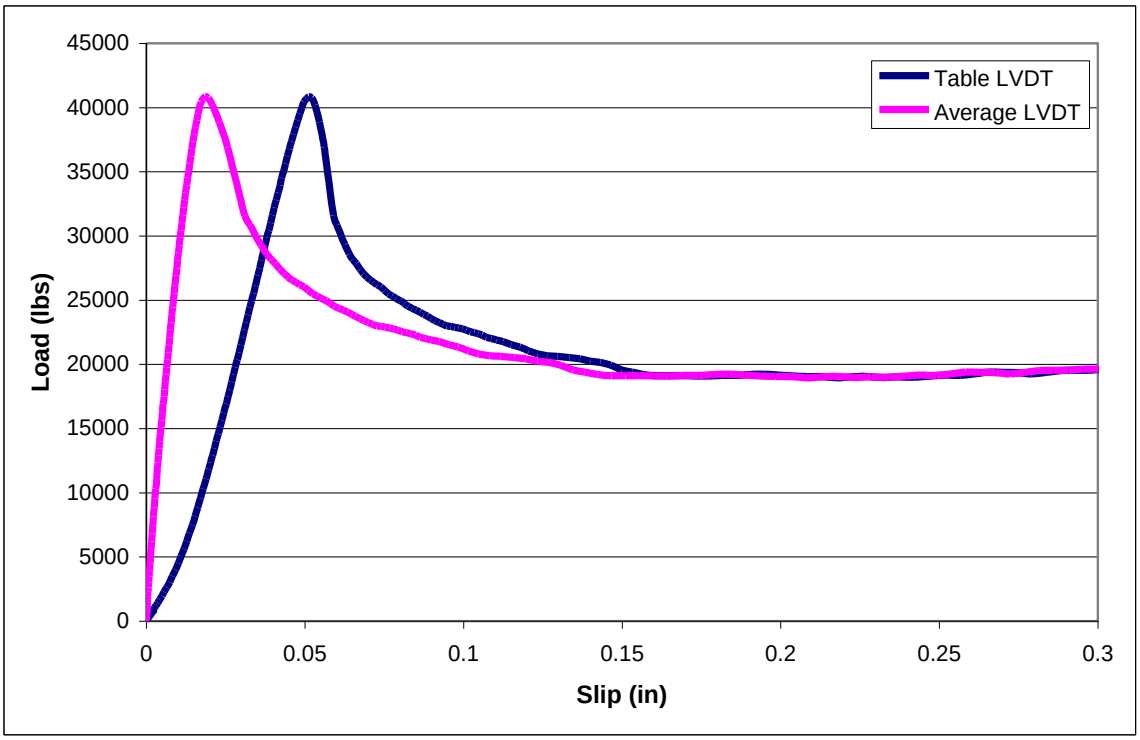

Figure C15. BP-1B.

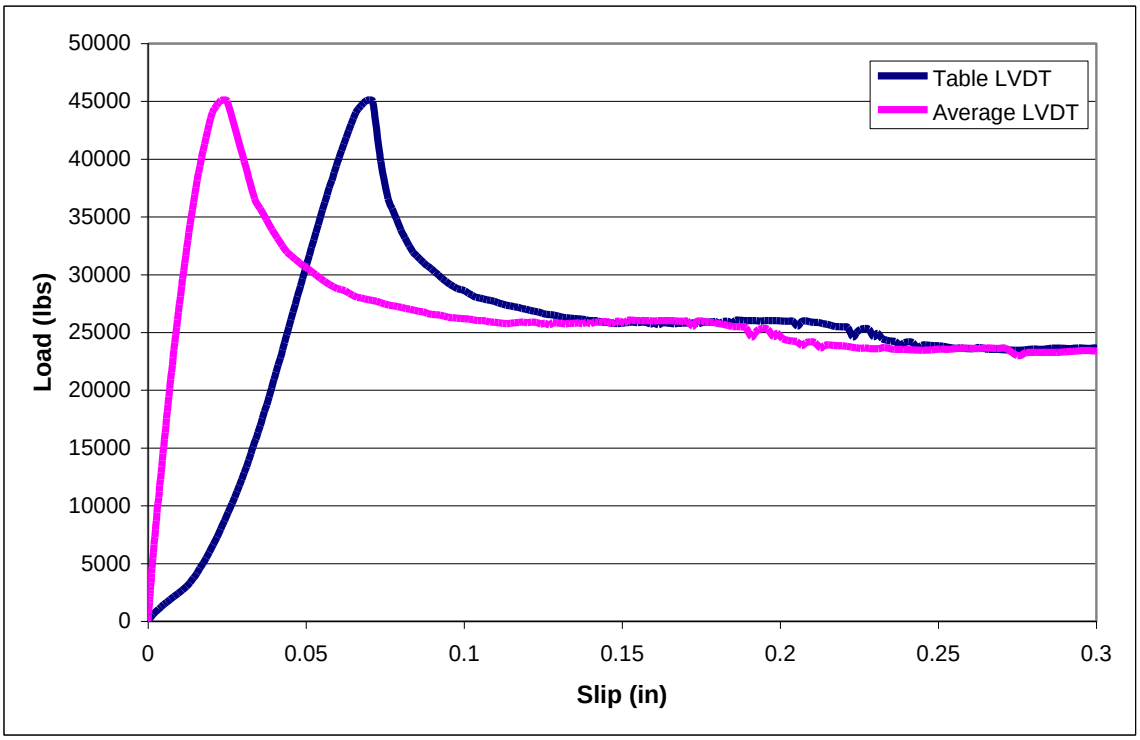

Figure C16. BP-1C.

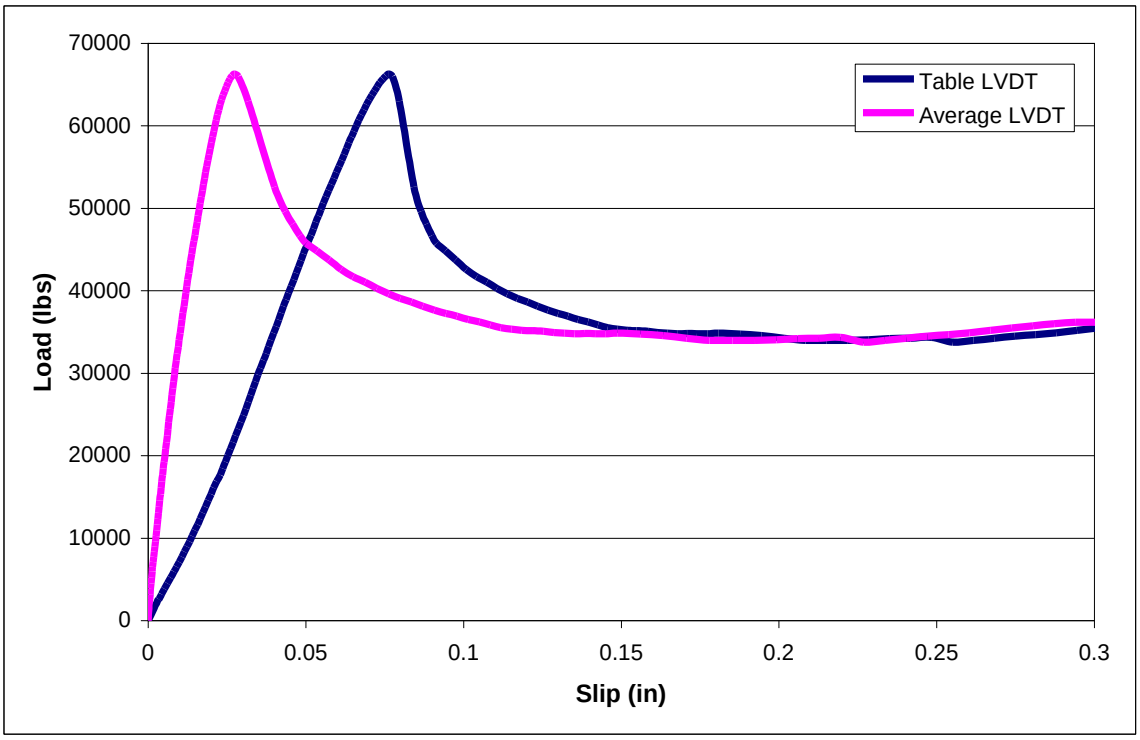

Figure C17. BP-2A.

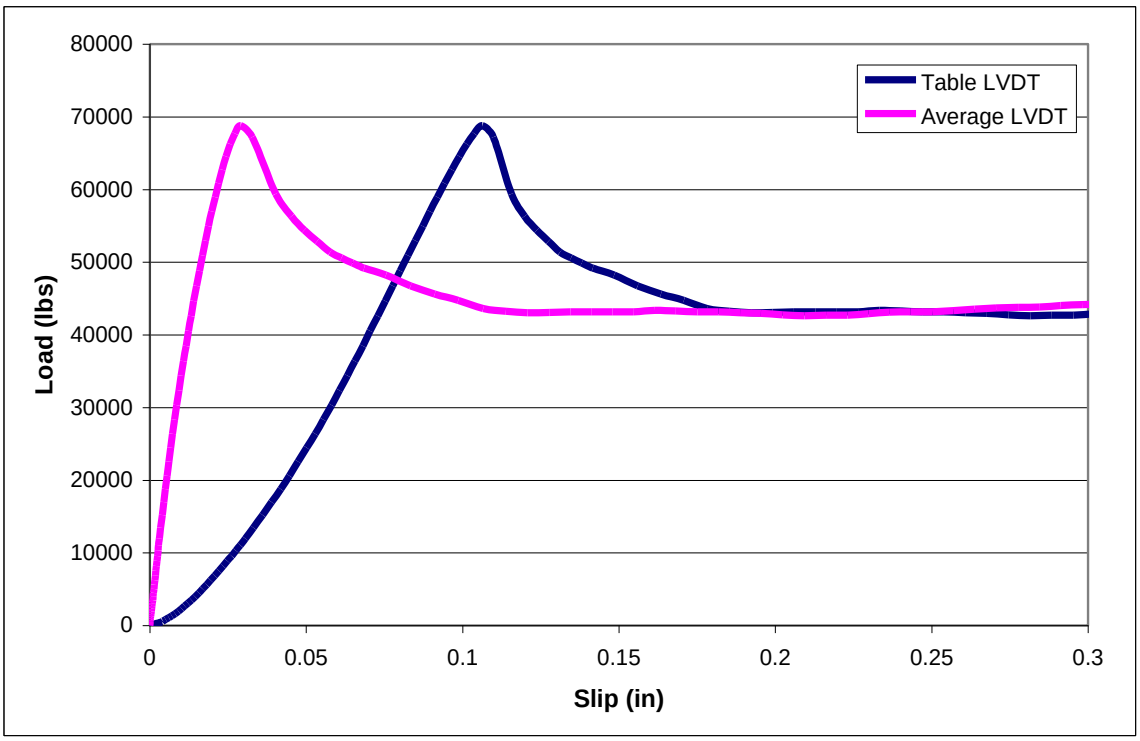

Figure C18. BP-2B.

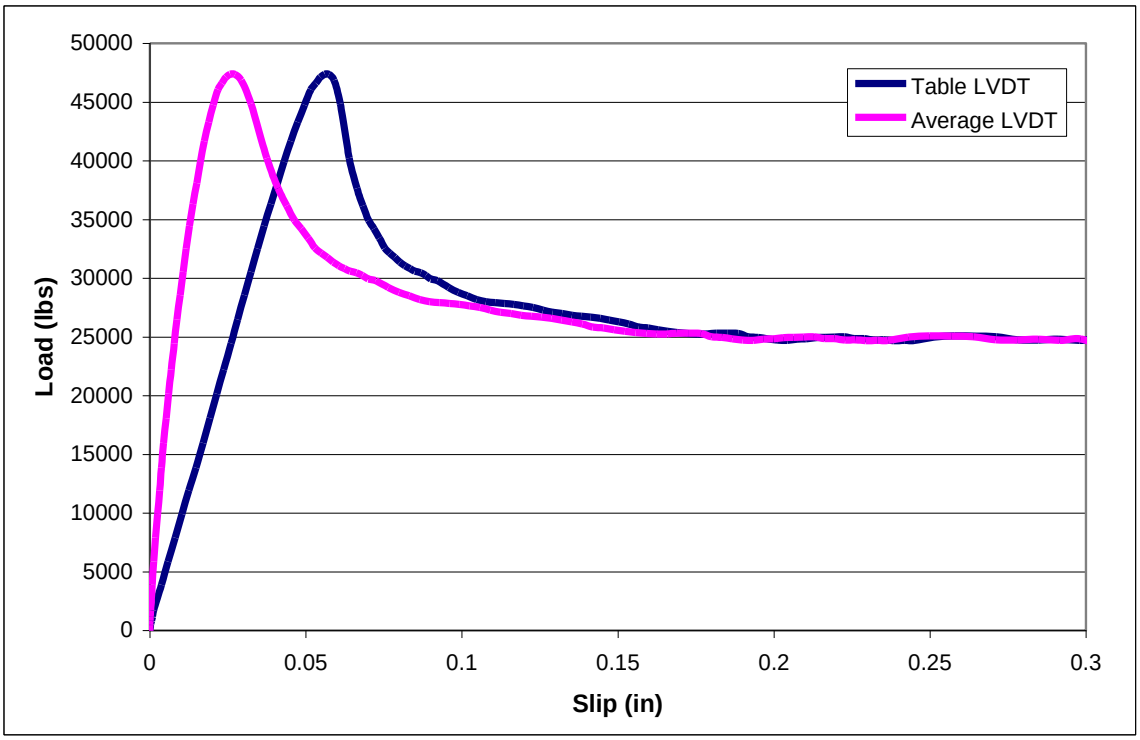

Figure C19. BP-2C.

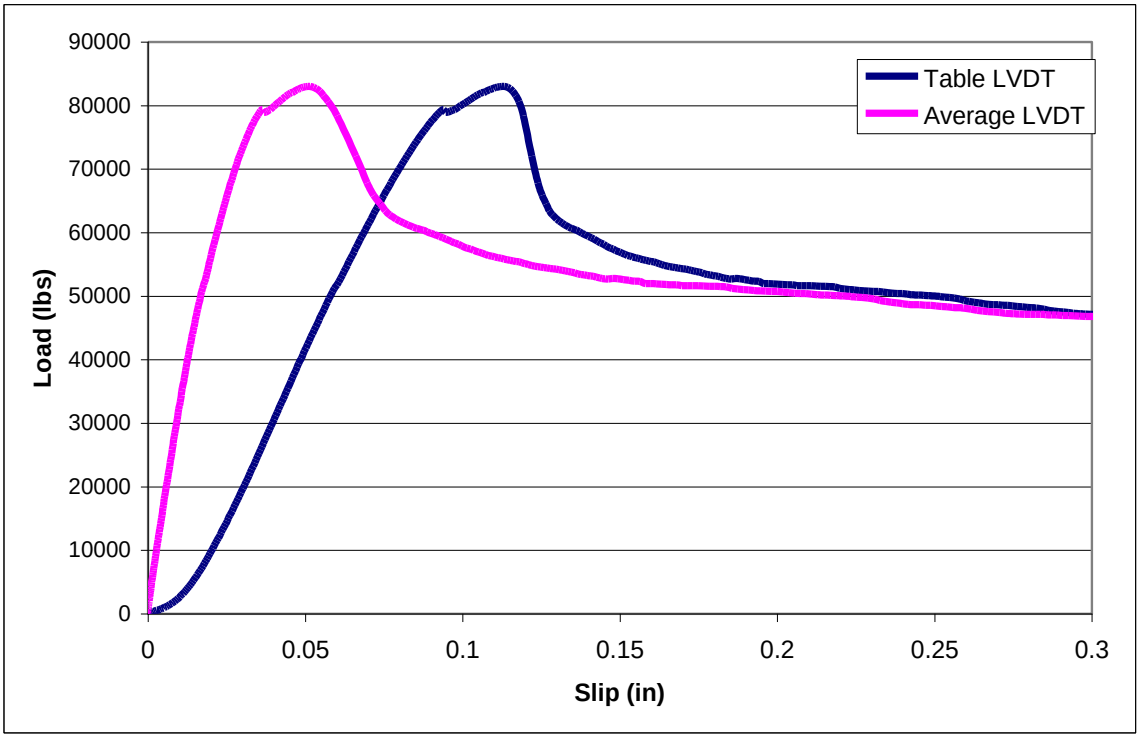

Figure C20. BP-3A.

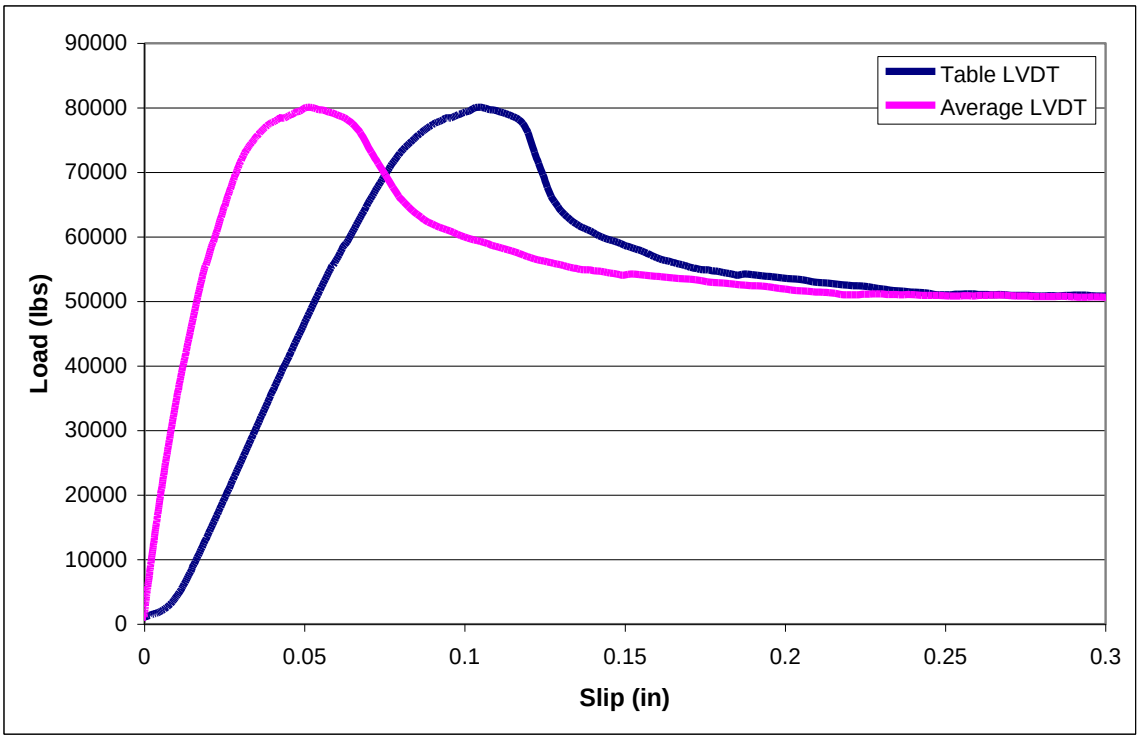

Figure C21. BP-3B.

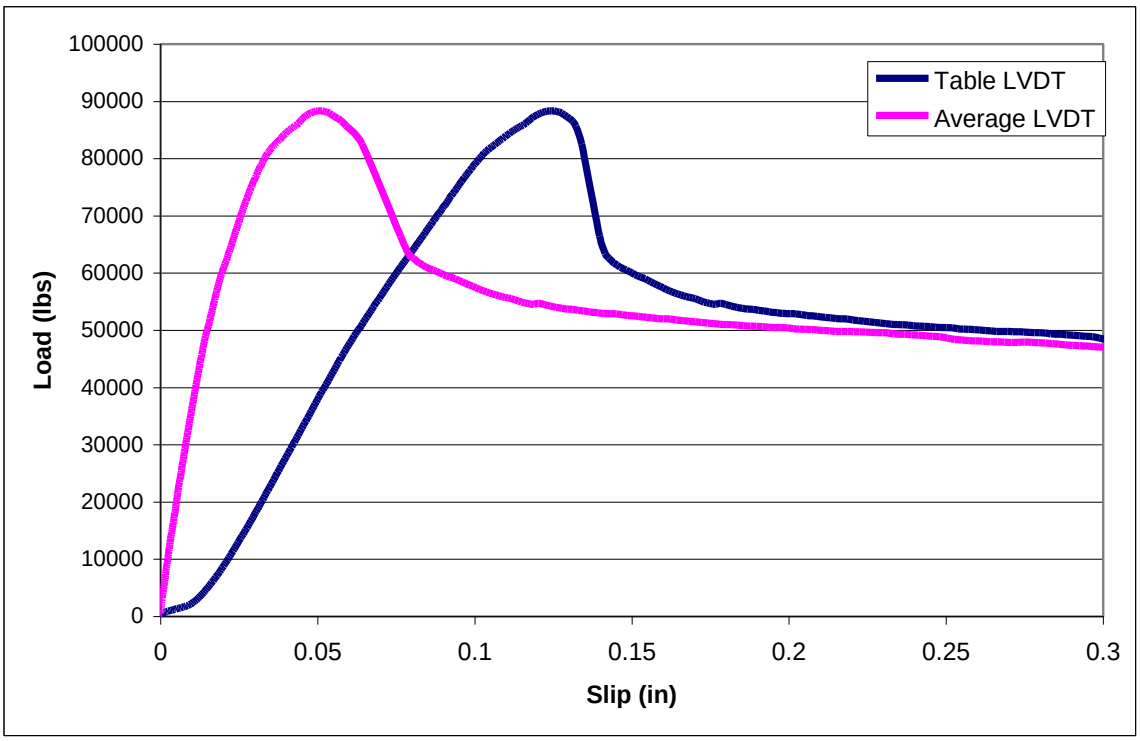

Figure C22. BP-3C.

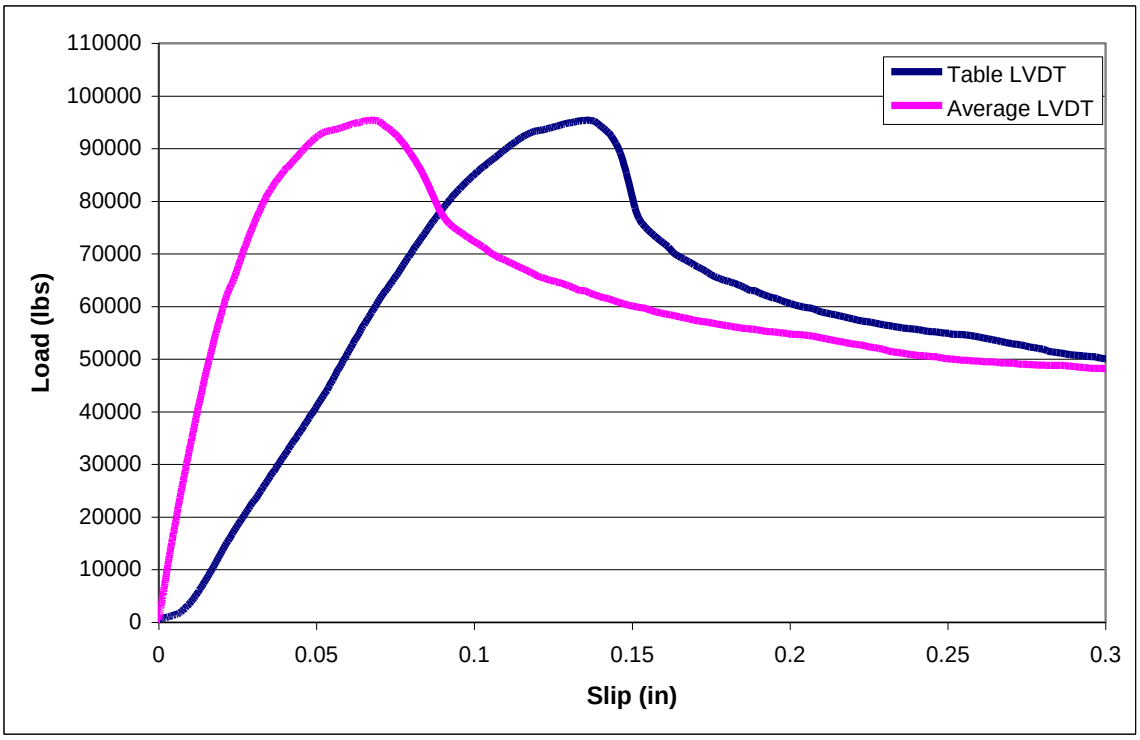

Figure C23. BP-4A.

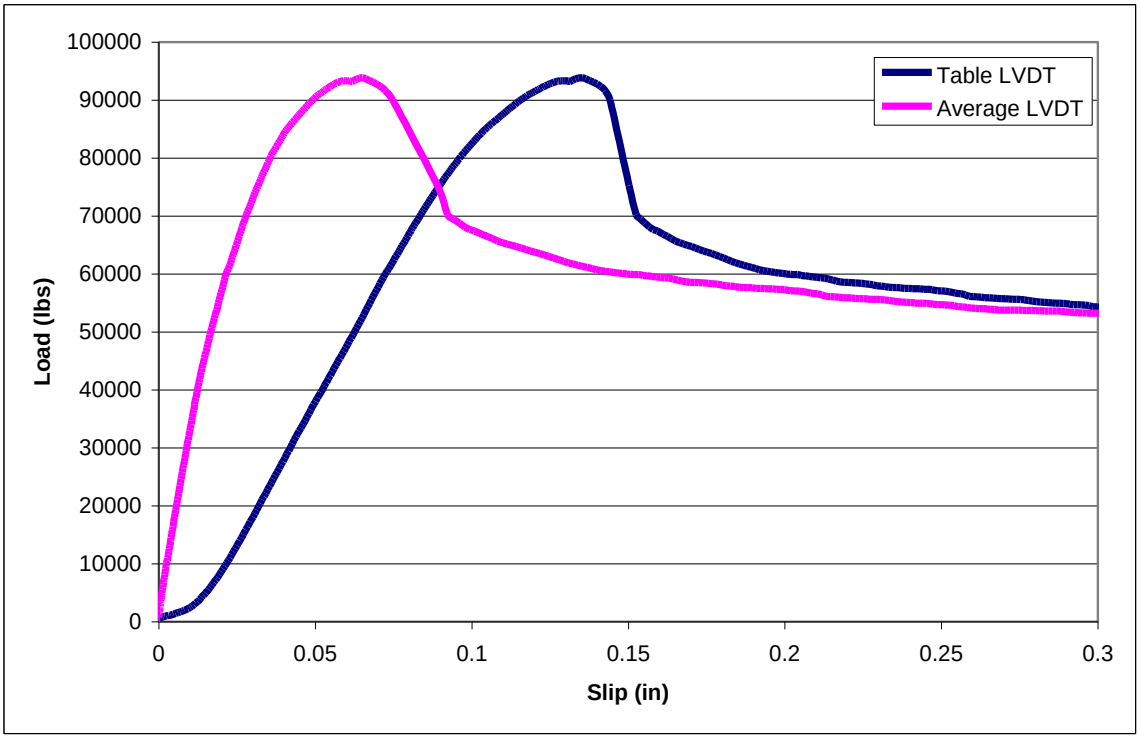

Figure C24. BP-4B.

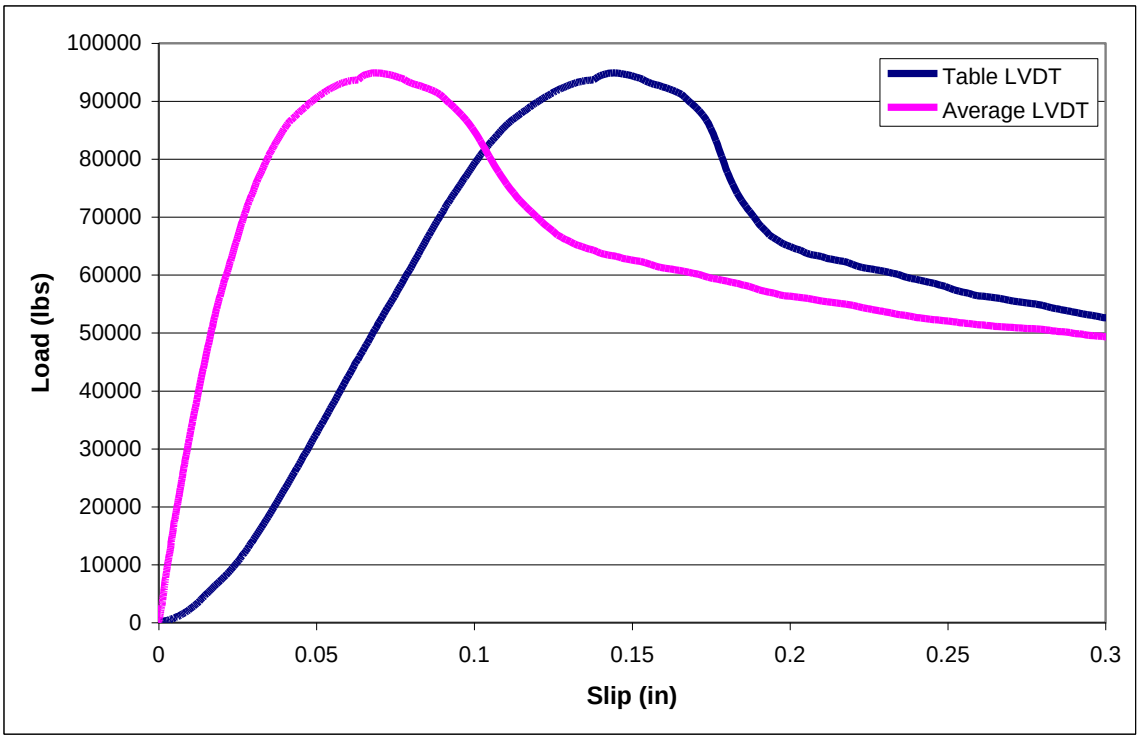

Figure C25. BP-4C.

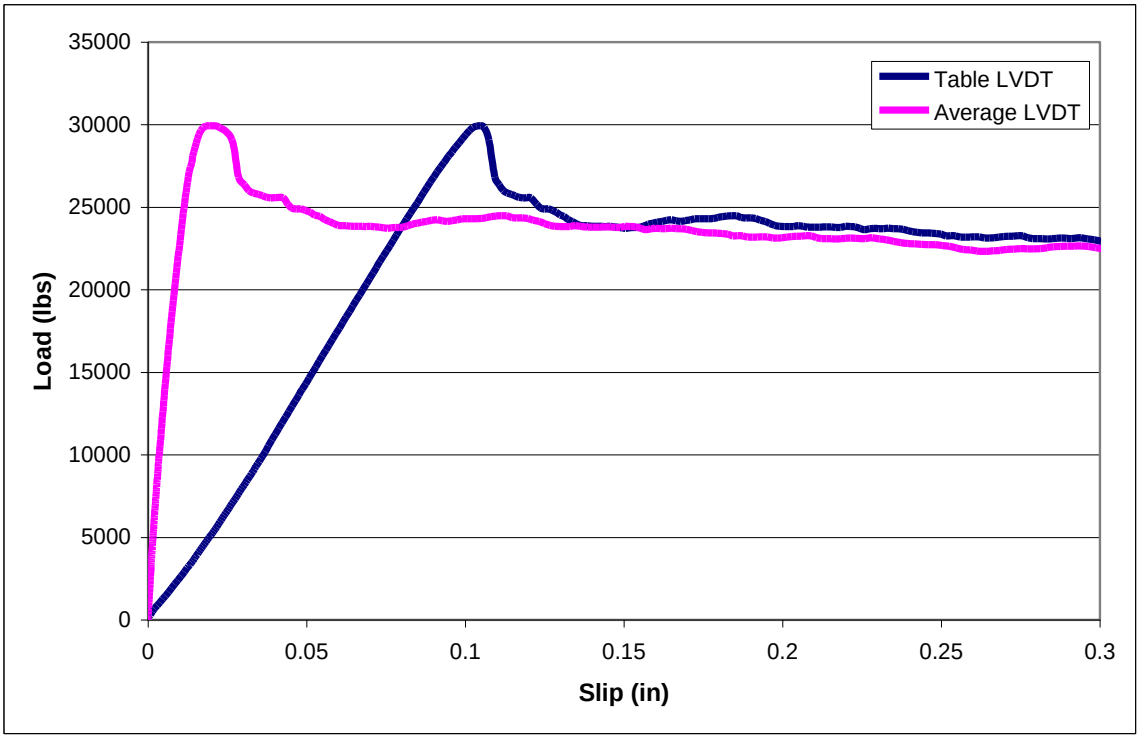

Figure C26. EP-1A.

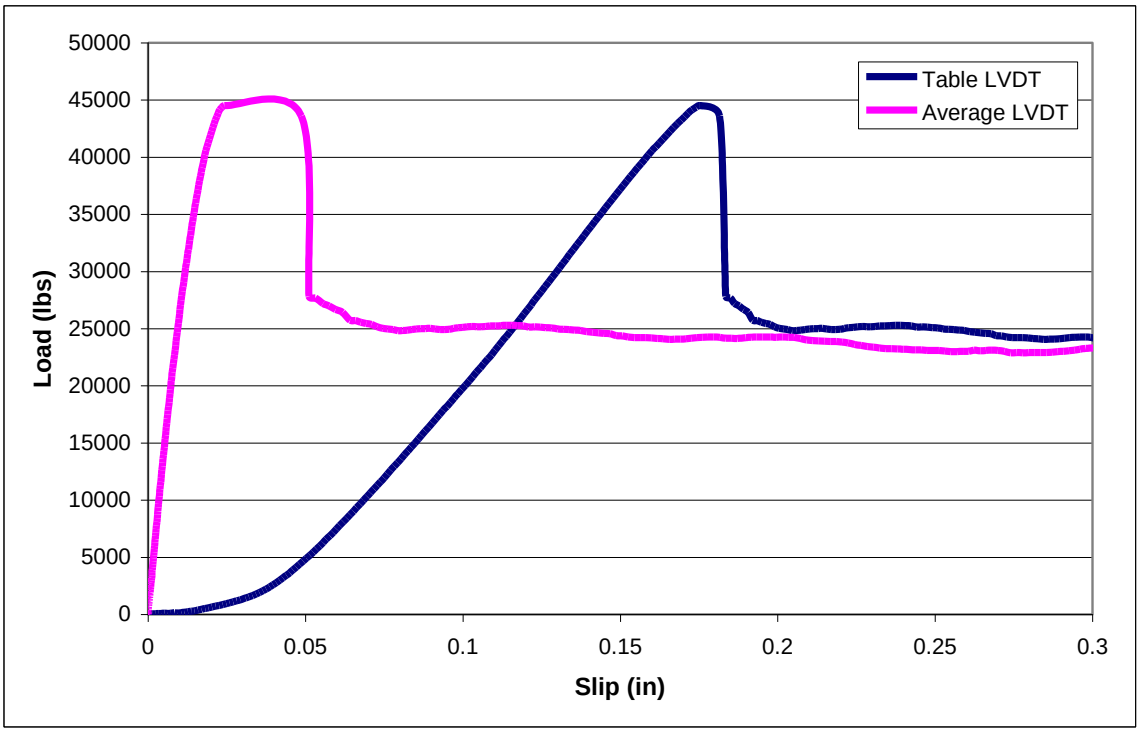

Figure C27. EP-1B.

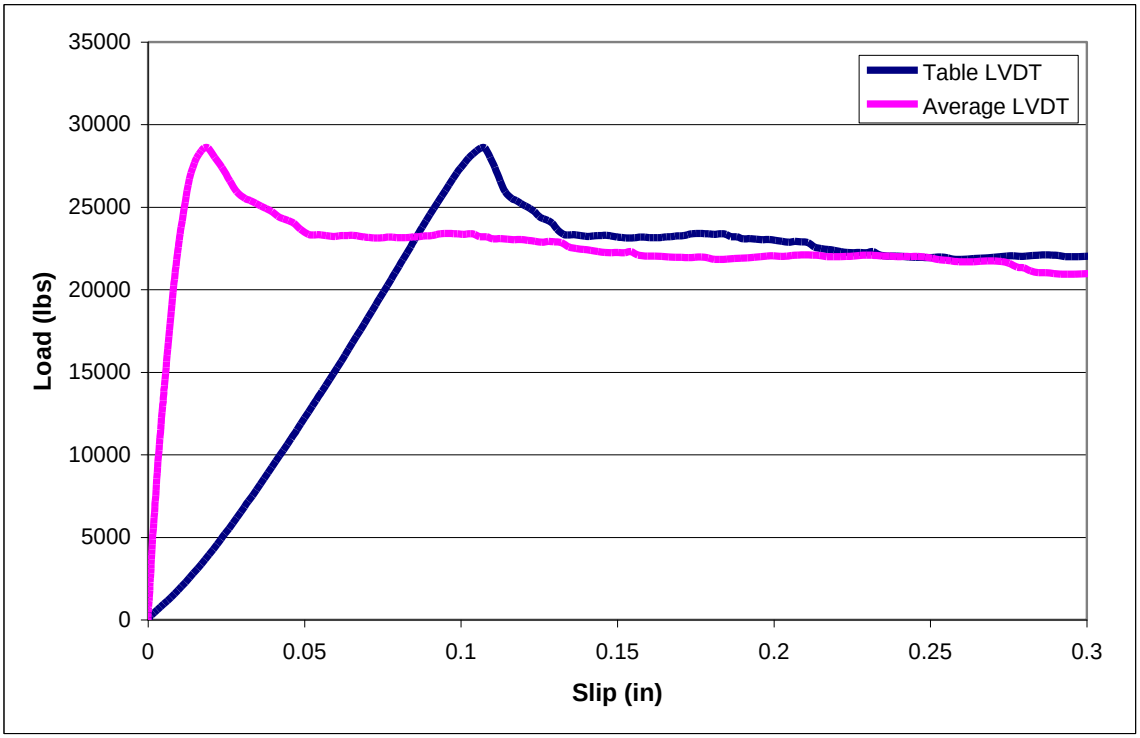

Figure C28. EP-1C.

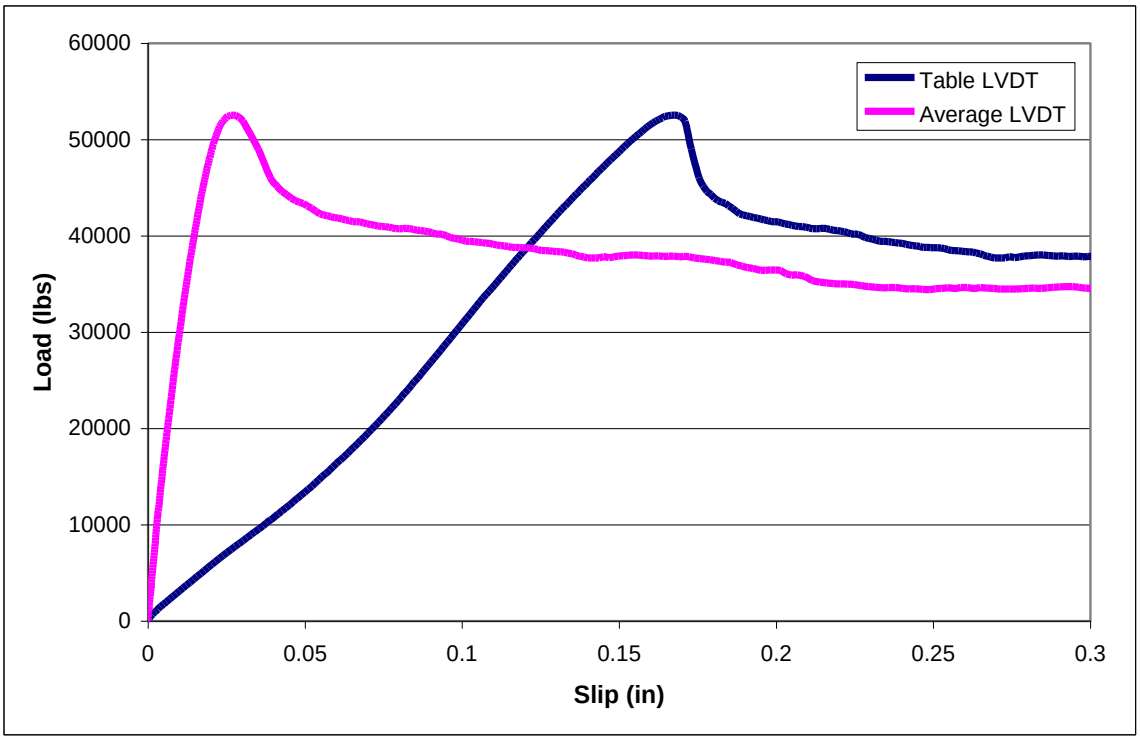

Figure C29. EP-2A.

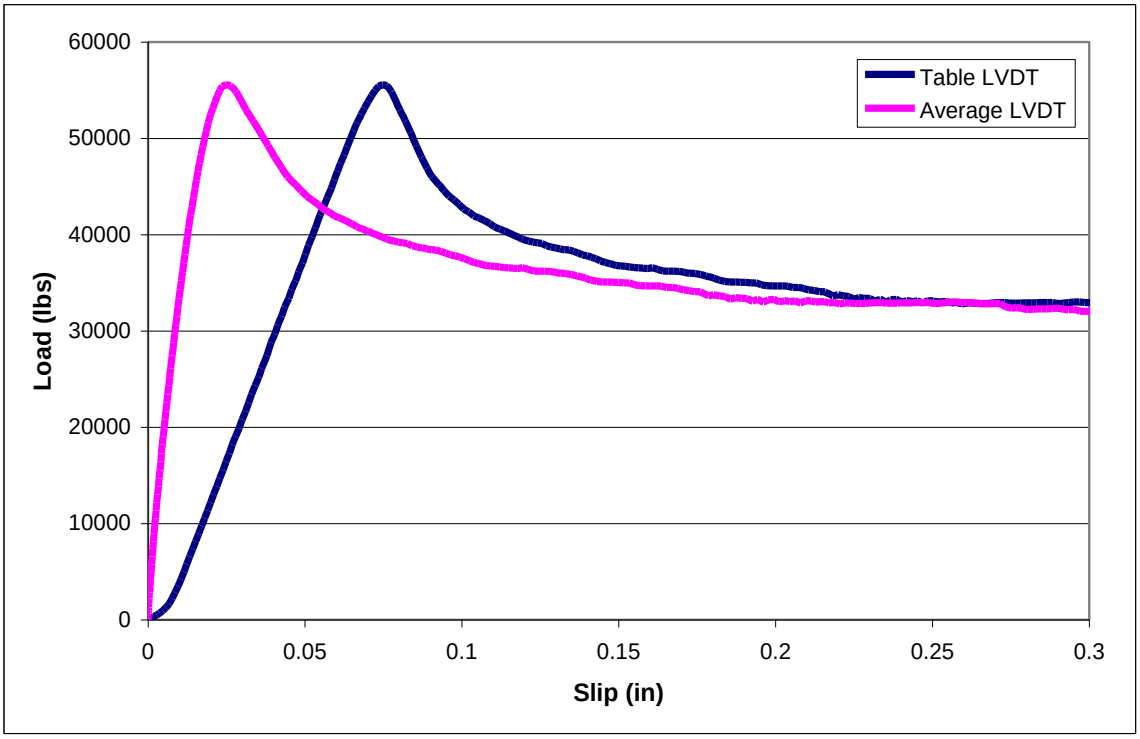

Figure C30. EP-2B.

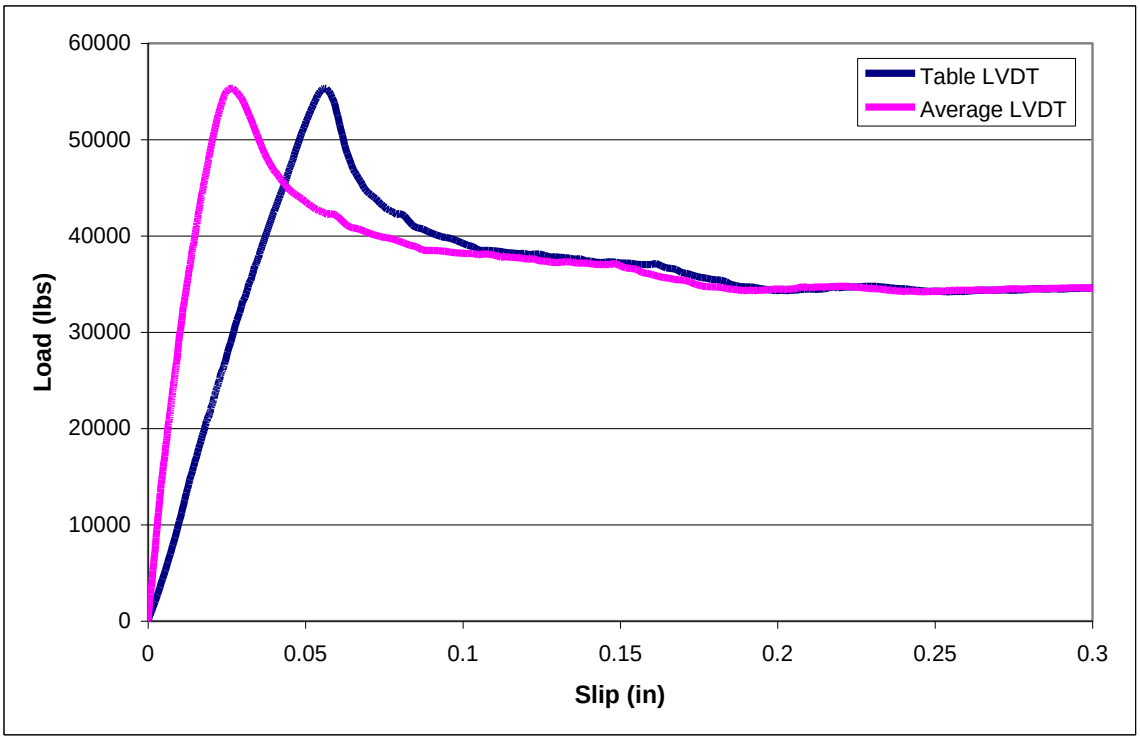

Figure C31. EP-2C.

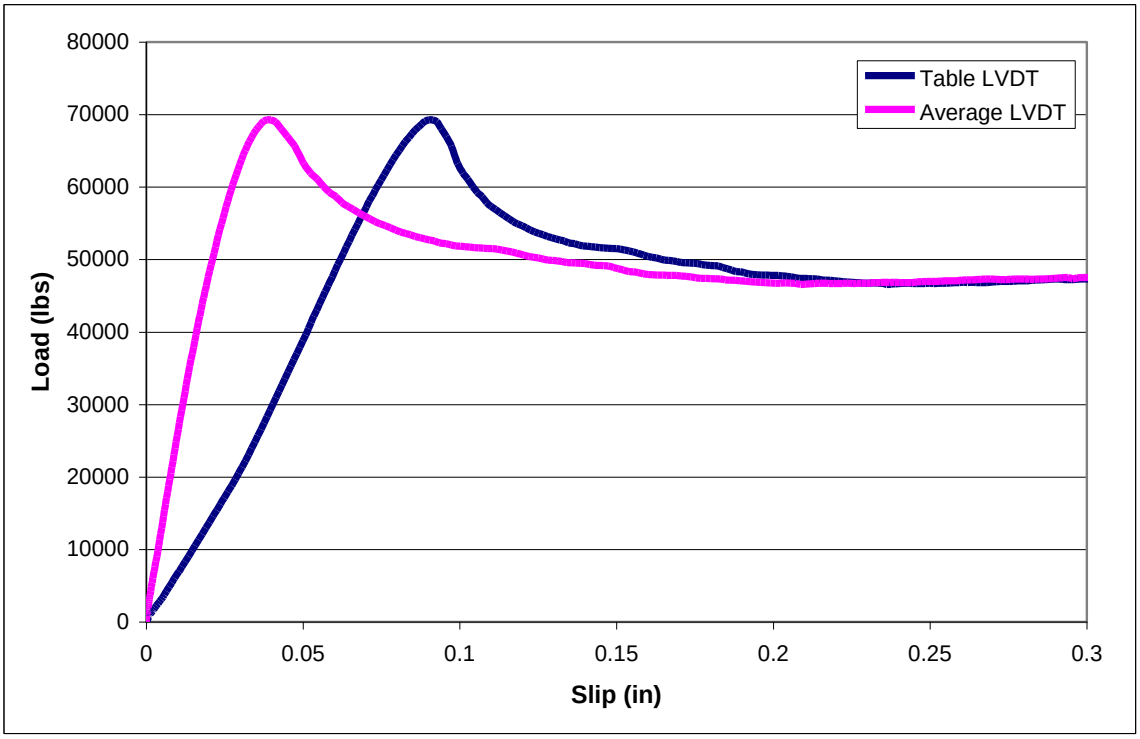

Figure C32. EP-3A.

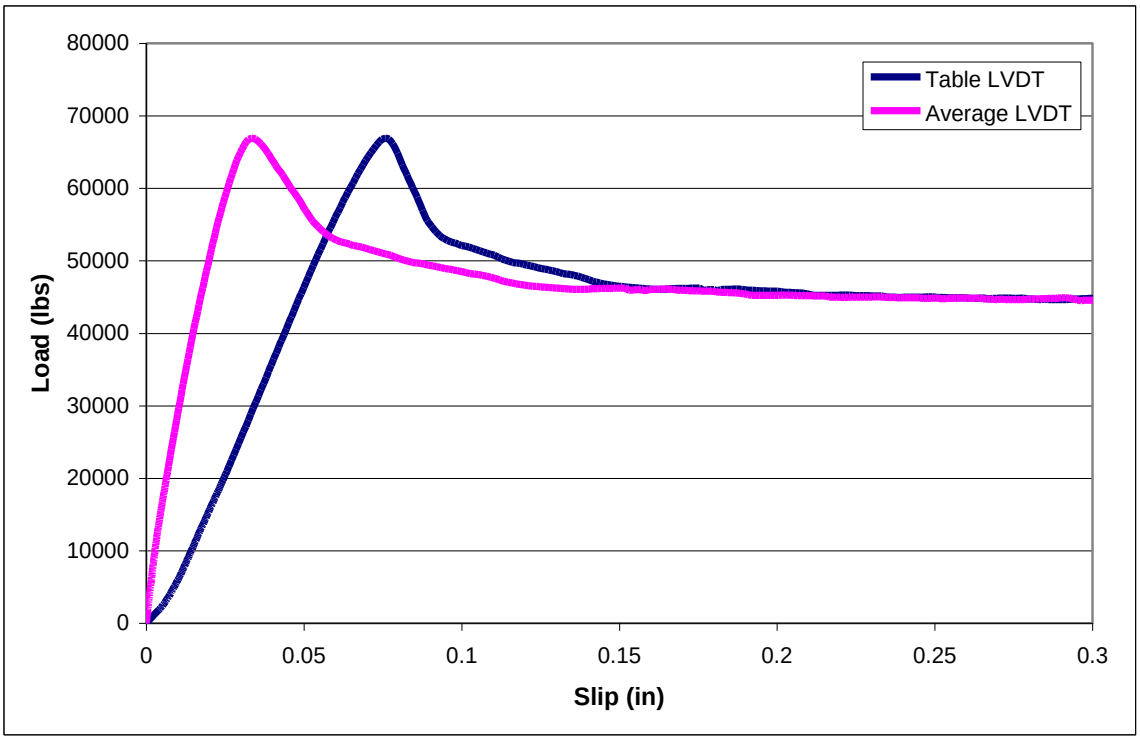

Figure C33. EP-3B.

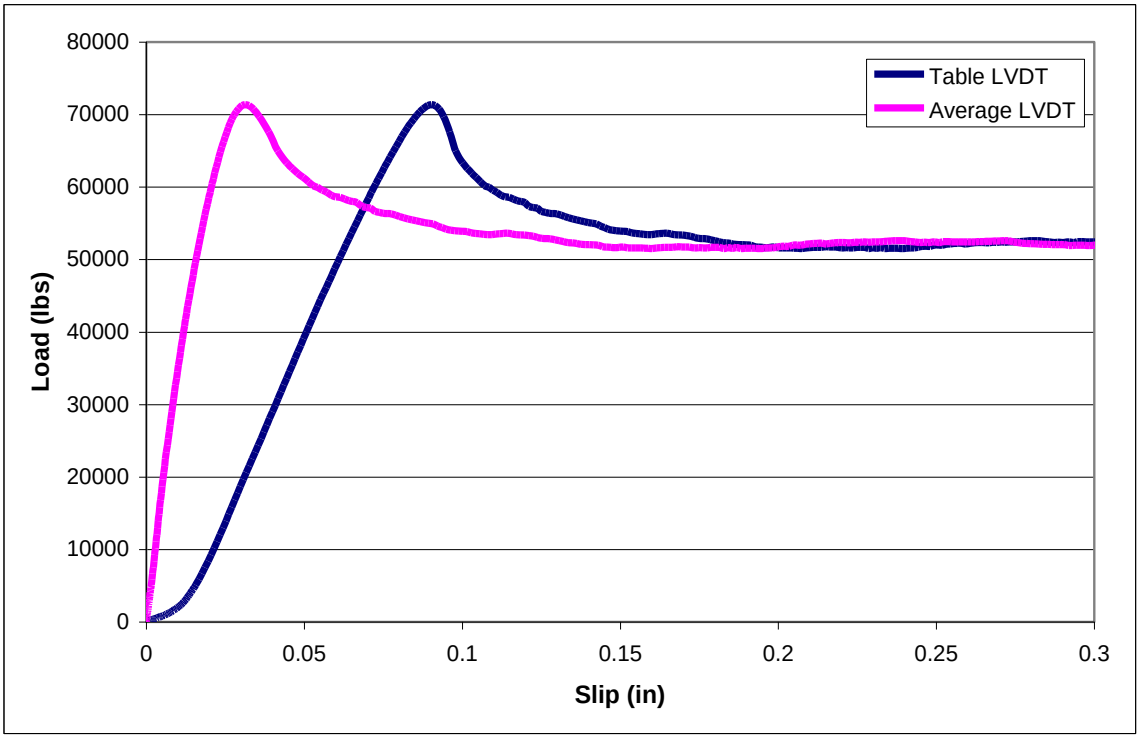

Figure C34. EP-3C.

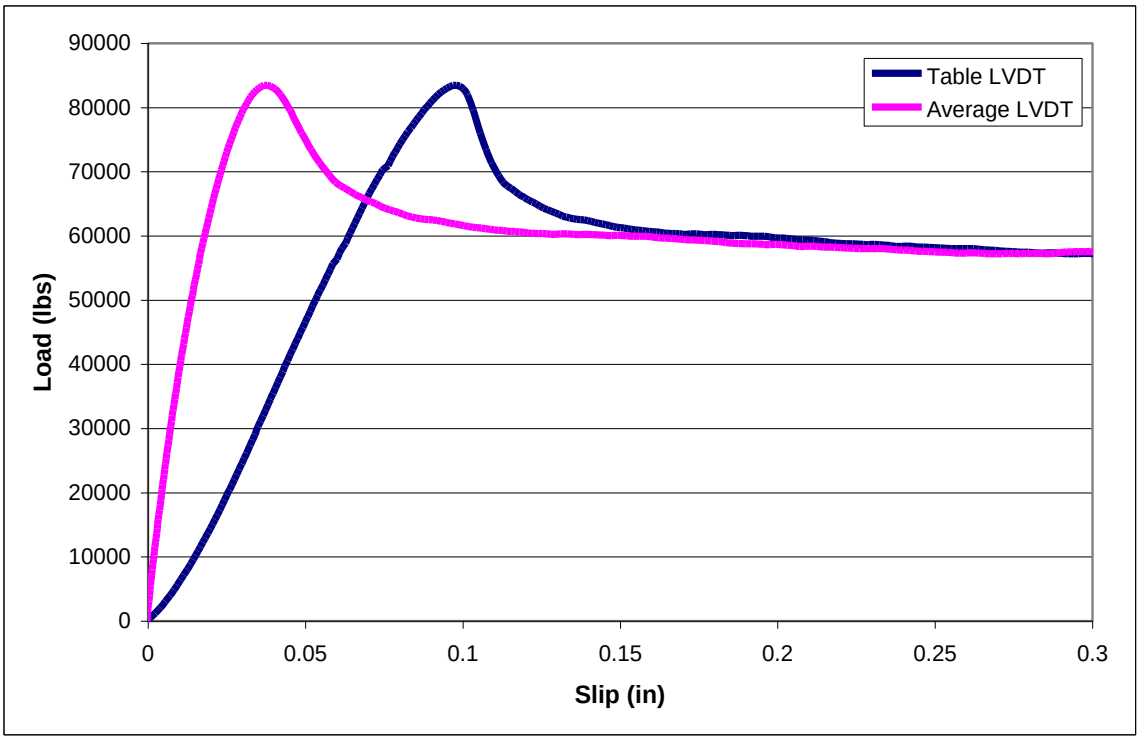

Figure C35. EP-4A.

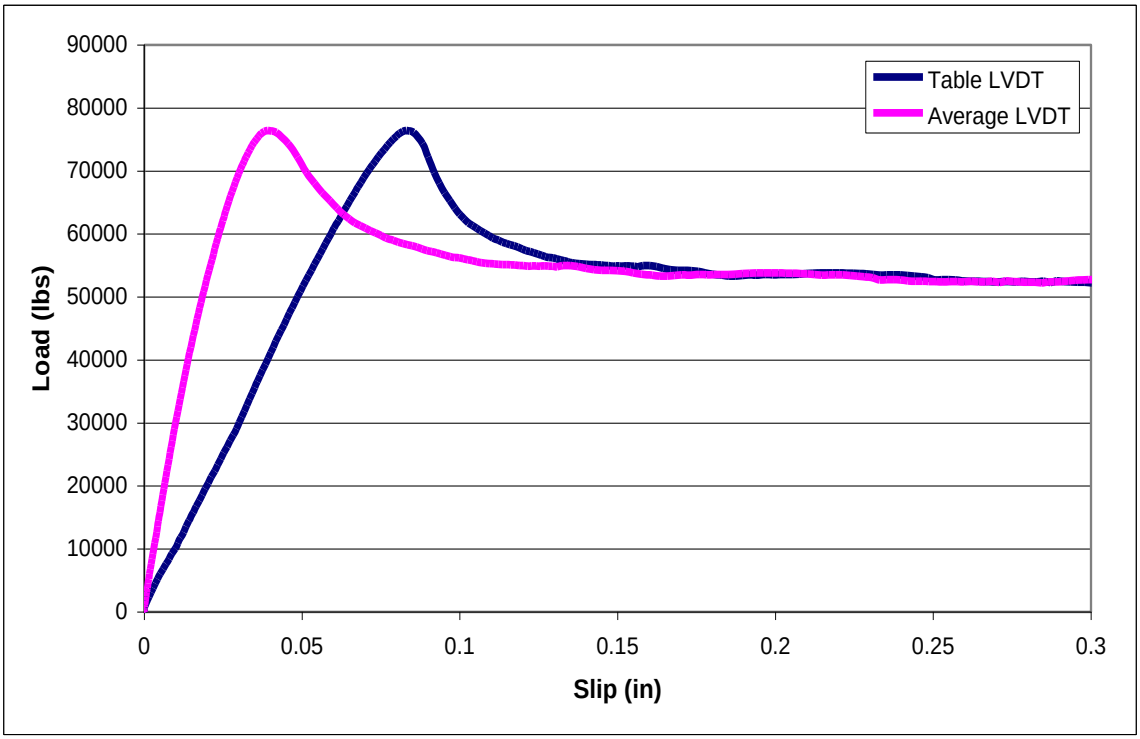

Figure C36. EP-4B.

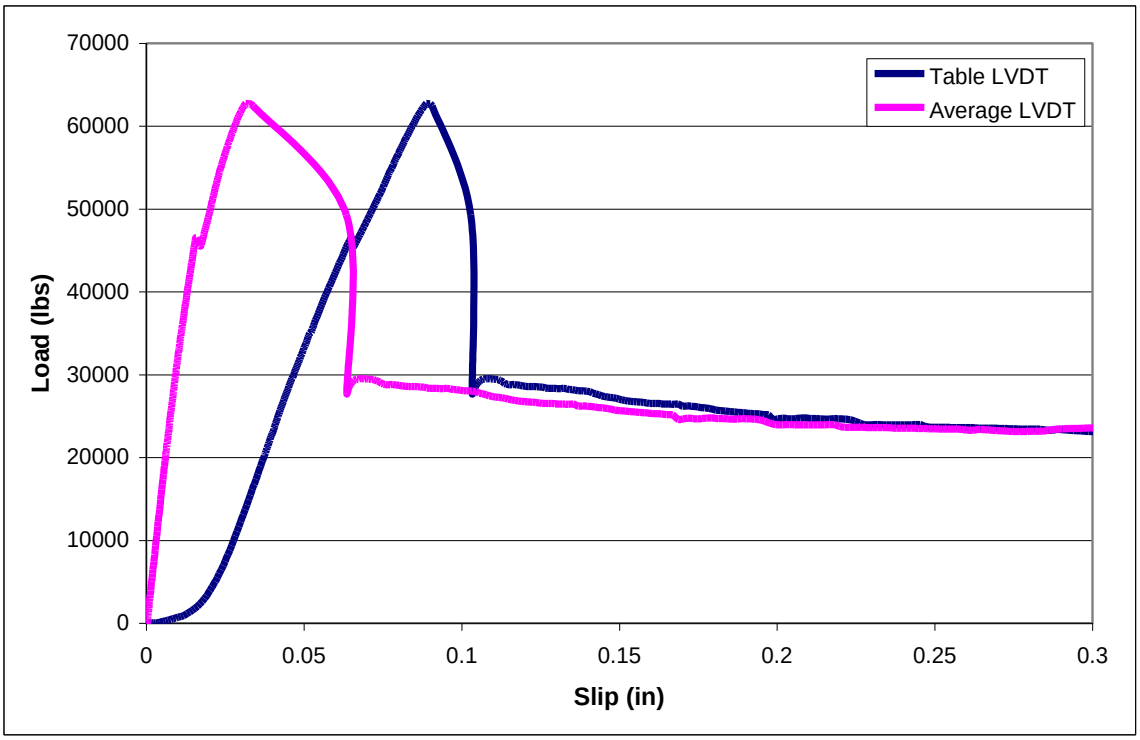

Figure C37. EP-4C.

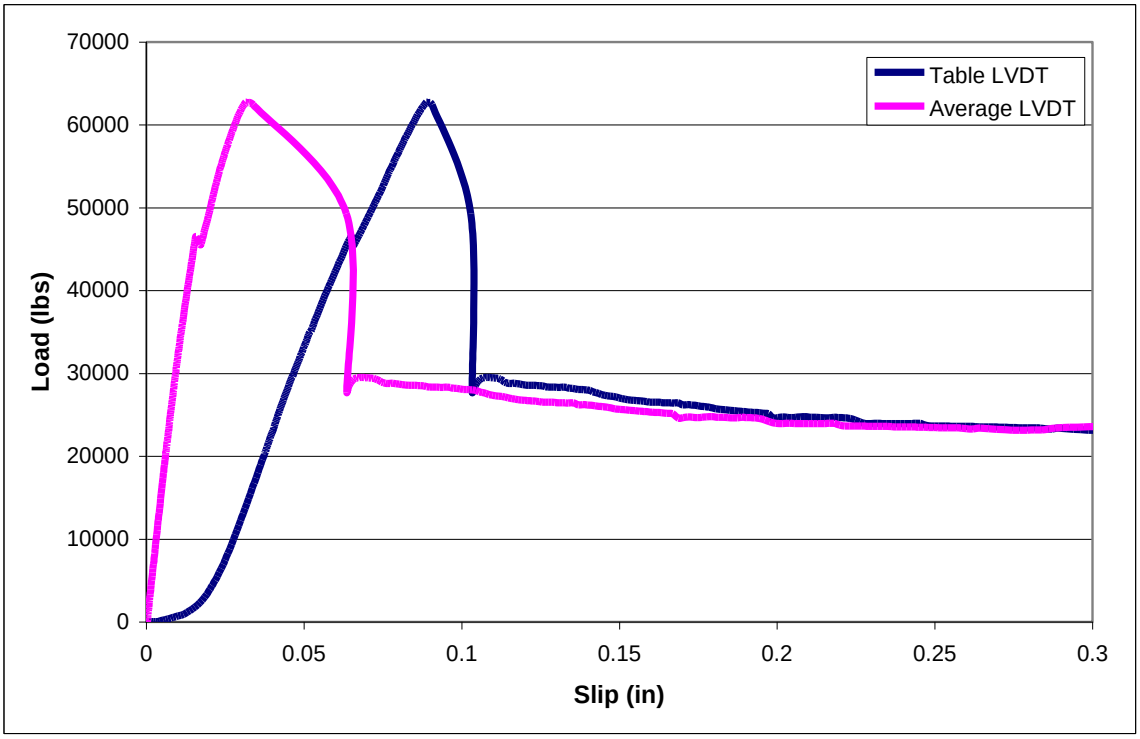

Figure C38. BU-1A.

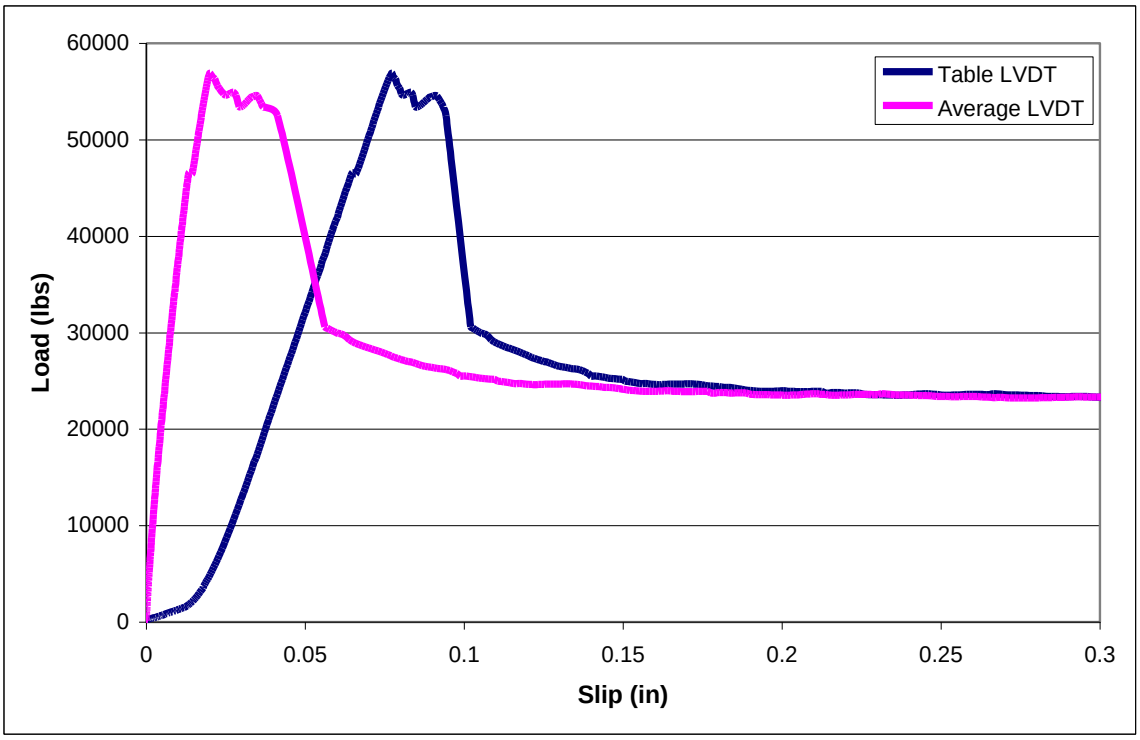

Figure C39. BU-1B.

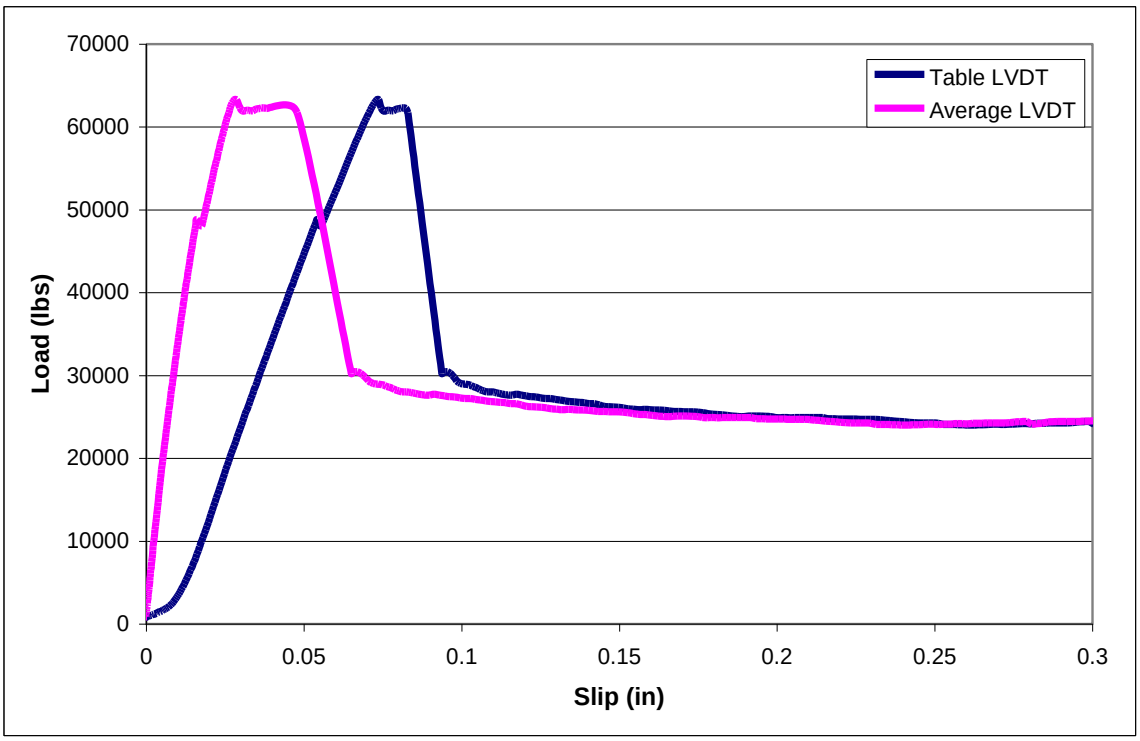

Figure C40. BU-1C.

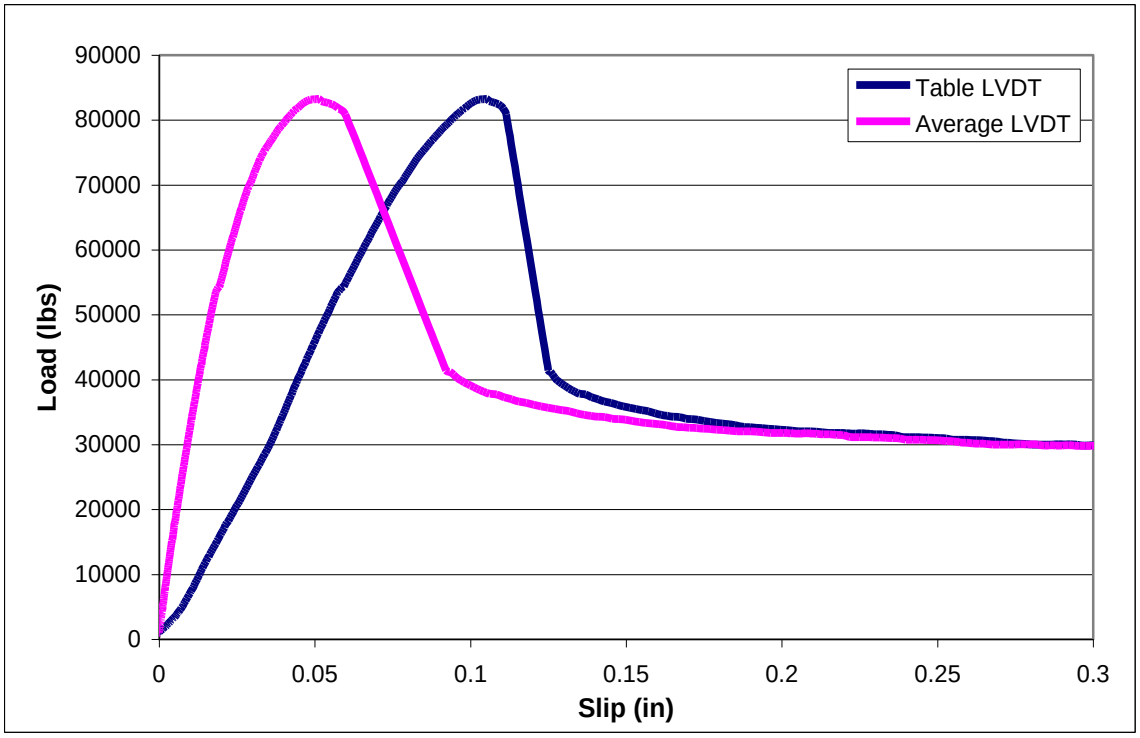

Figure C41. BU-2A.

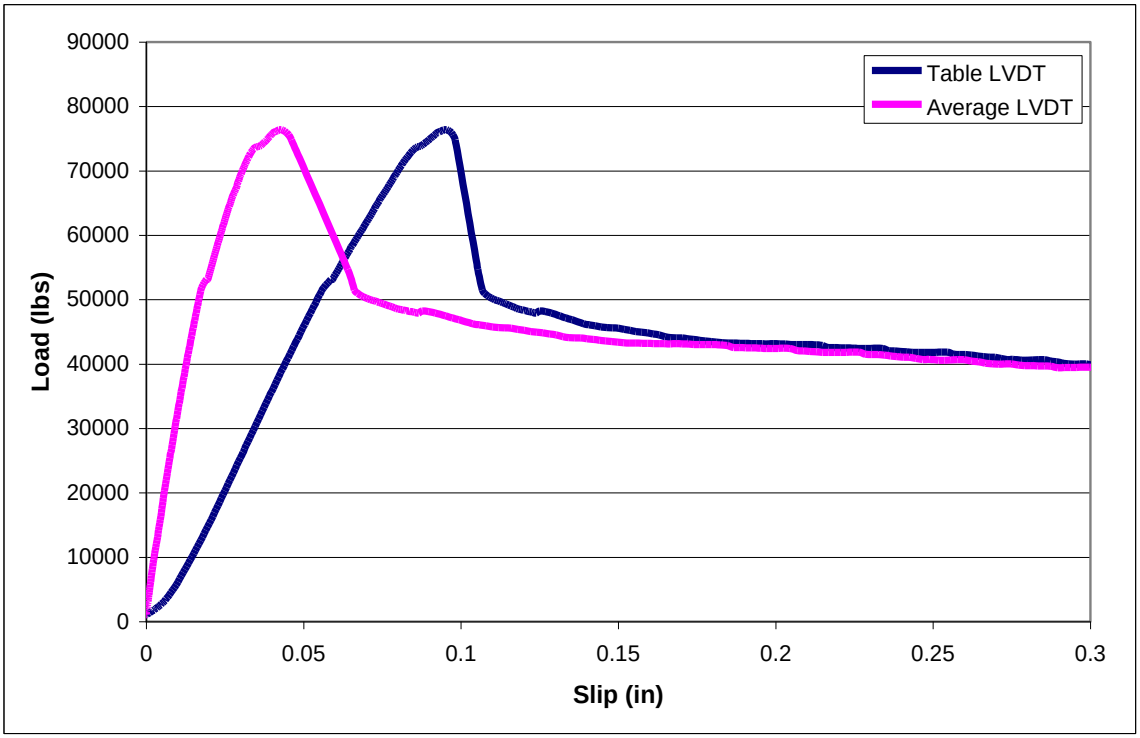

Figure C42. BU-2B.

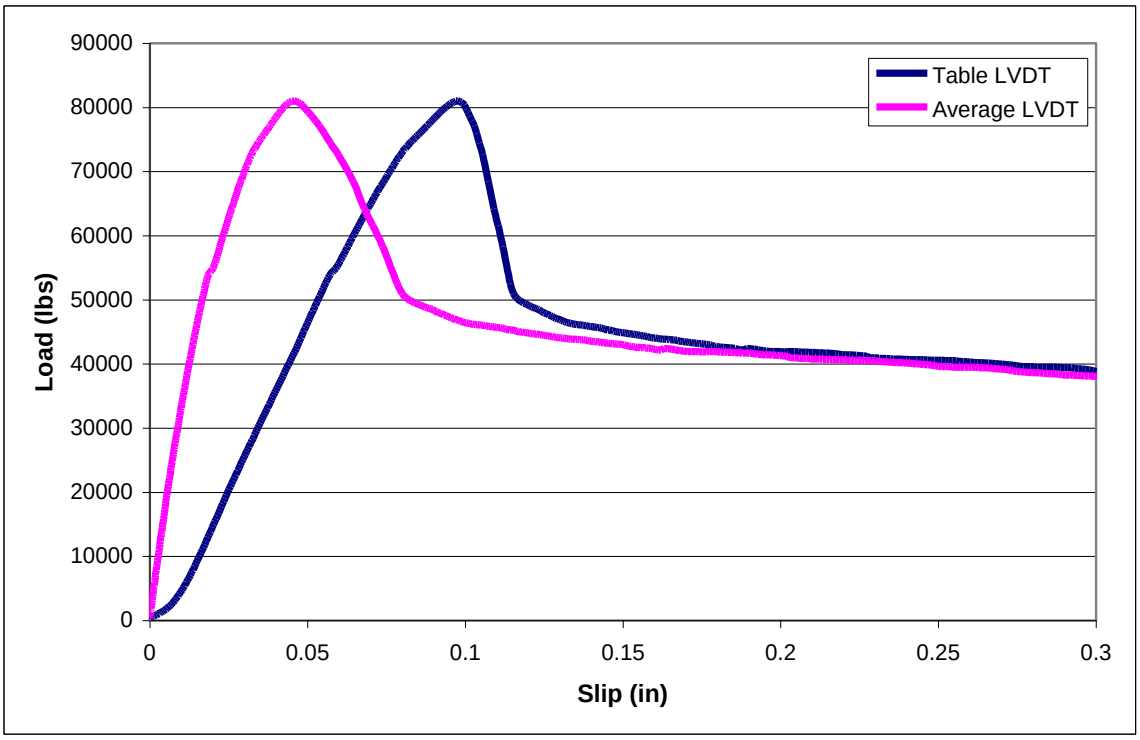

Figure C43. BU-2C.

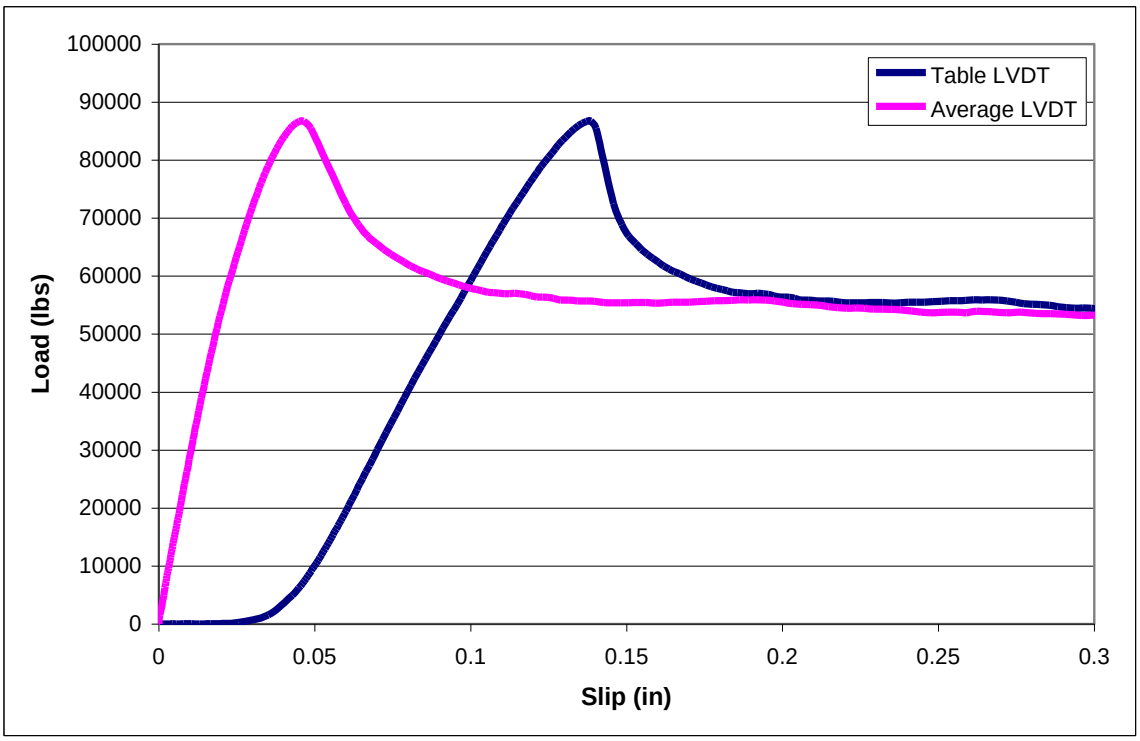

Figure C44. BU-3A.

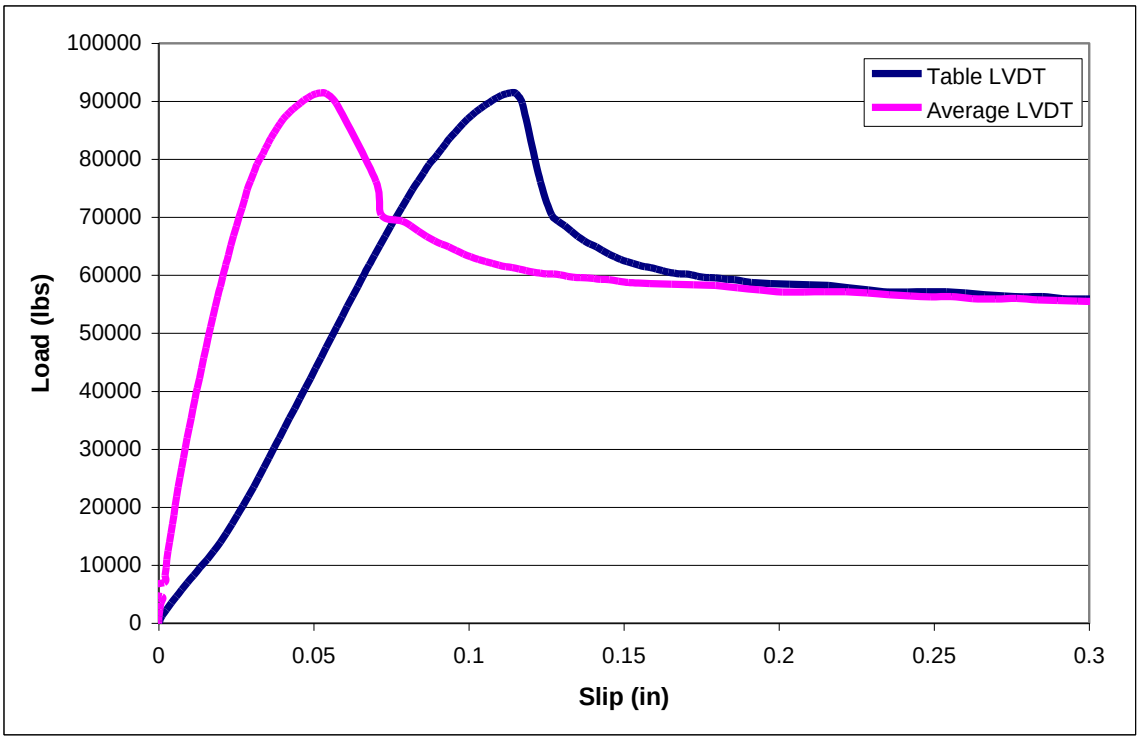

Figure C45. BU-3B.

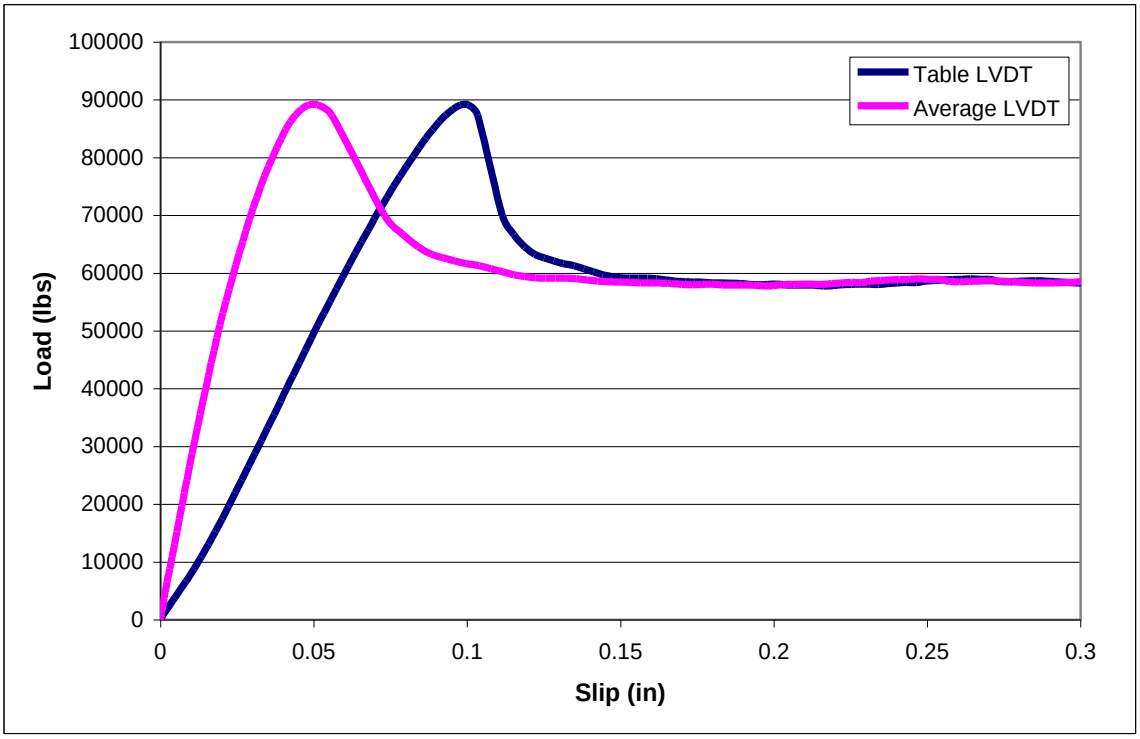

Figure C46. BU-3C.

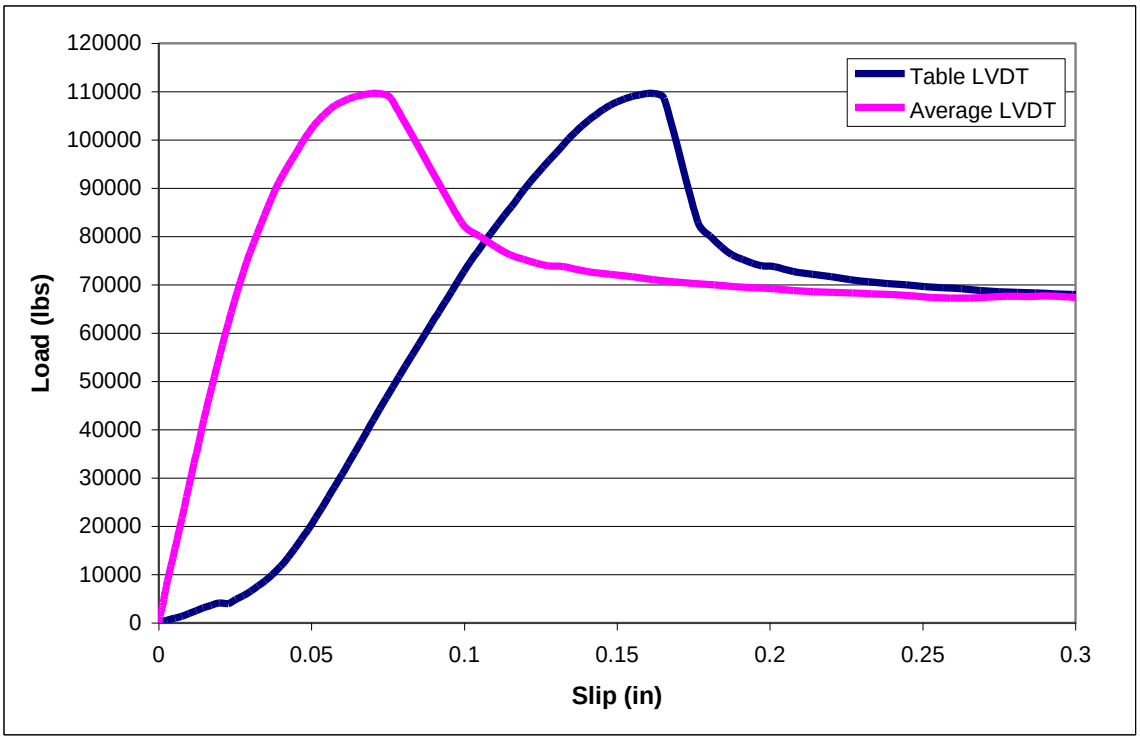

Figure C47. BU-4A.

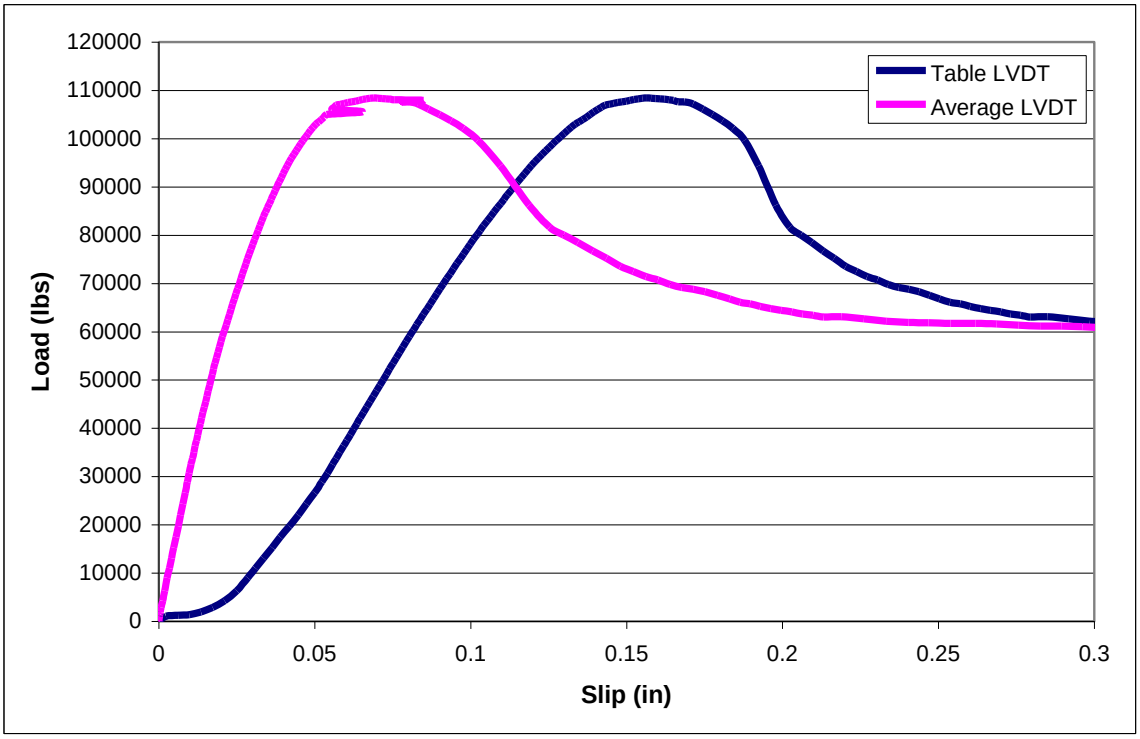

Figure C48. BU-4B.

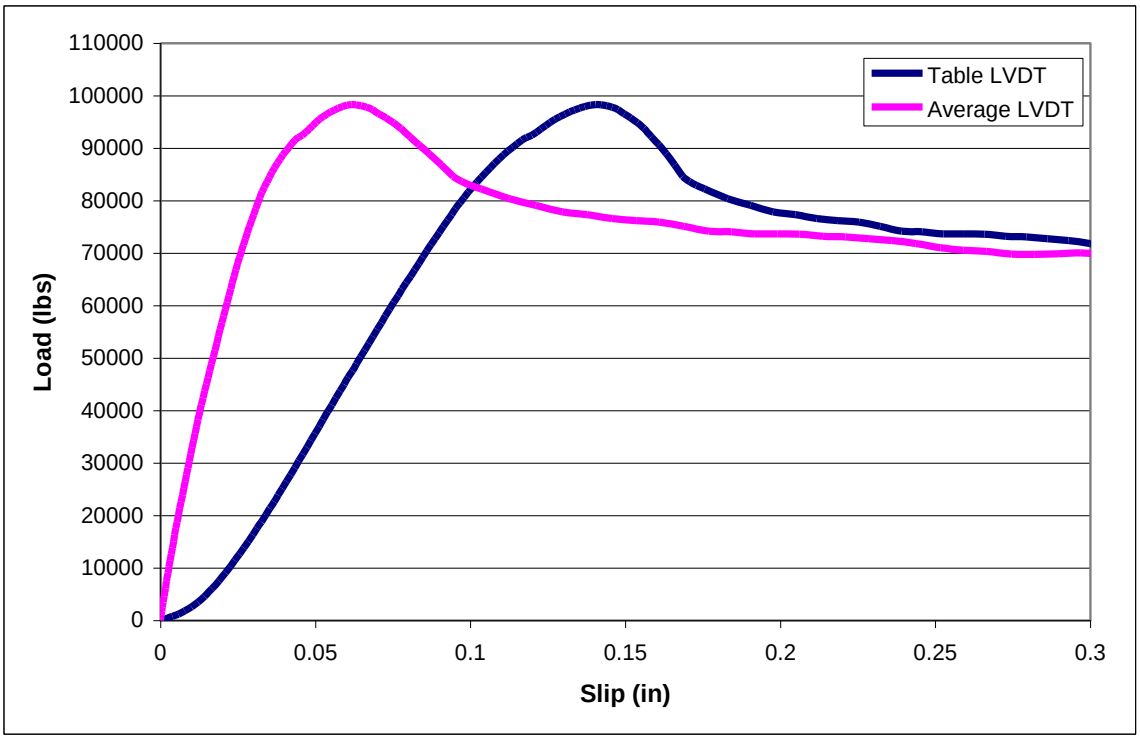

Figure C49. BU-4C.

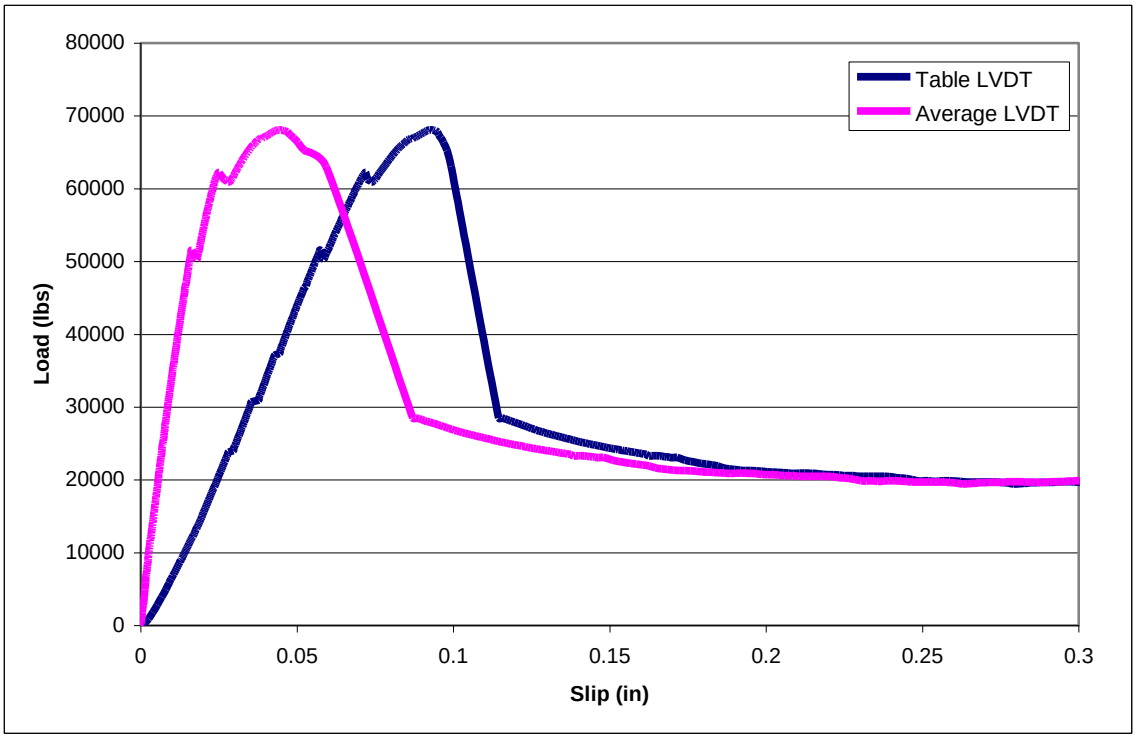

Figure C50. EU-1A.

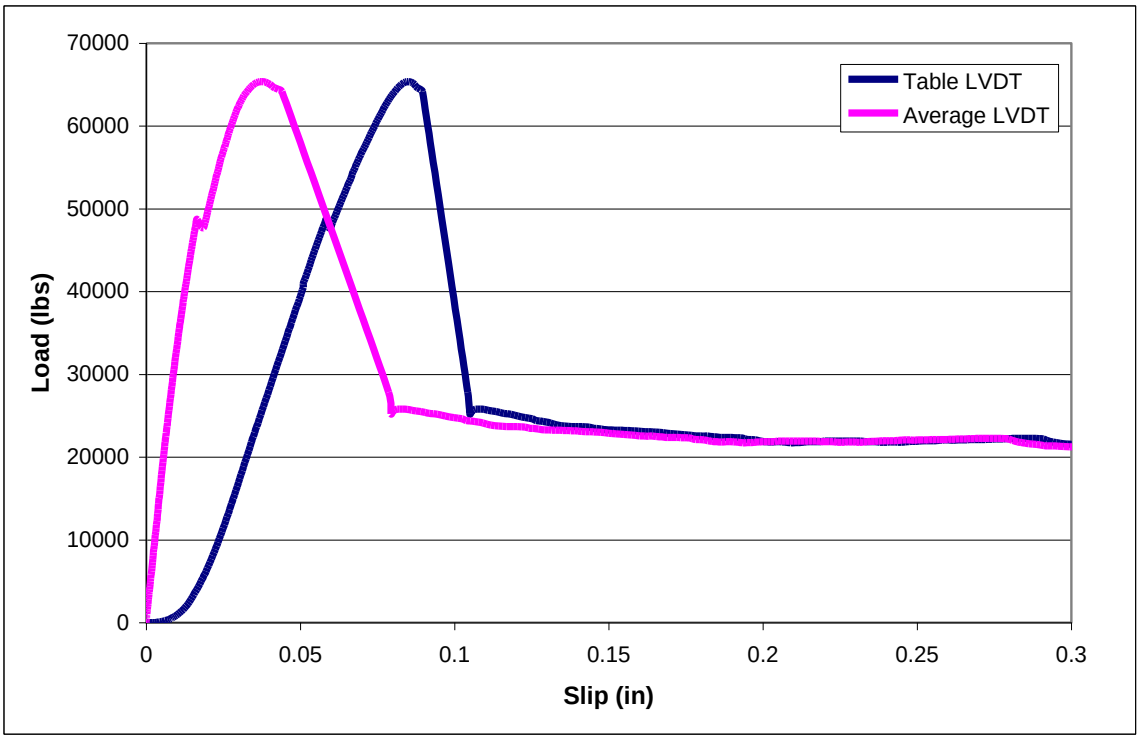

Figure C51. EU-1B.

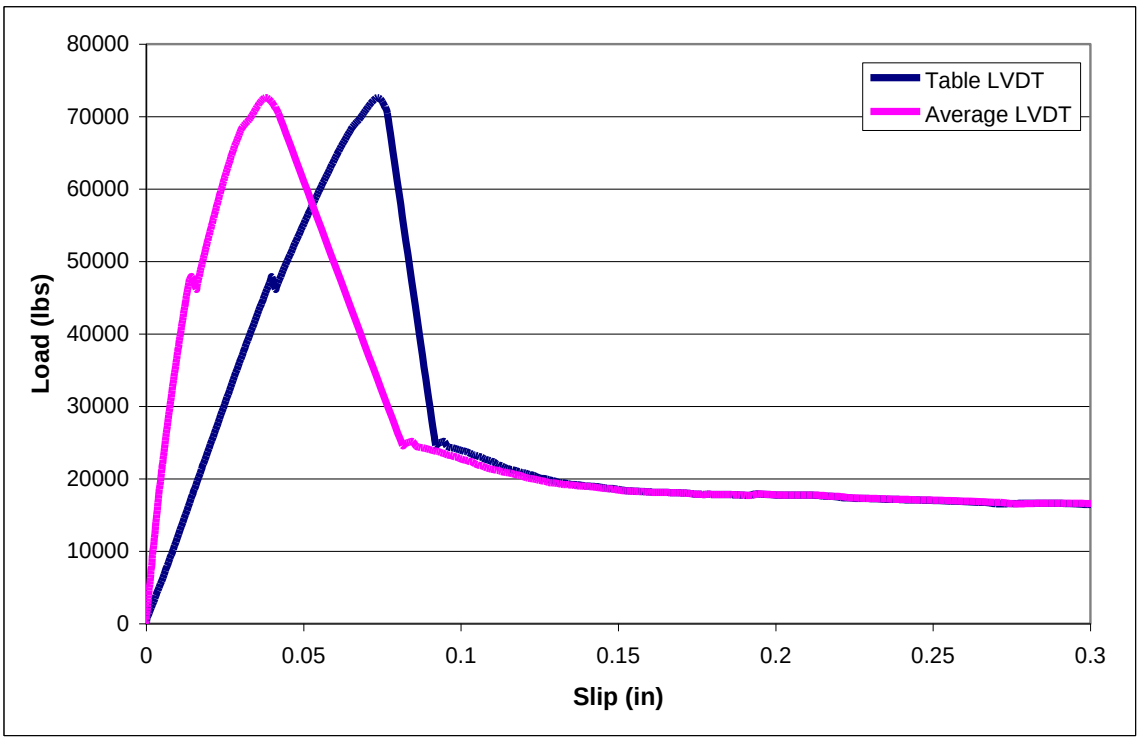

Figure C52. EU-1C.

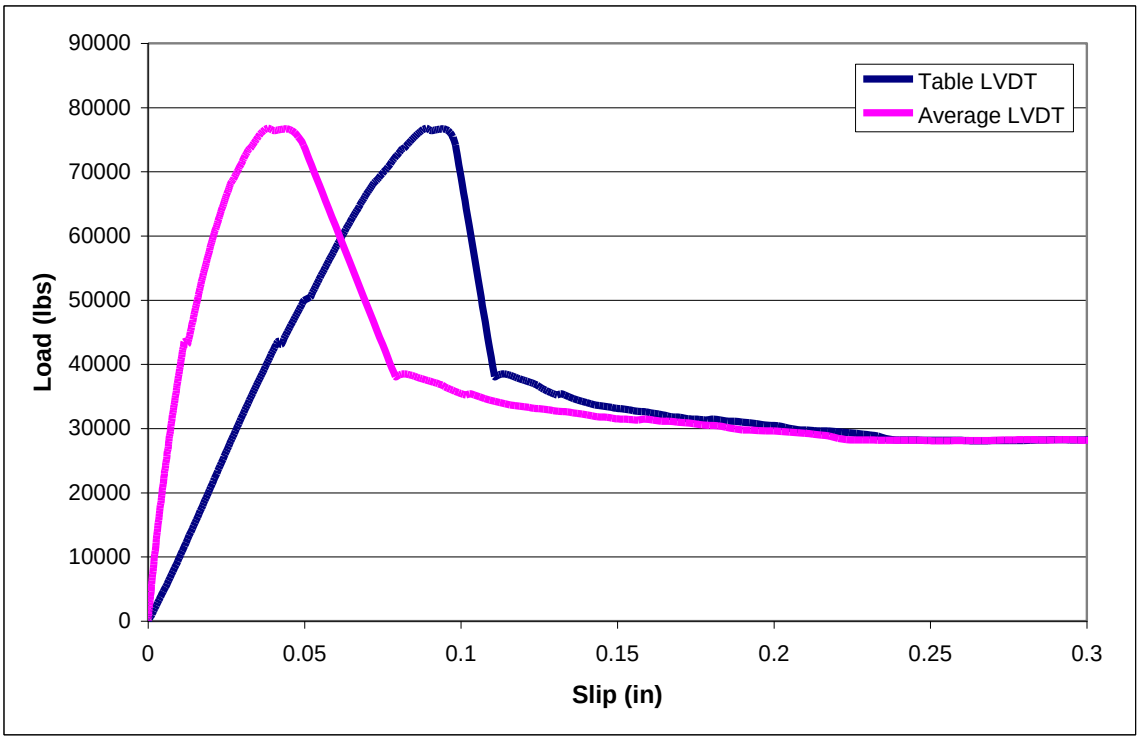

Figure C53. EU-2A.

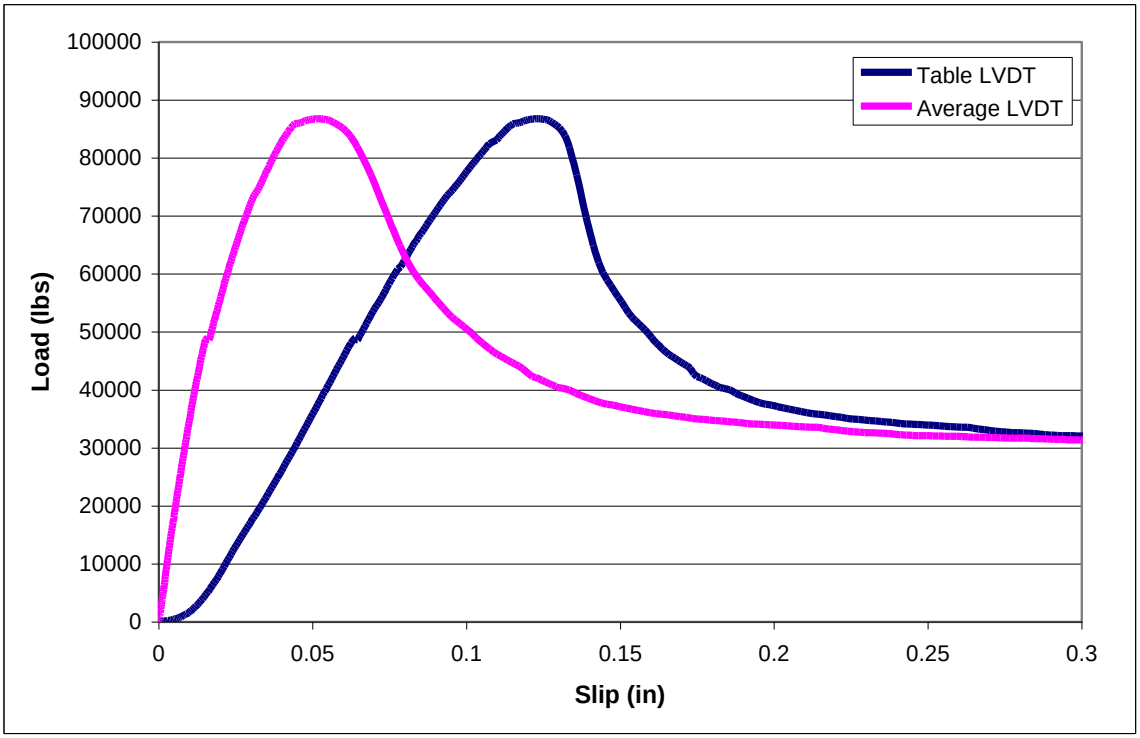

Figure C54. EU-2B.

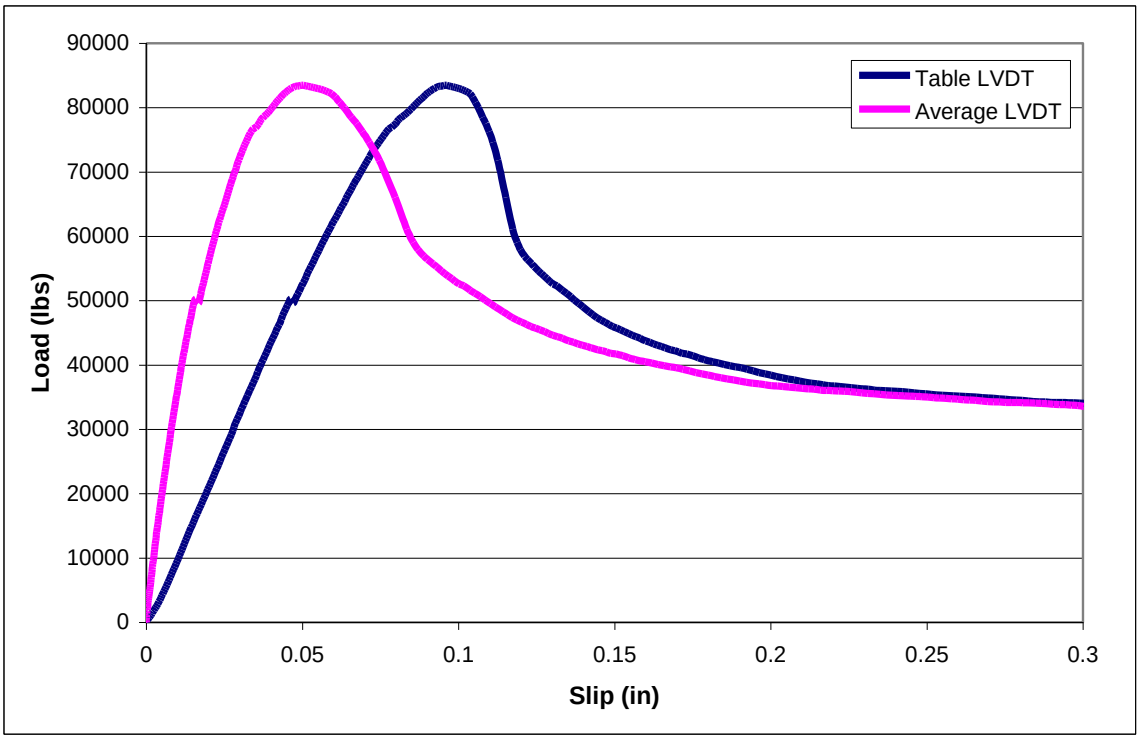

Figure C55. EU-2C.

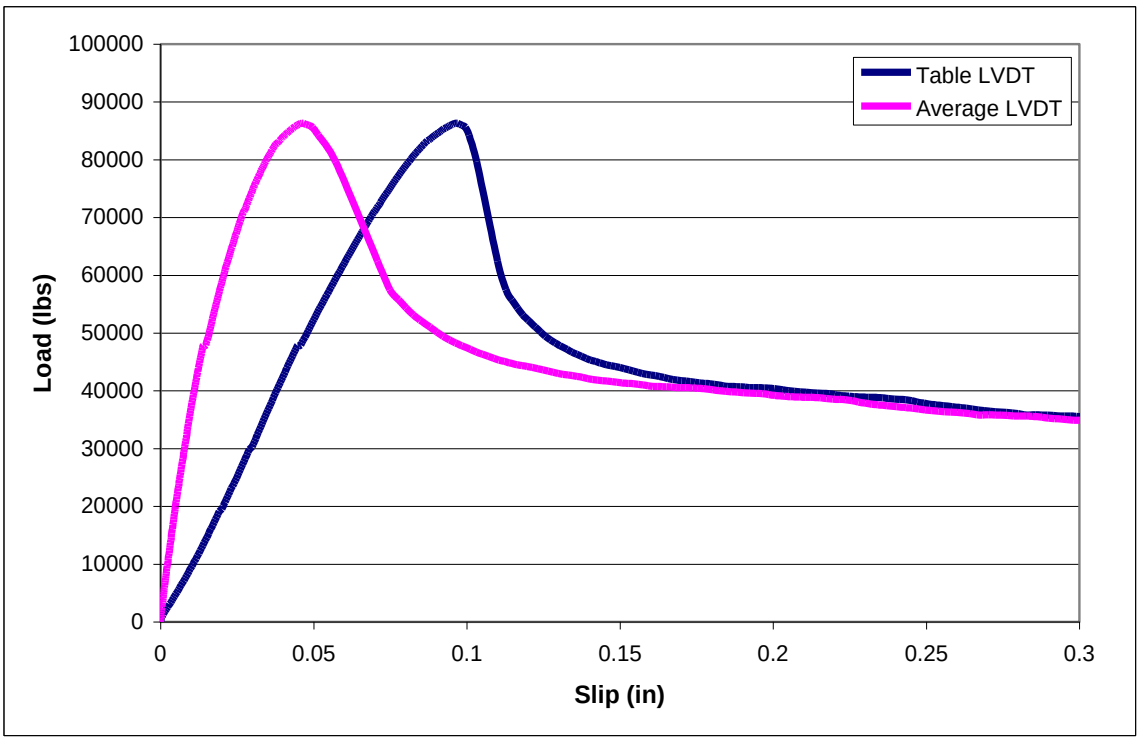

Figure C56. EU-3A.

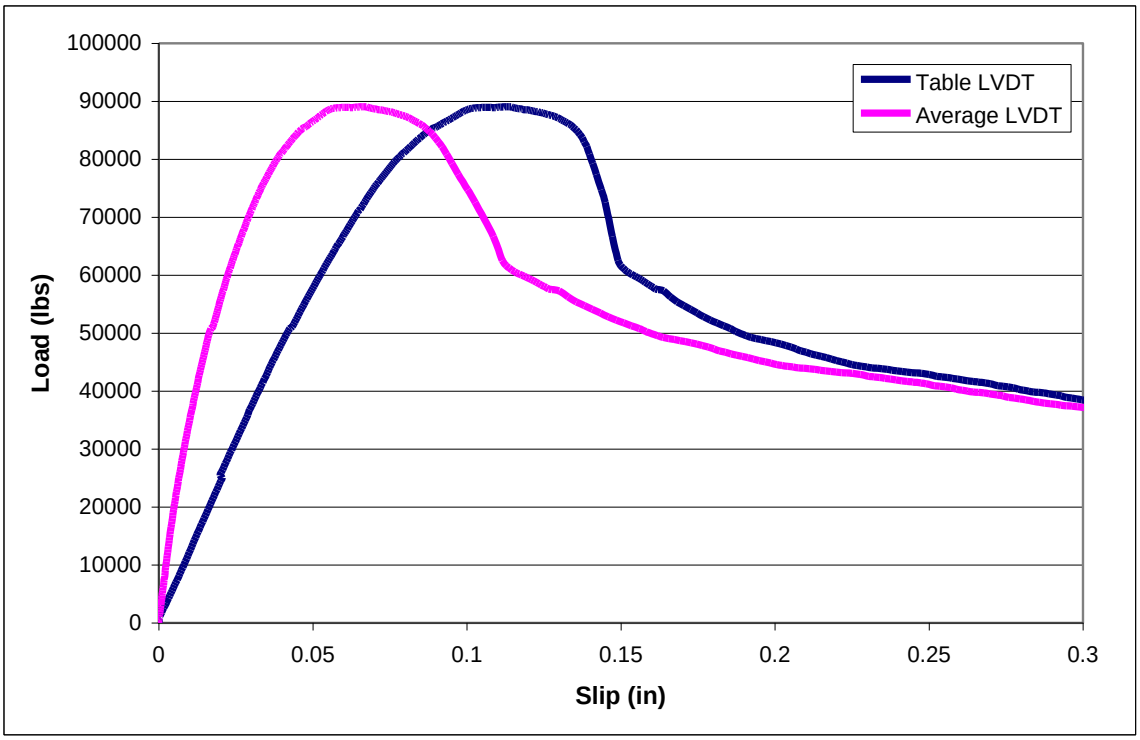

Figure C57. EU-3B.

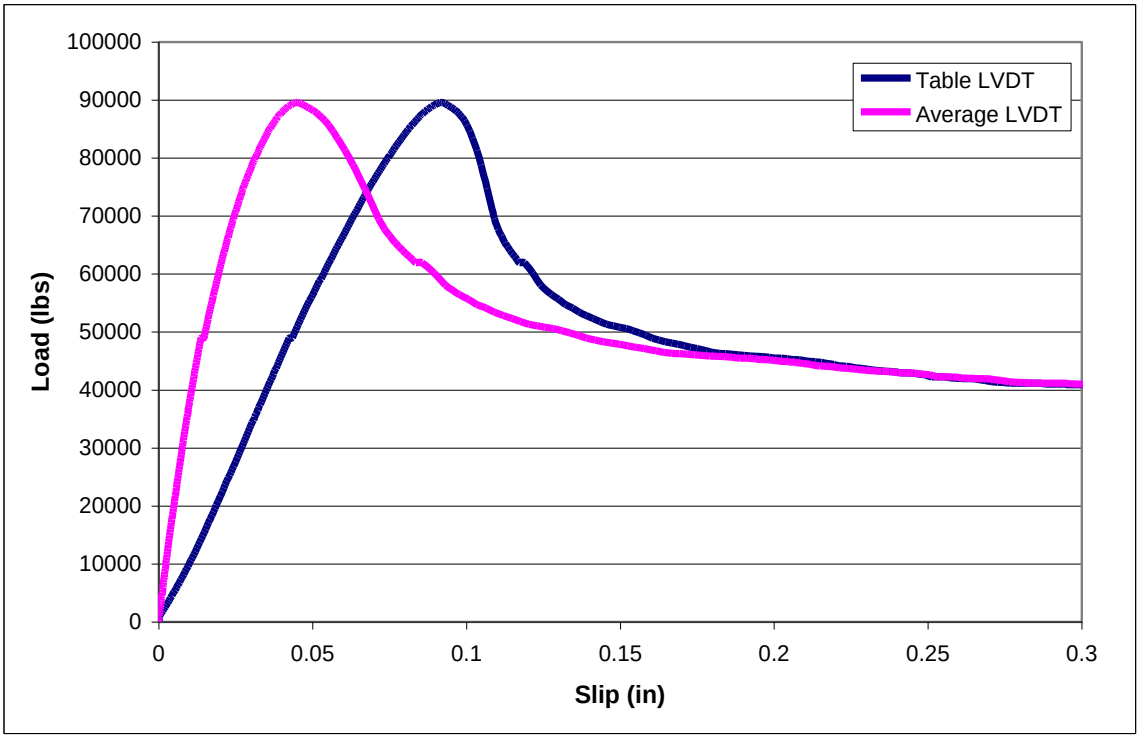

Figure C58. EU-3C.

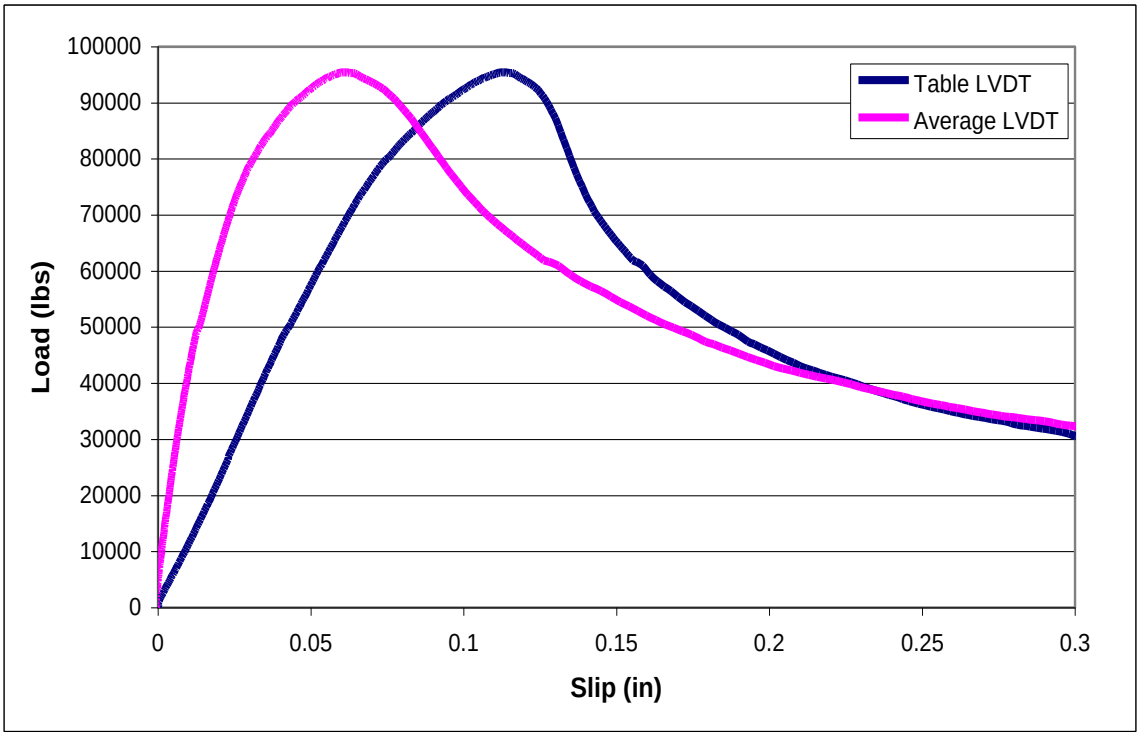

Figure C59. EU-4A.

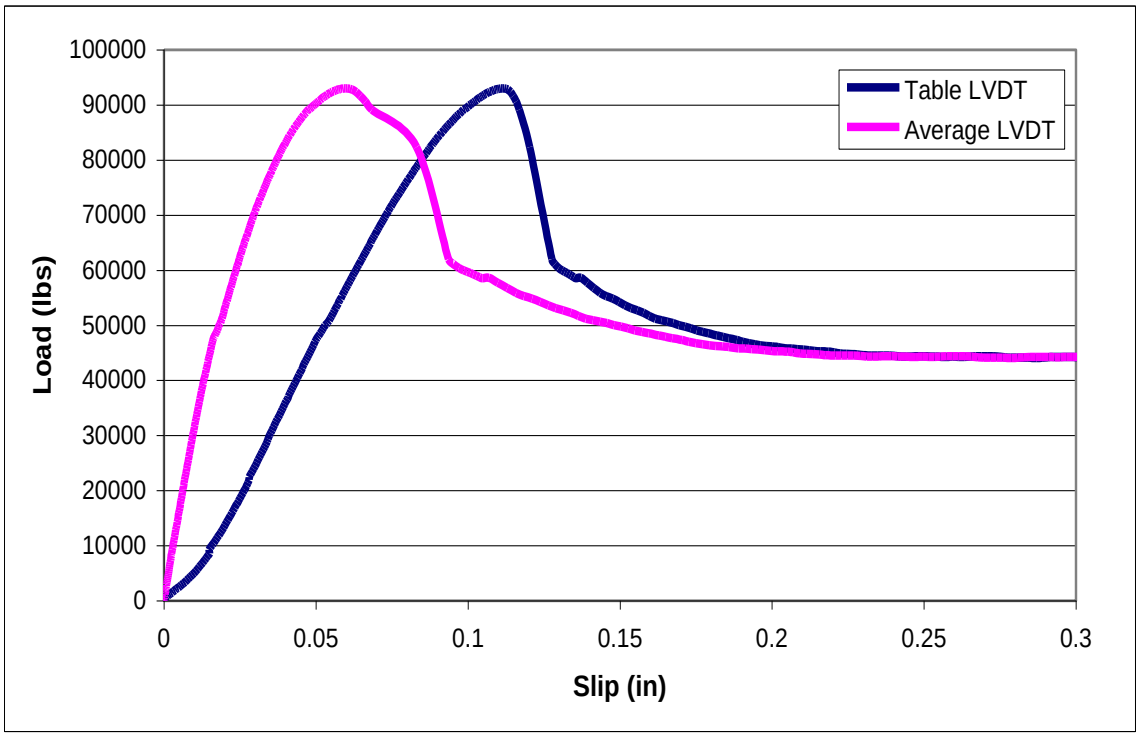

Figure C60. EU-4B.

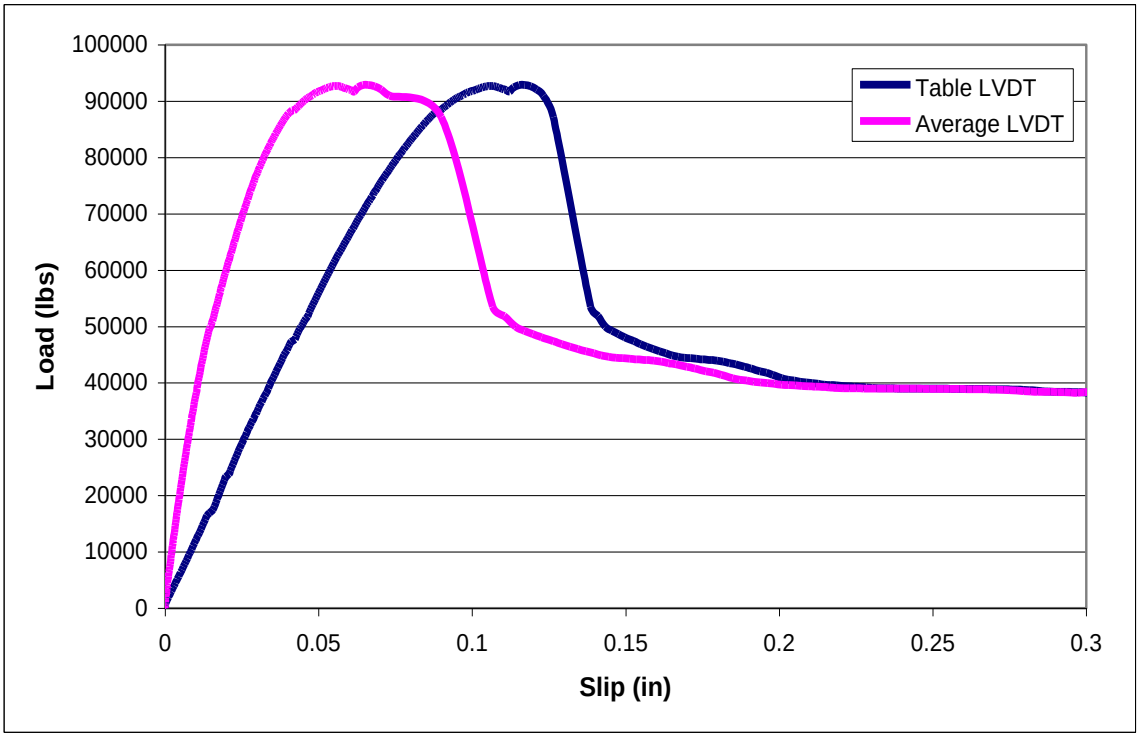

Figure C61. EU-4C.

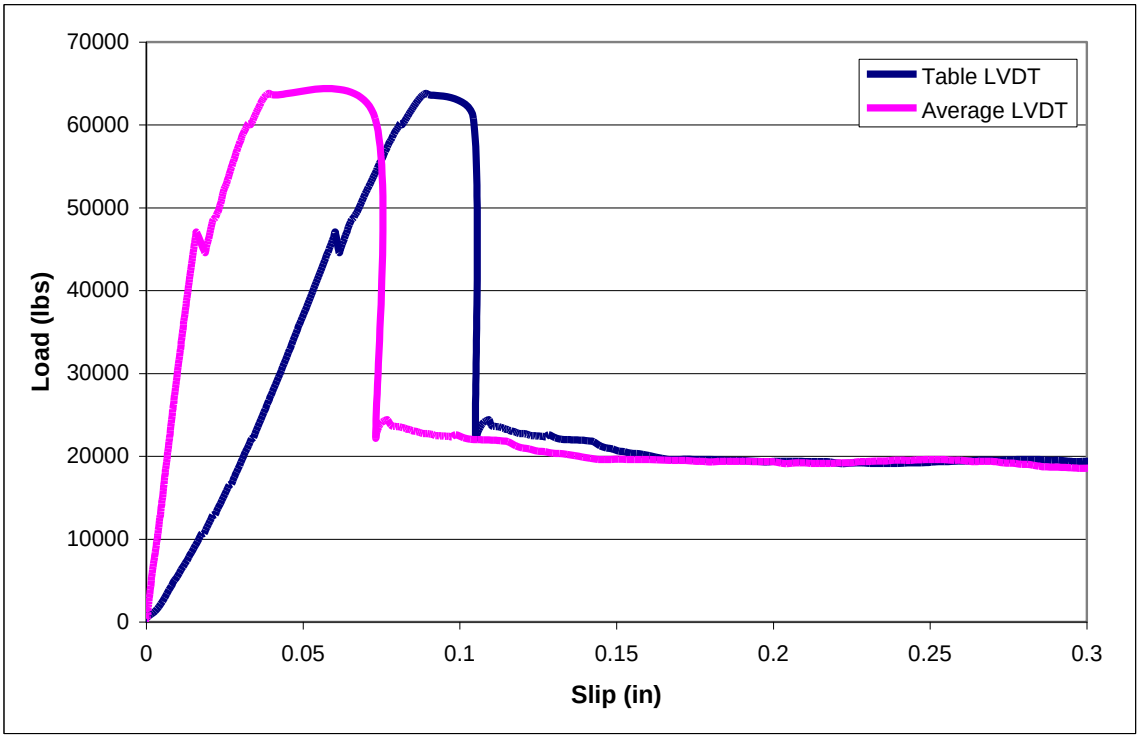

Figure C62. OH-1A.

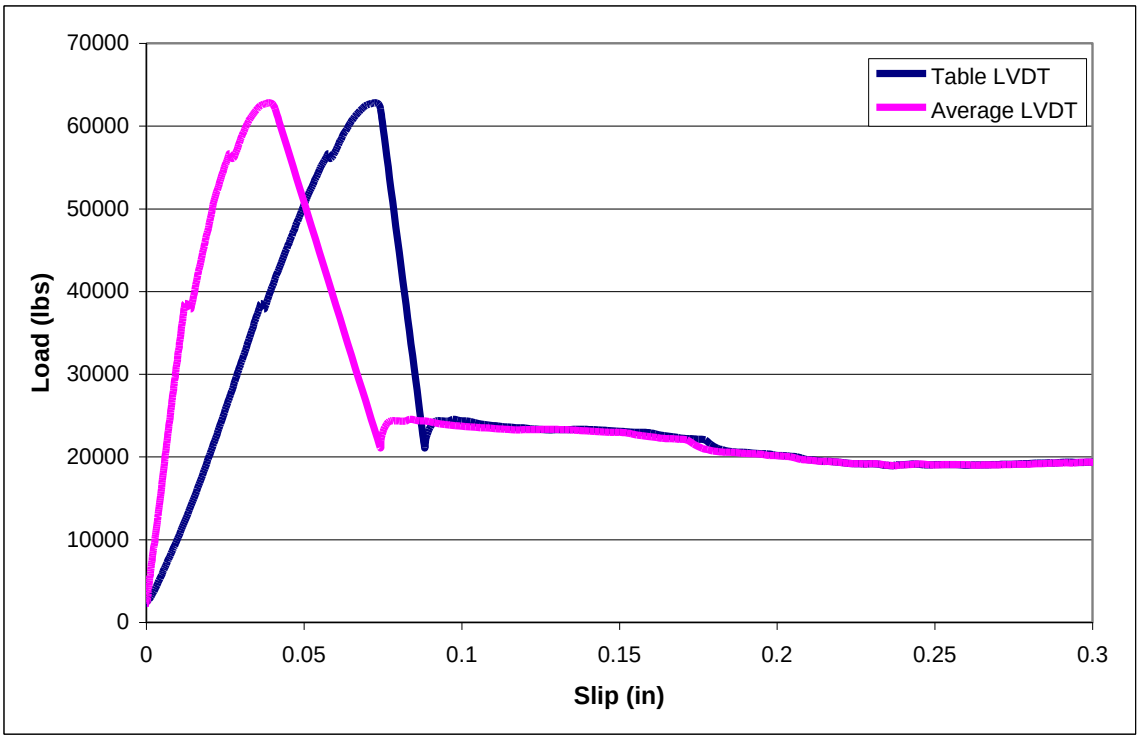

Figure C63. OH-1B.

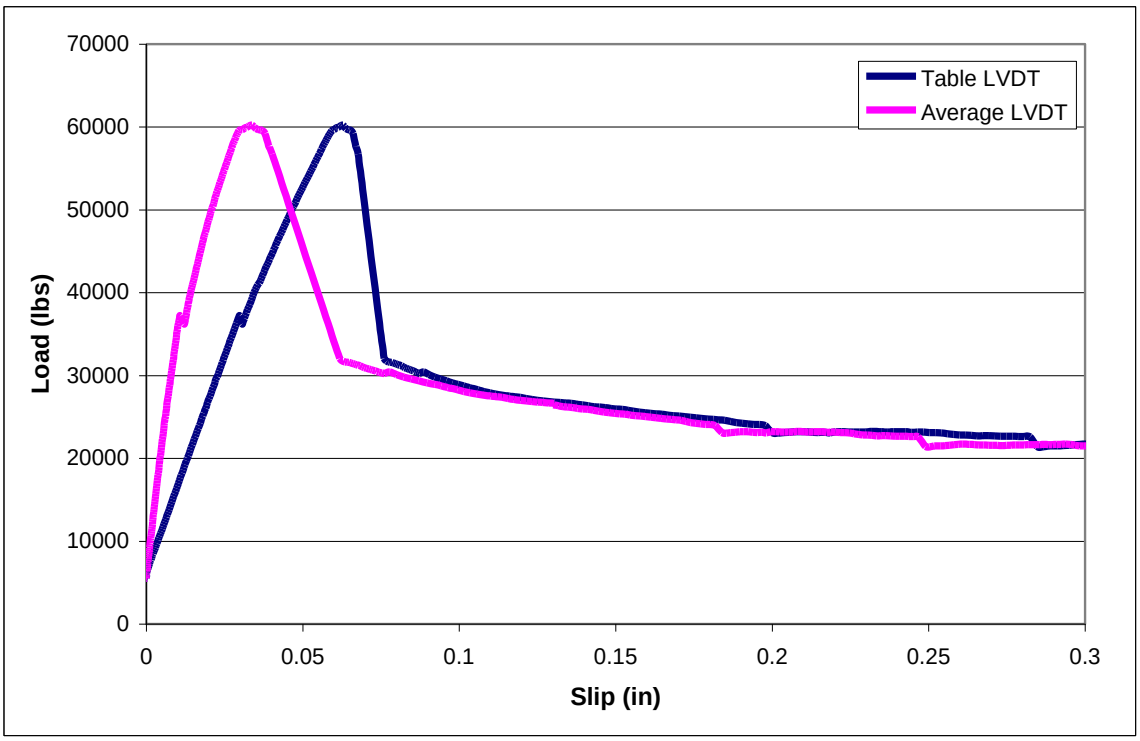

Figure C64. OH-1C.

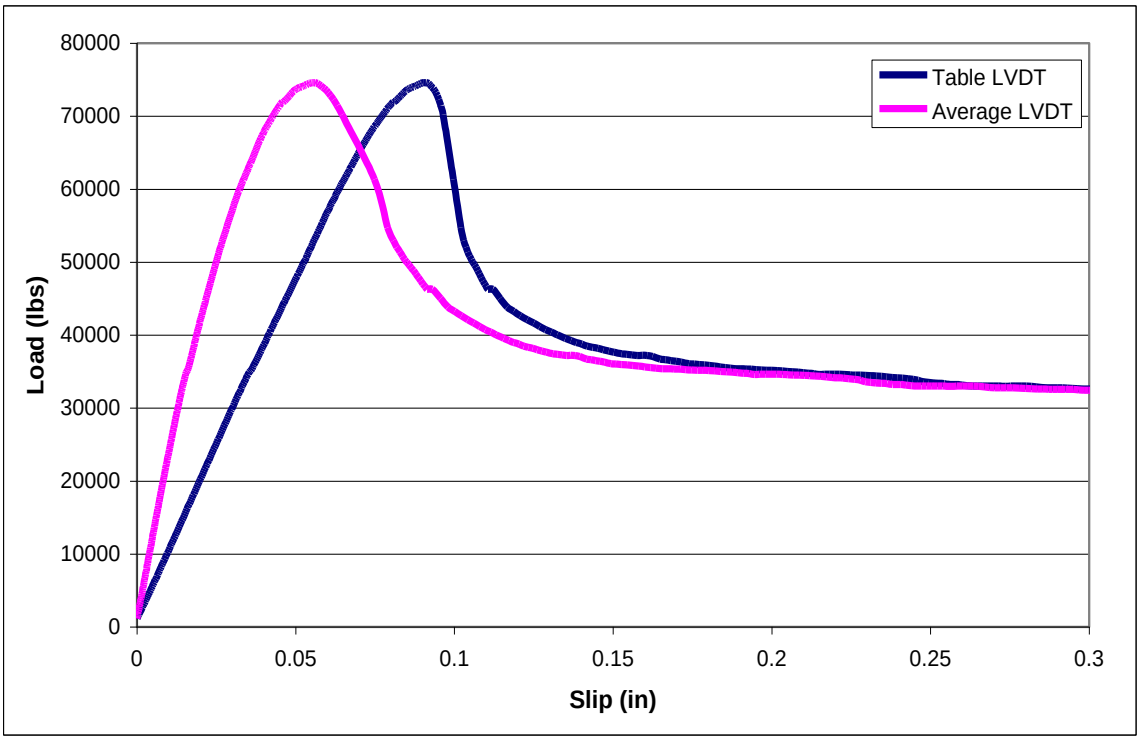

Figure C65. OH-2A.

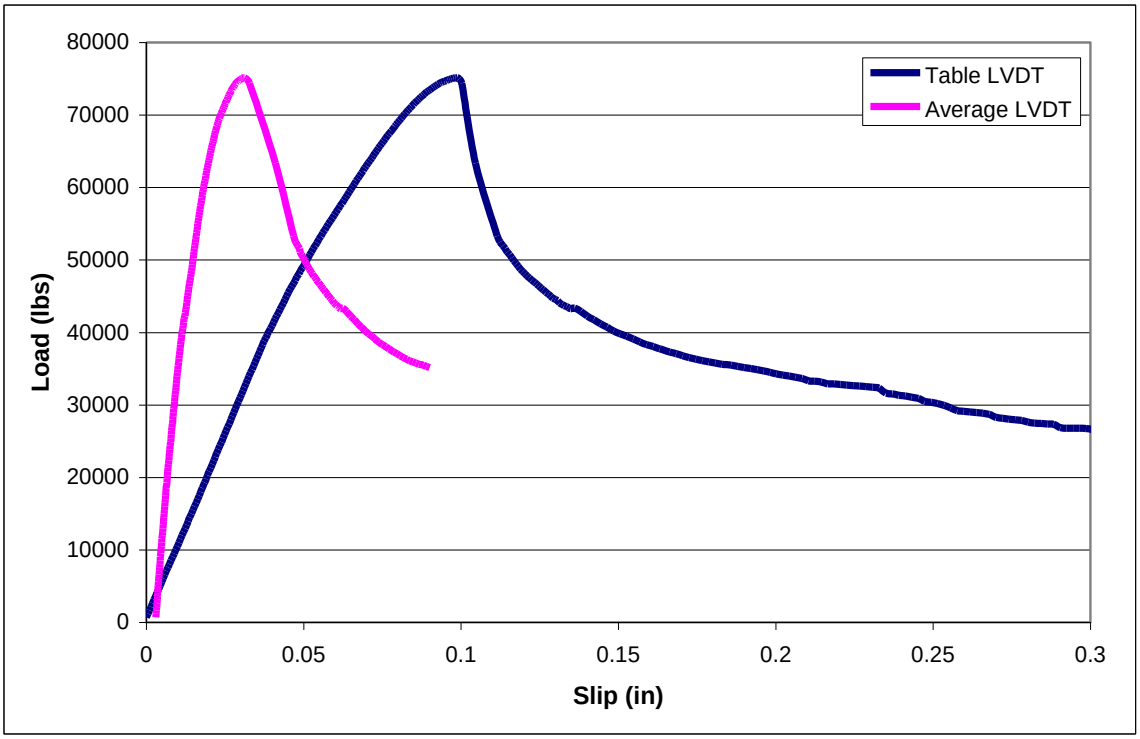

Figure C66. OH-2B.

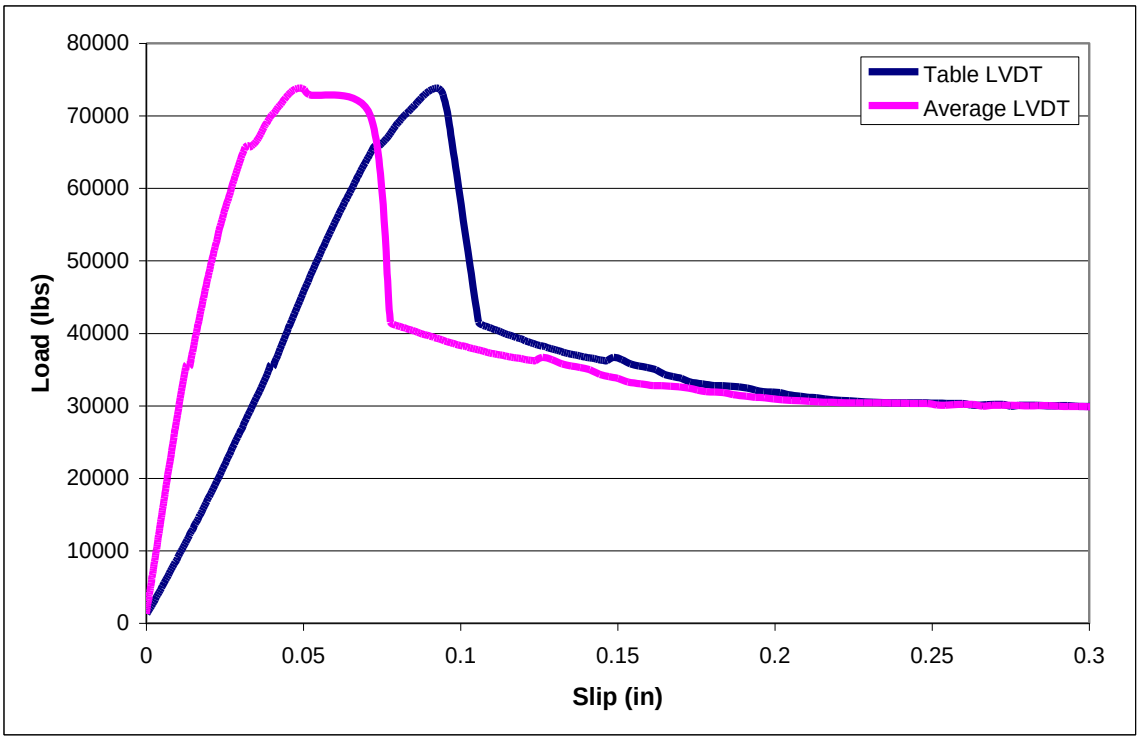

Figure C67. OH-2C.

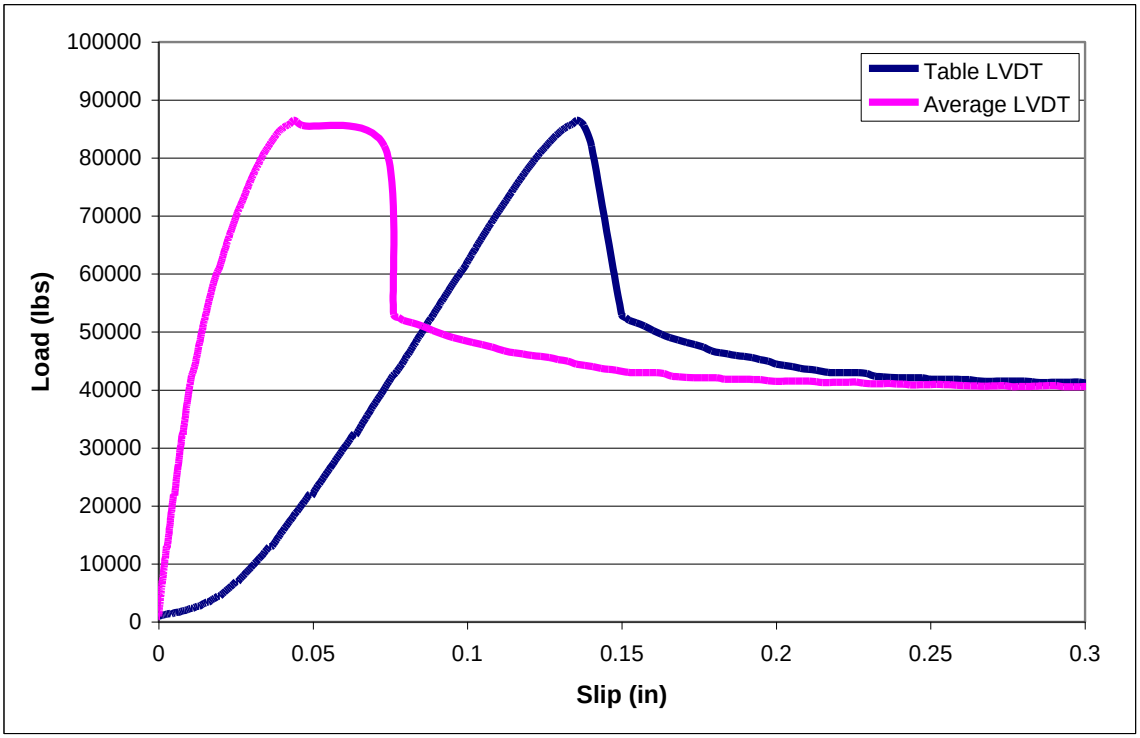

Figure C68. OH-3A.

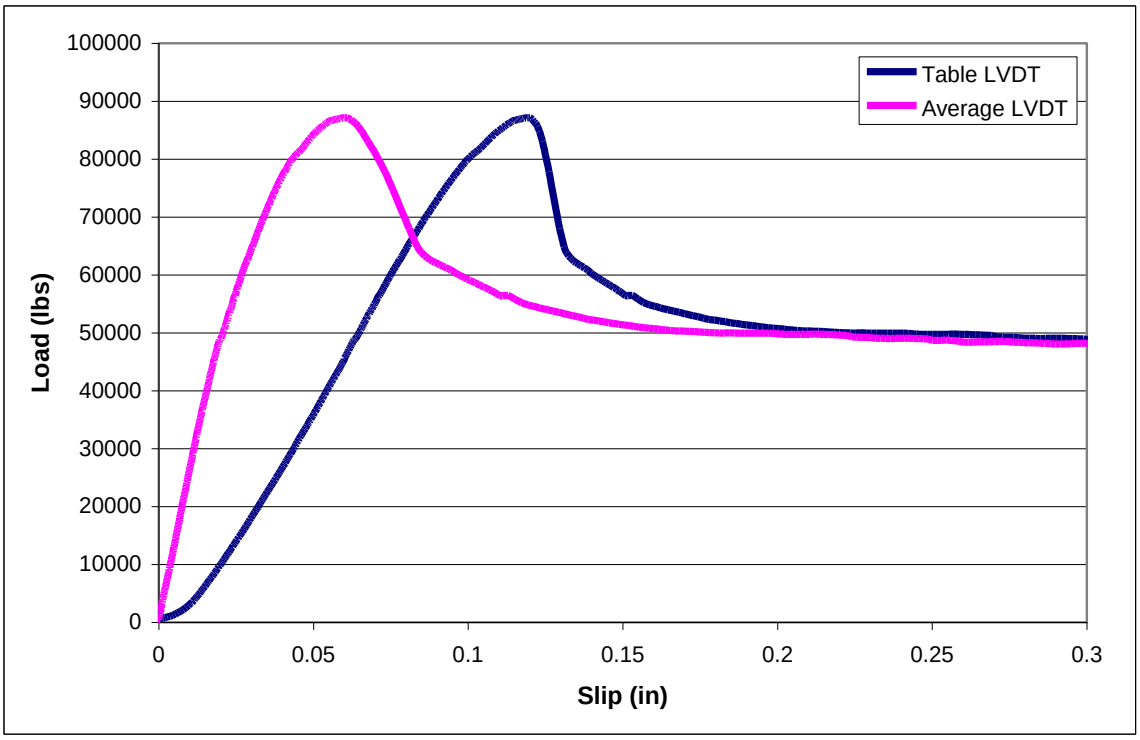

Figure C69. OH-3B.

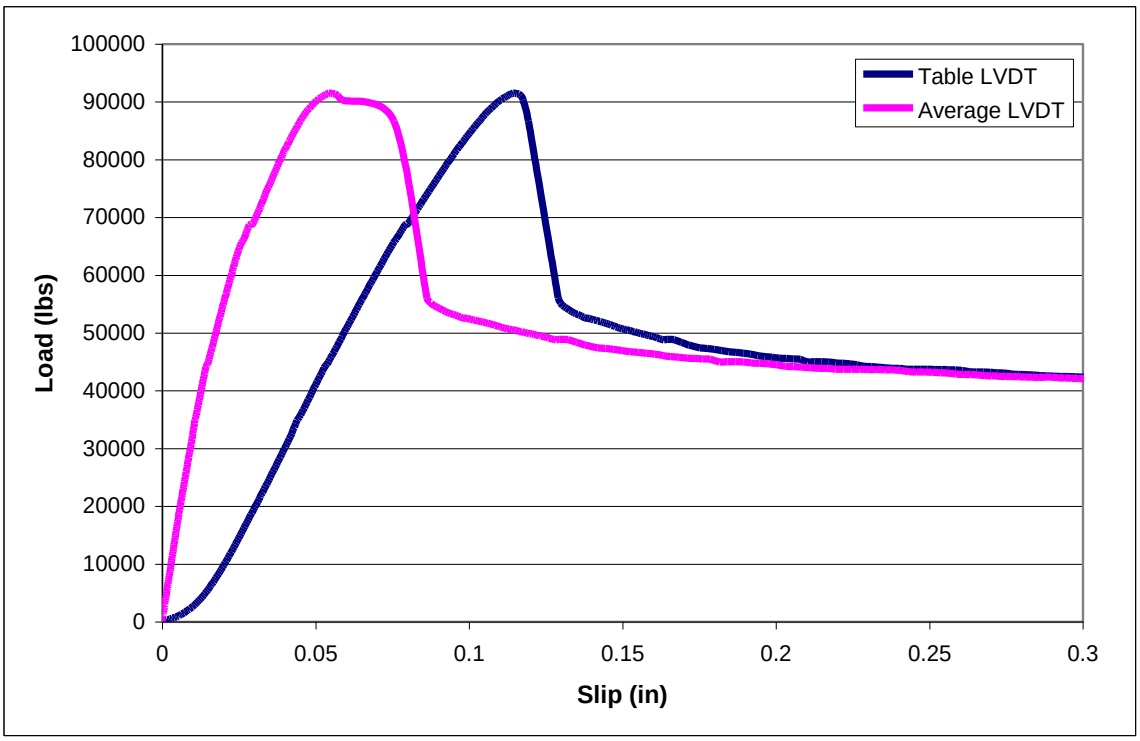

Figure C70. OH-3C.

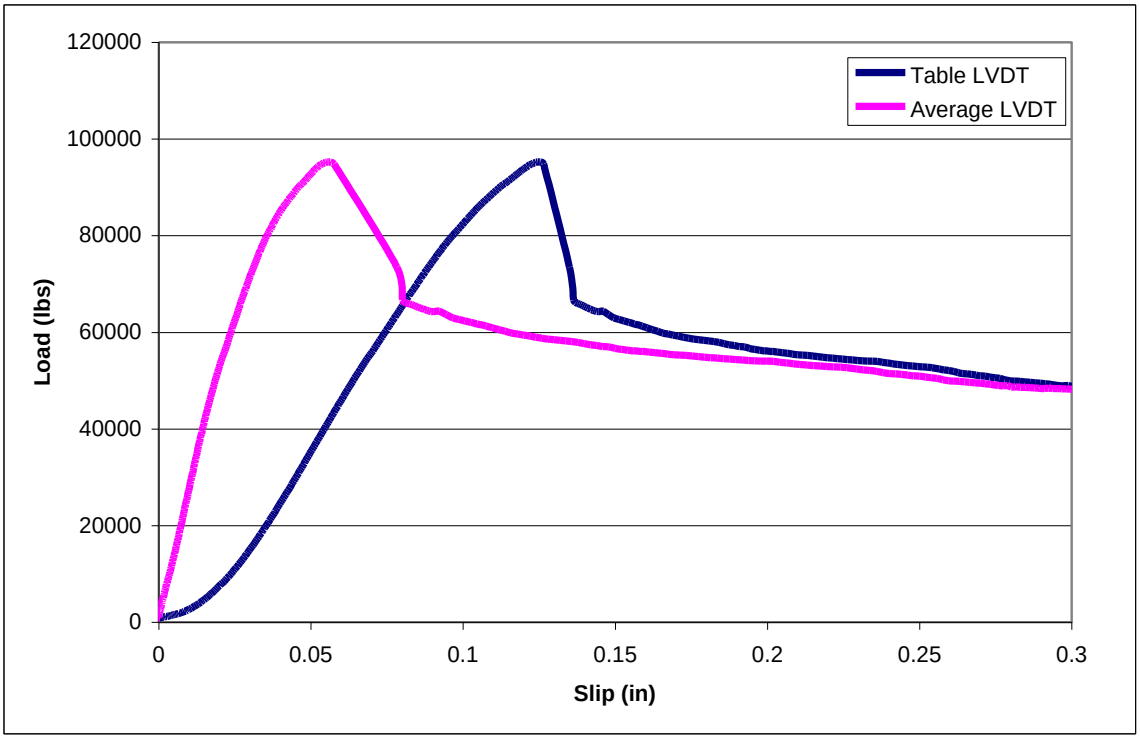

Figure C71. OH-4A.

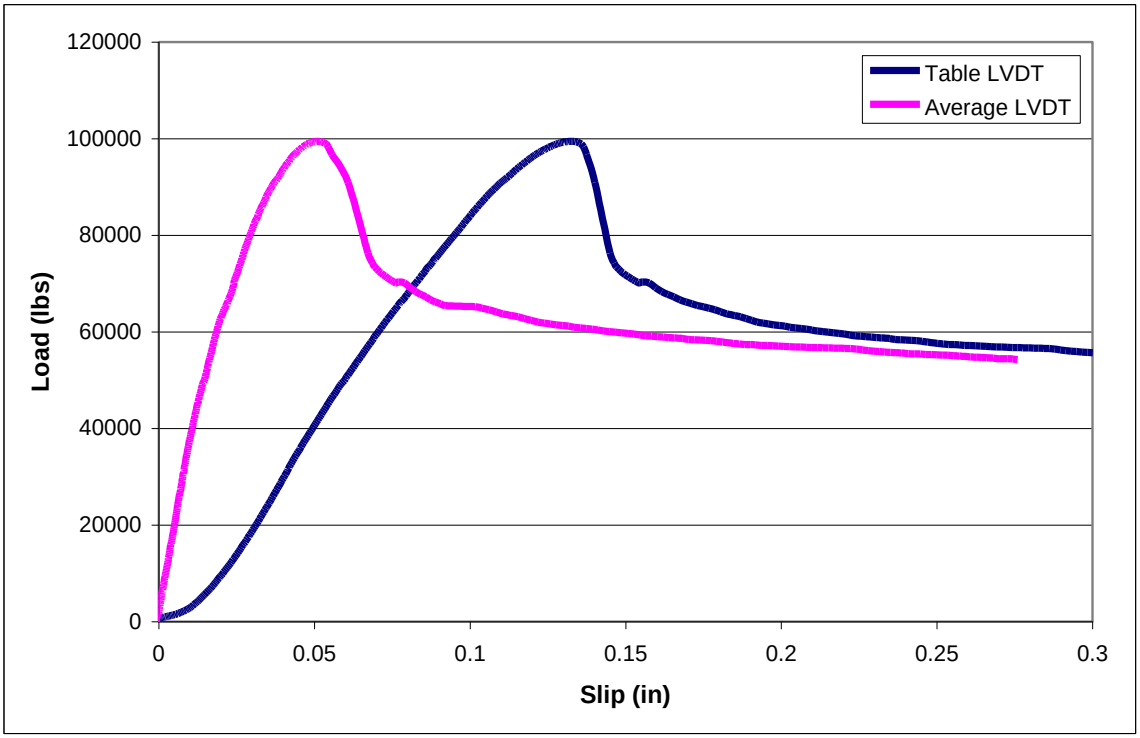

Figure C72. OH-4B.

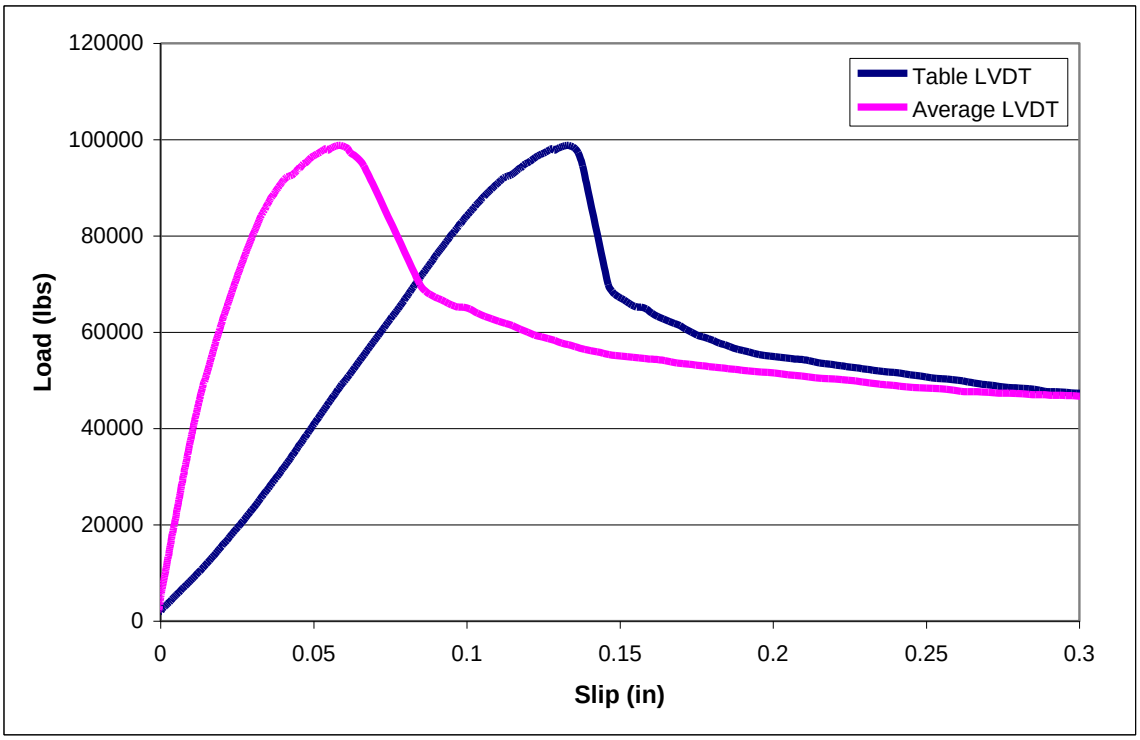

Figure C73. OH-4C.

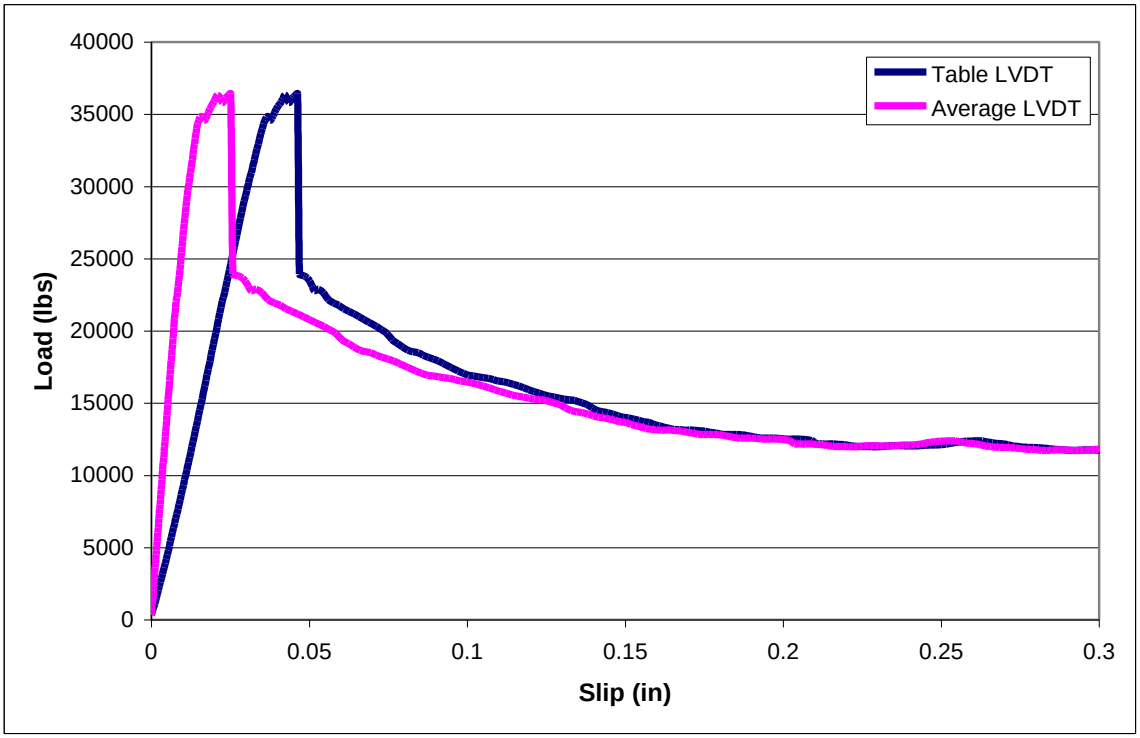

Figure C74. CJC-1A.

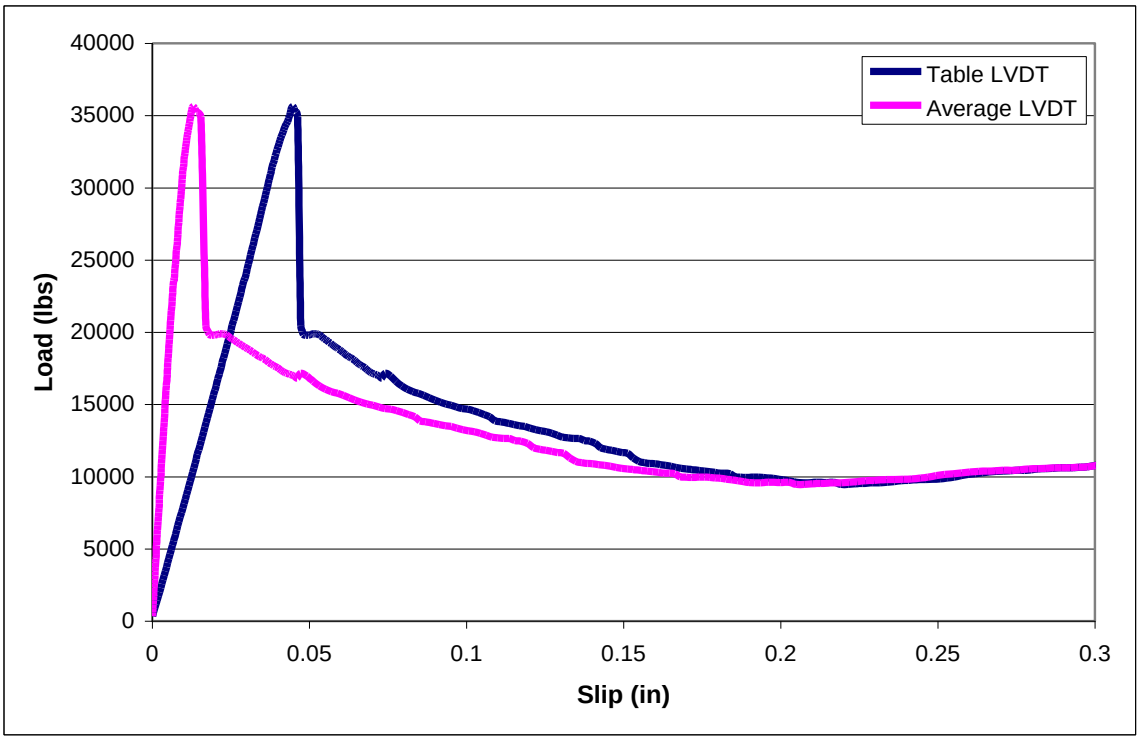

Figure C75. CJC-1B.

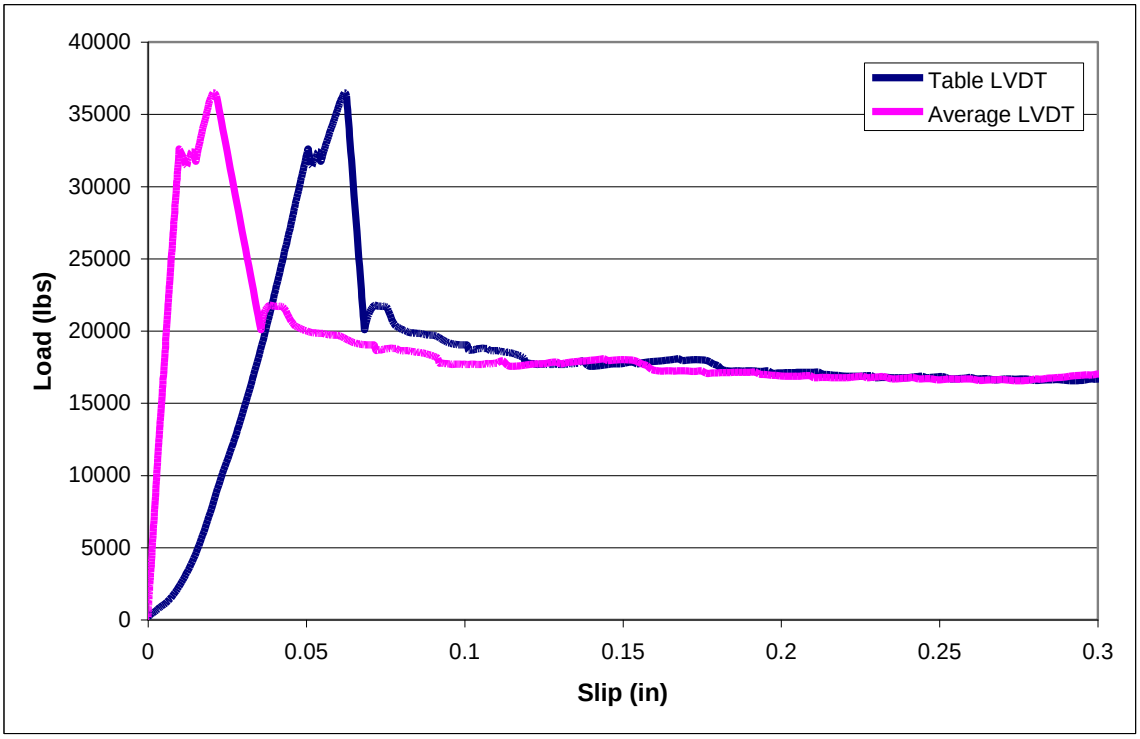

Figure C76. CJC-1C.

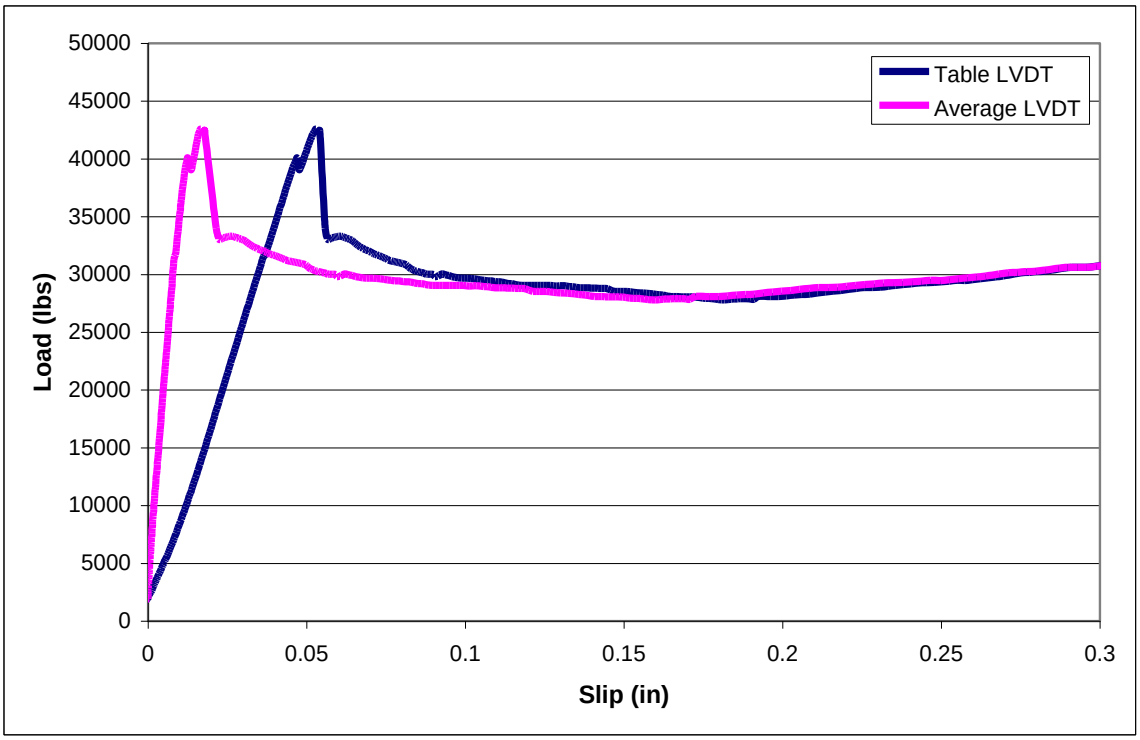

Figure C77. CJC-2A.

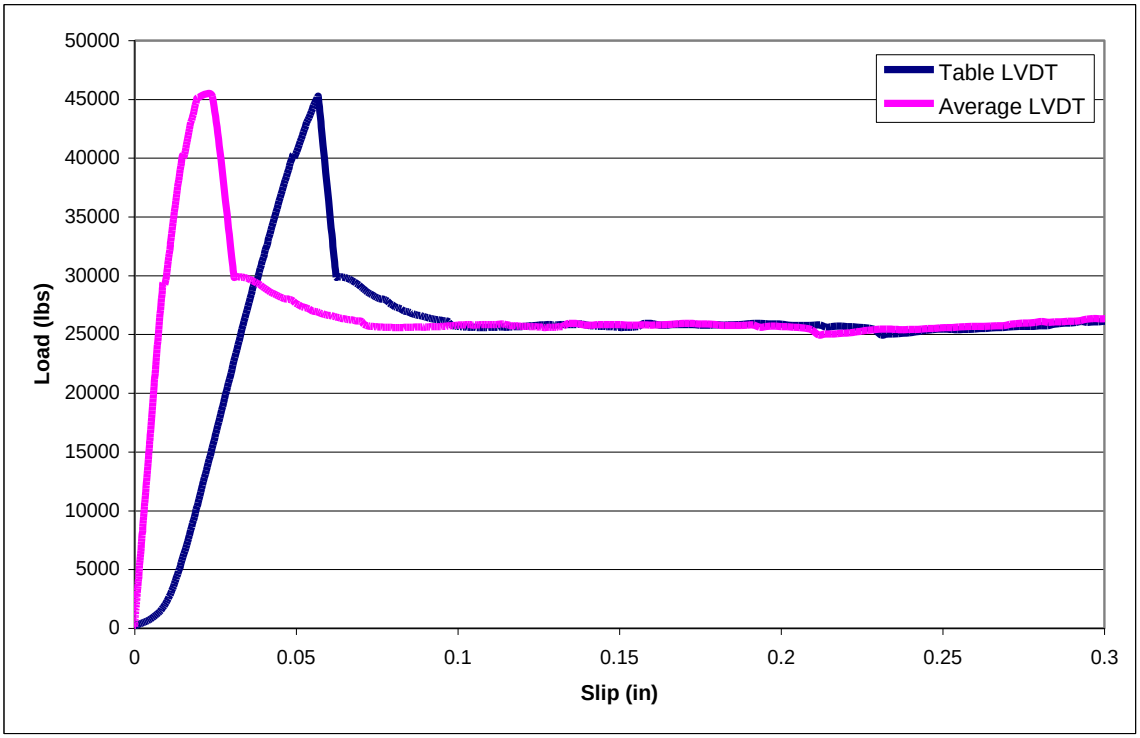

Figure C78. CJC-2B.

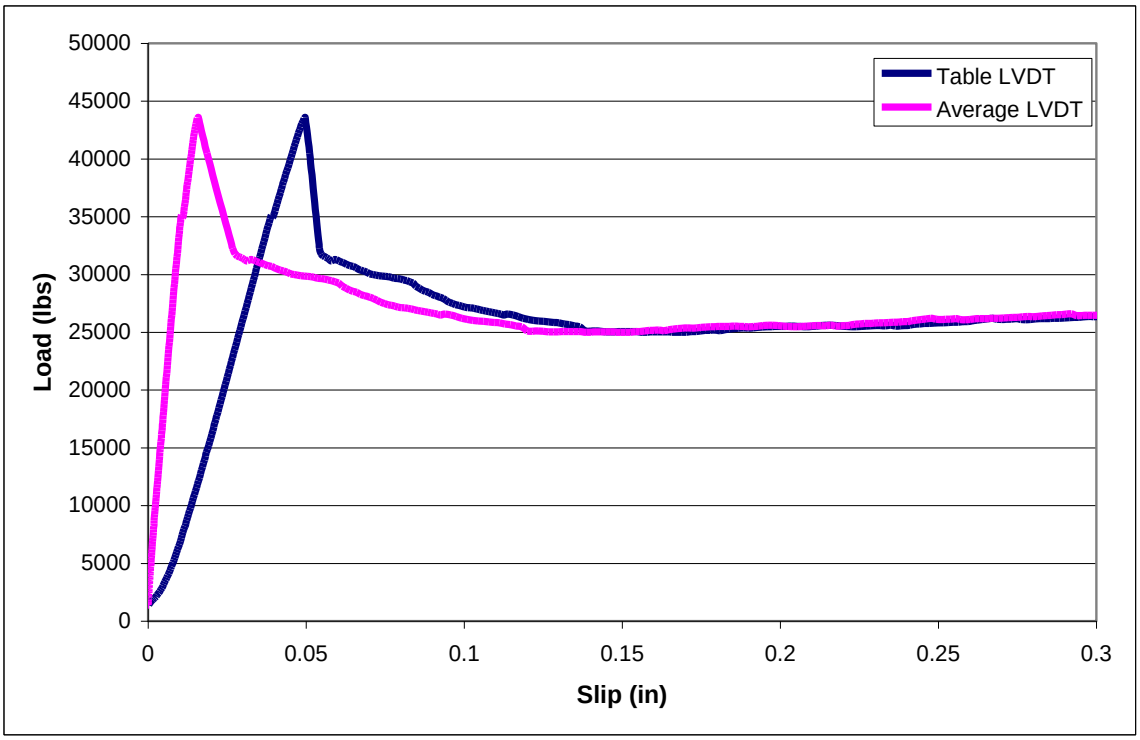

Figure C79. CJC-2C.

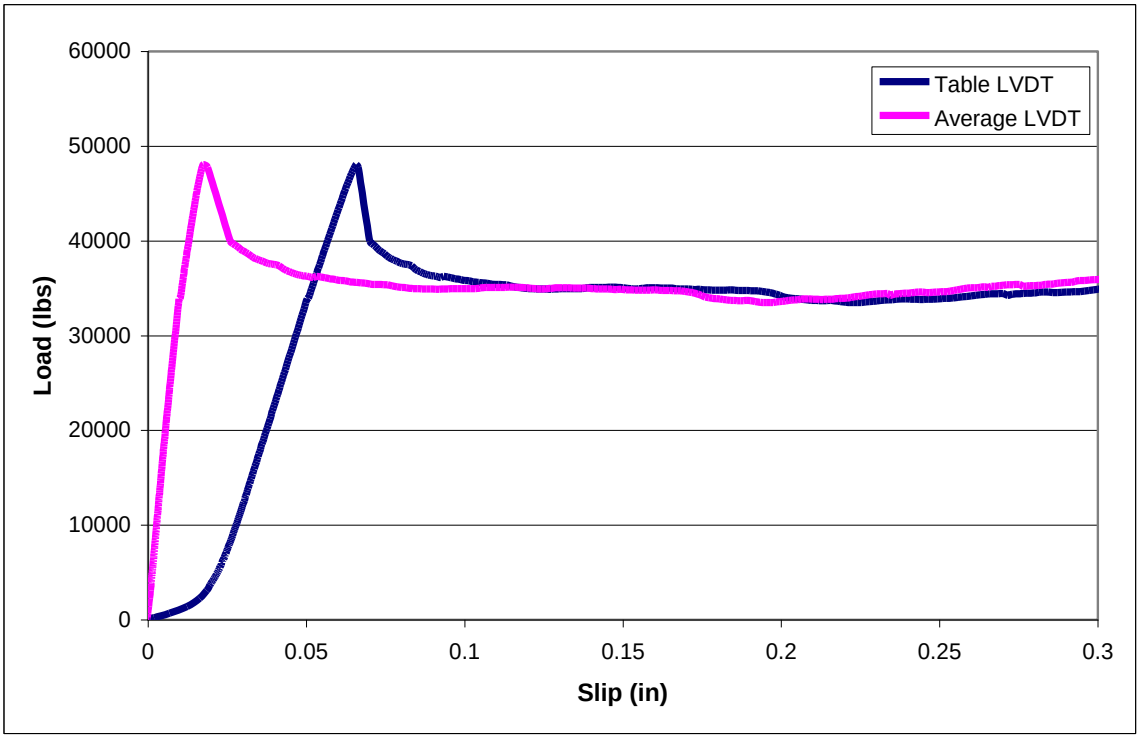

Figure C80. CJC-3A.

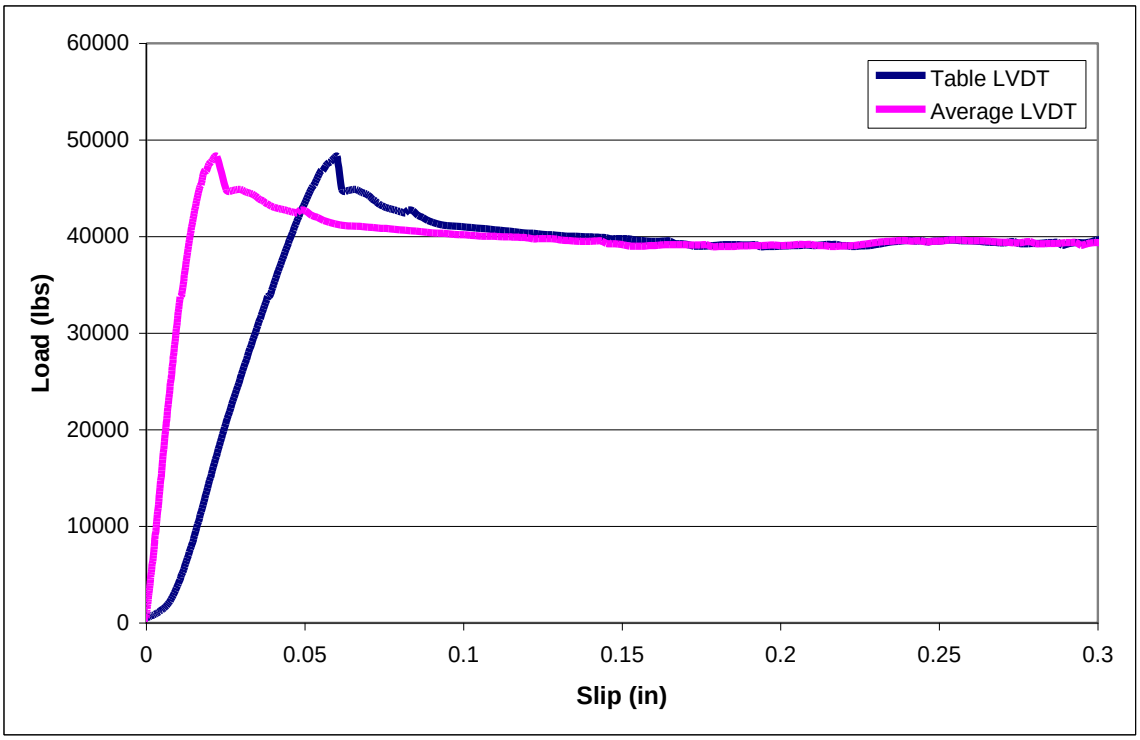

Figure C81. CJC-3B.

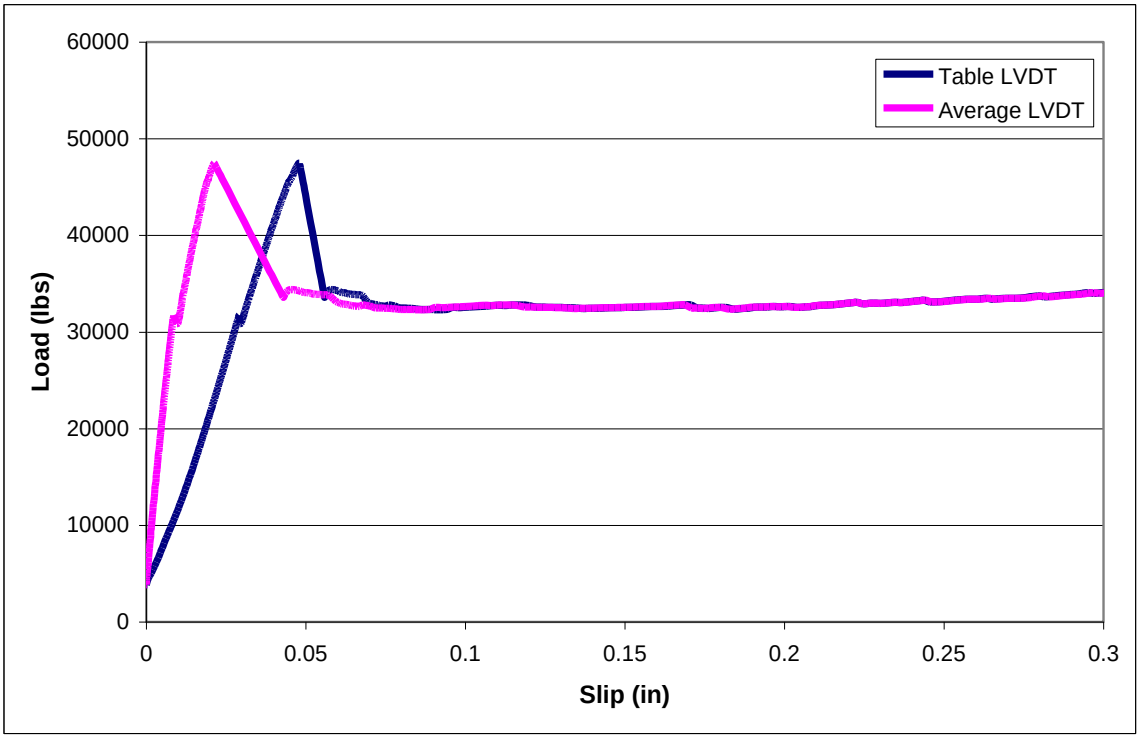

Figure C82. CJC-3C.

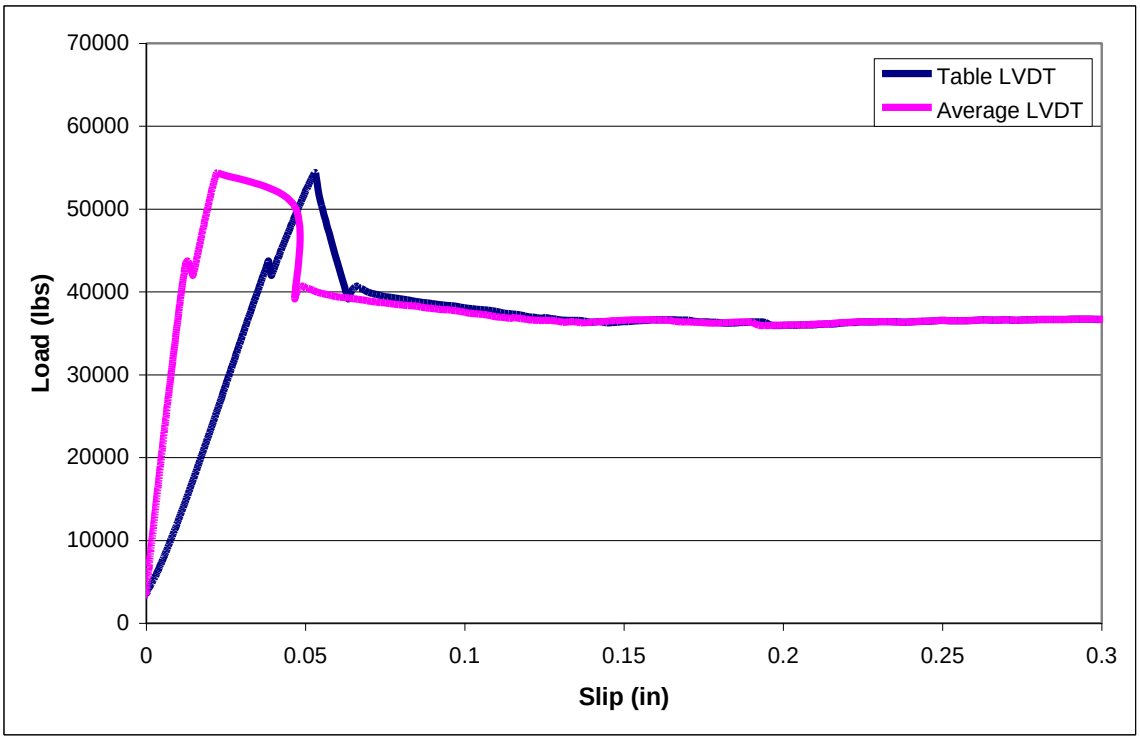

Figure C83. CJC-4A.

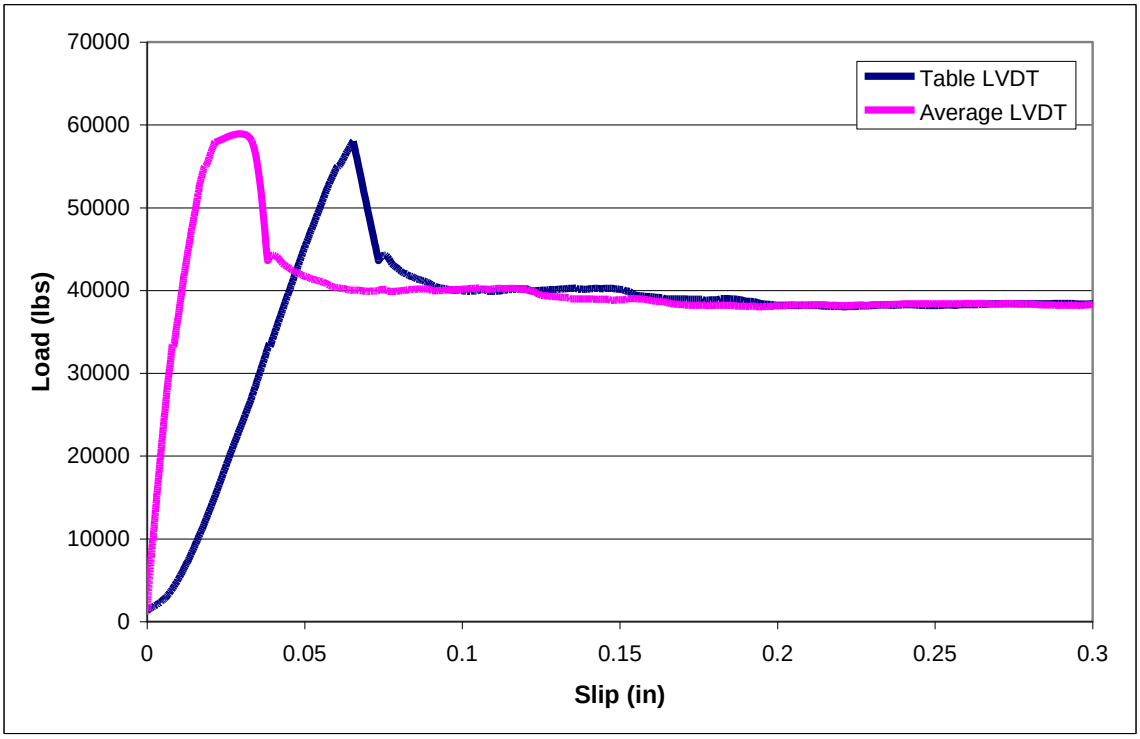

Figure C84. CJC-4B.

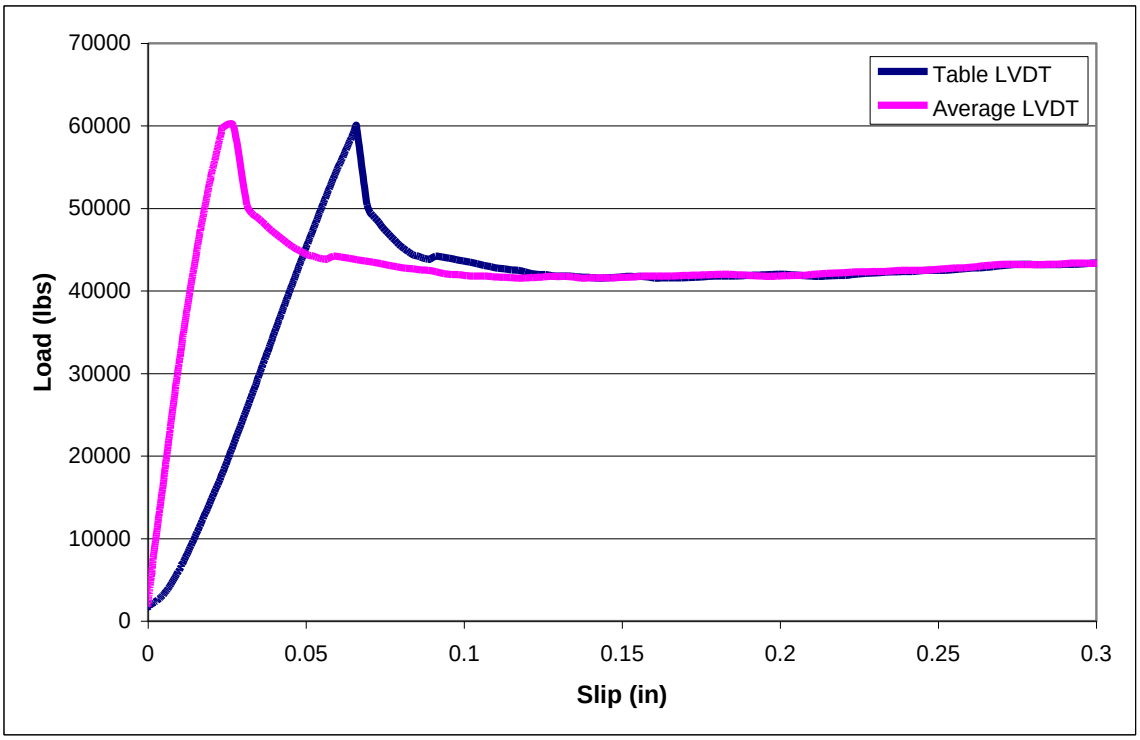

Figure C85. CJC-4C.

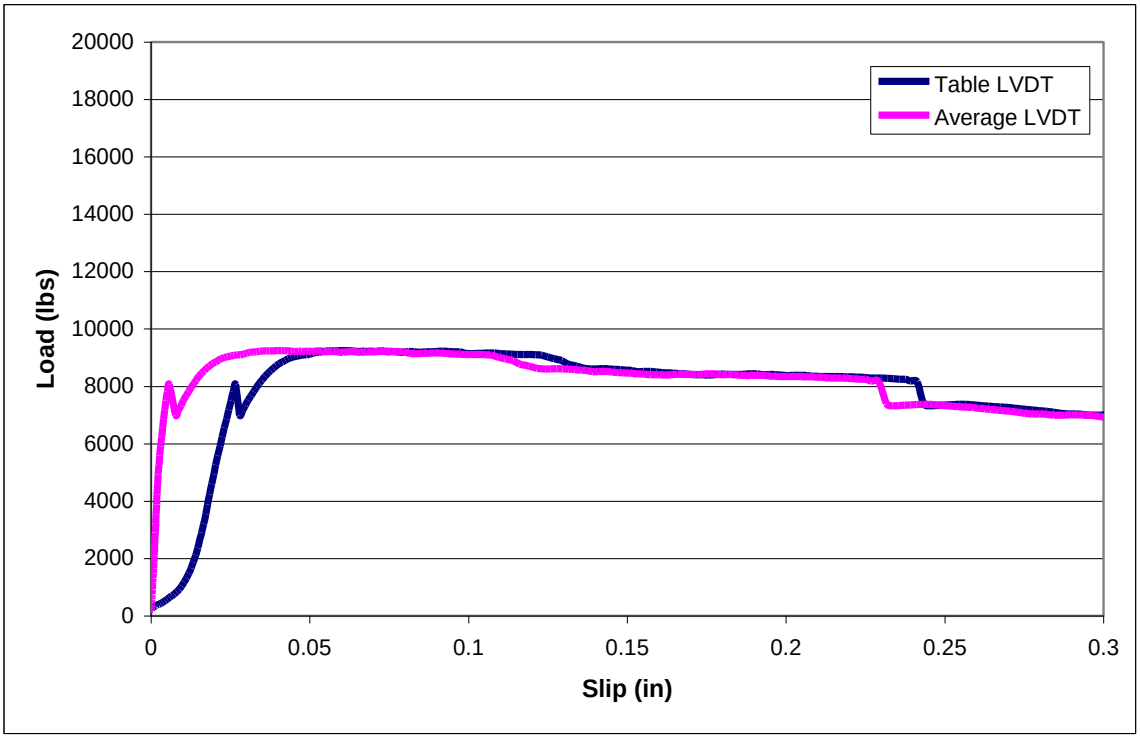

Figure C86. CJO-1A.

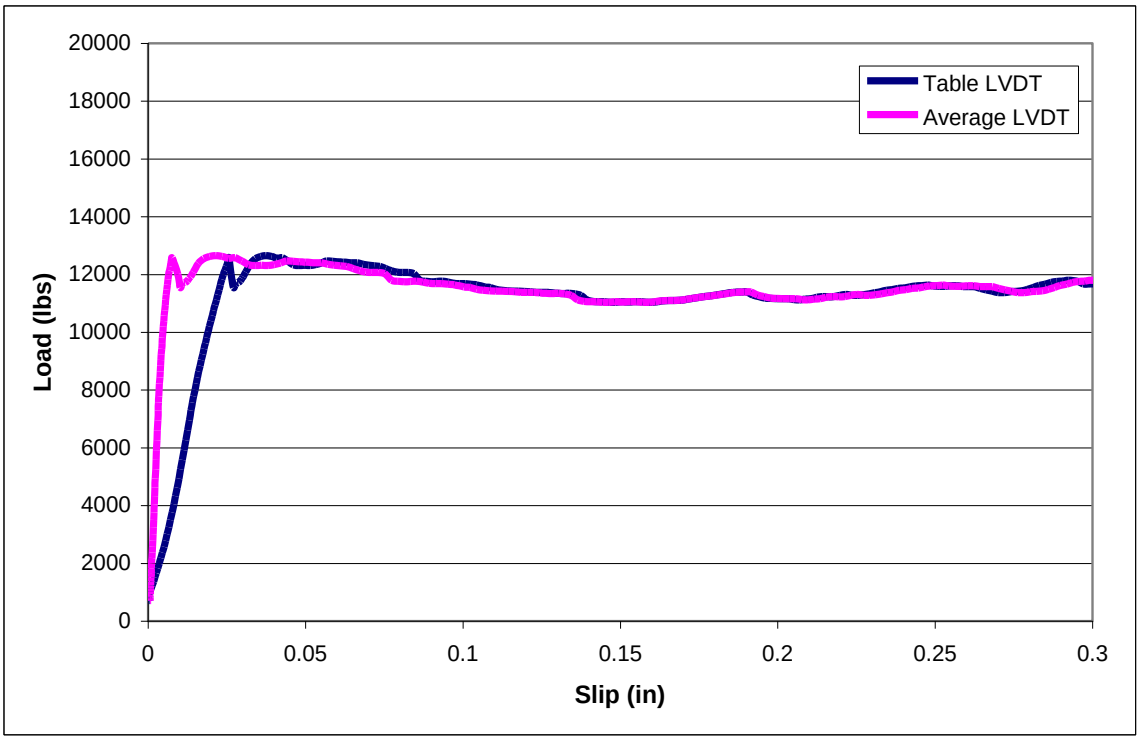

Figure C87. CJO-1B.

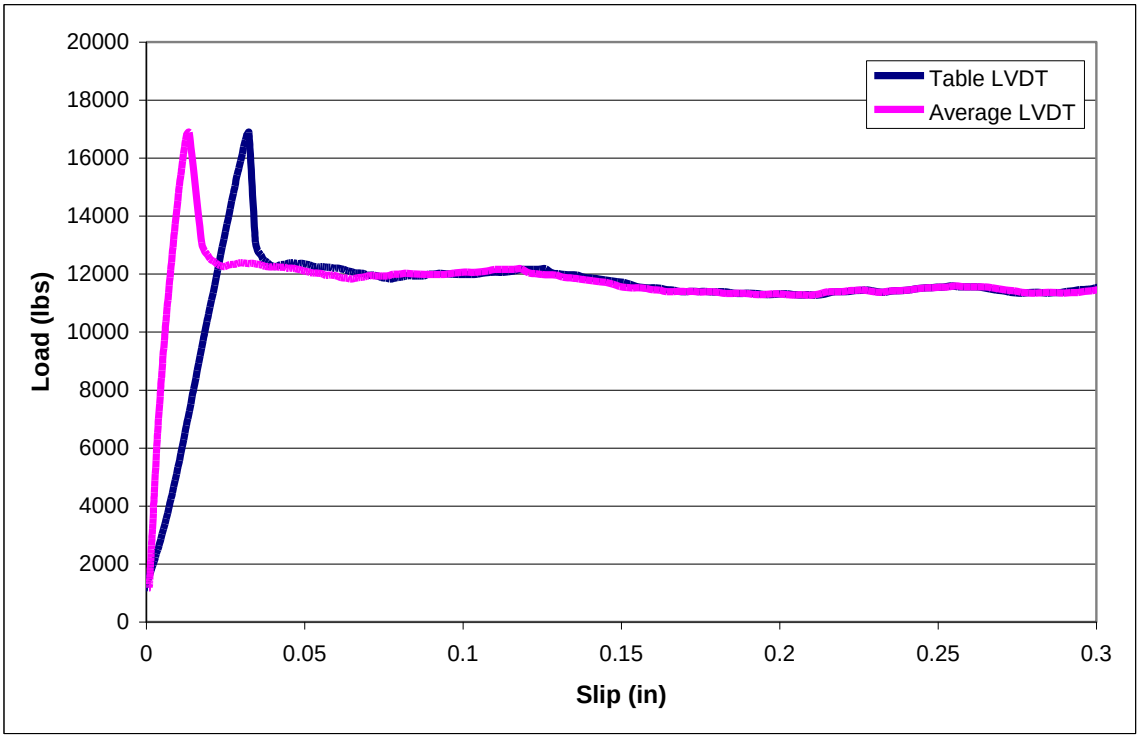

Figure C88. CJO-1C.

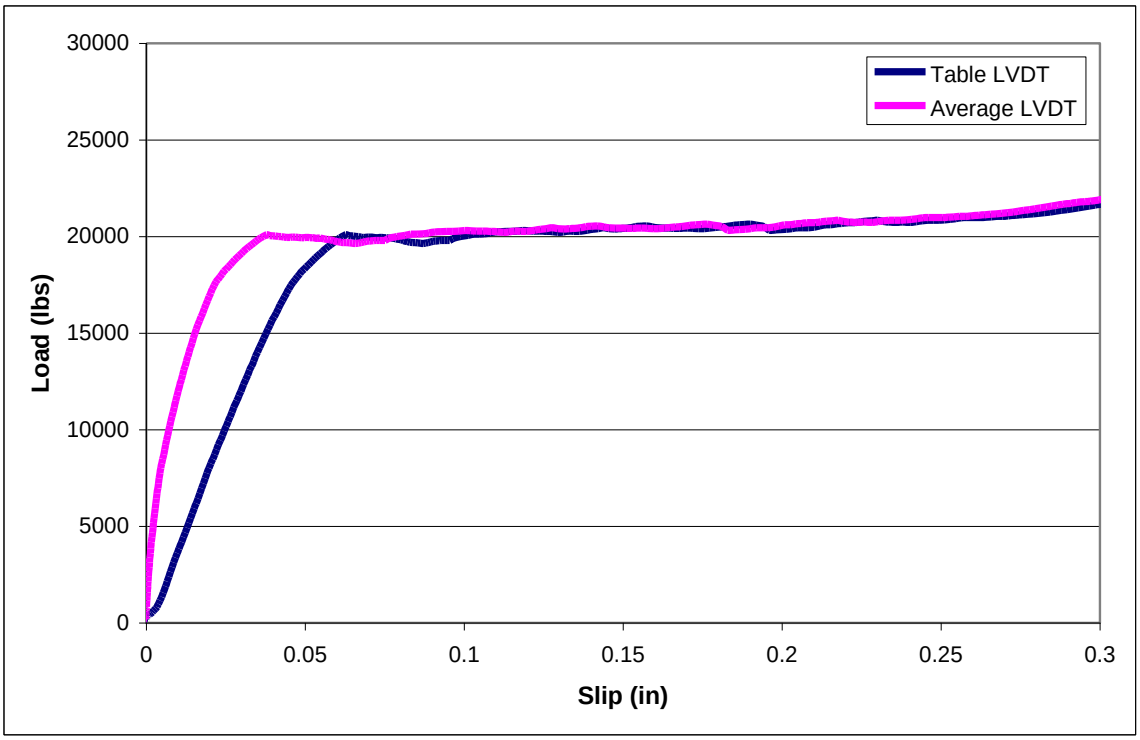

Figure C89. CJO-2A.

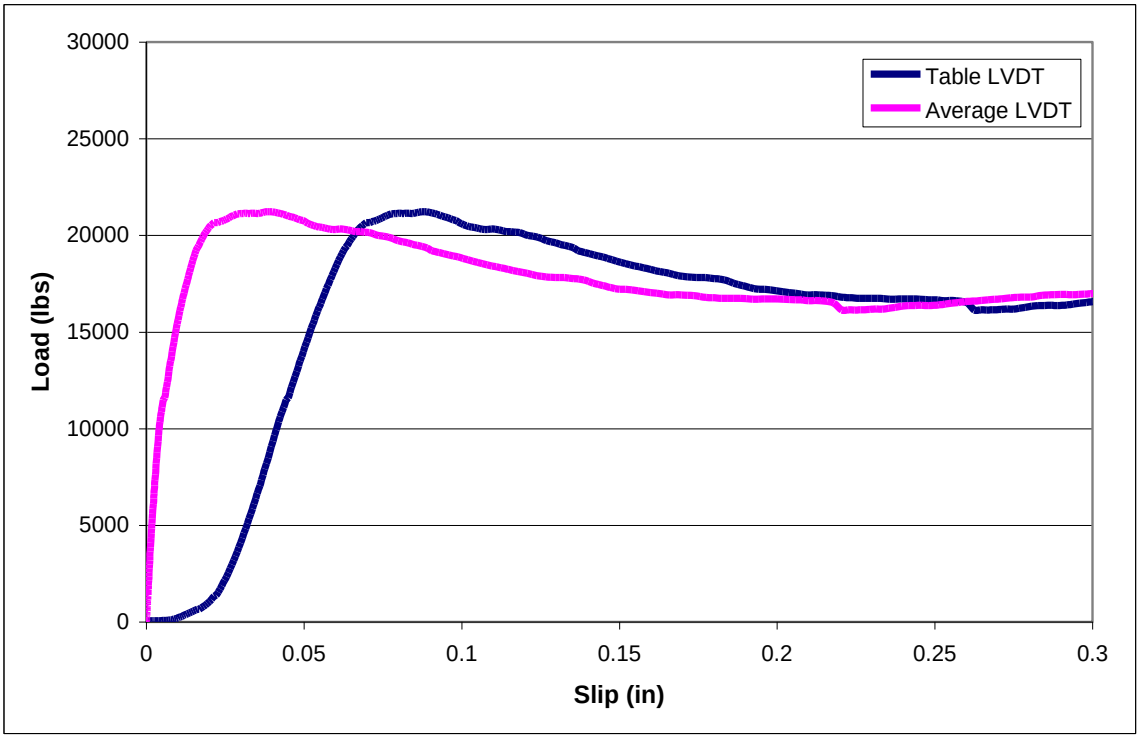

Figure C90. CJO-2B.

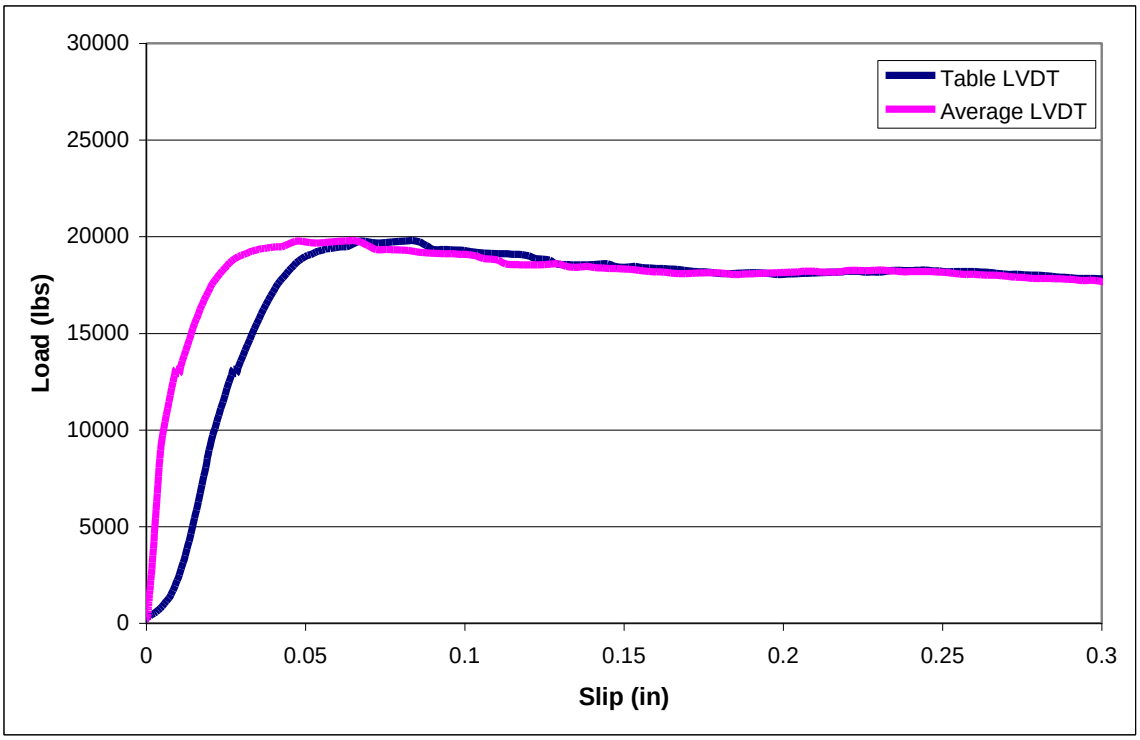

Figure C91. CJO-2C.

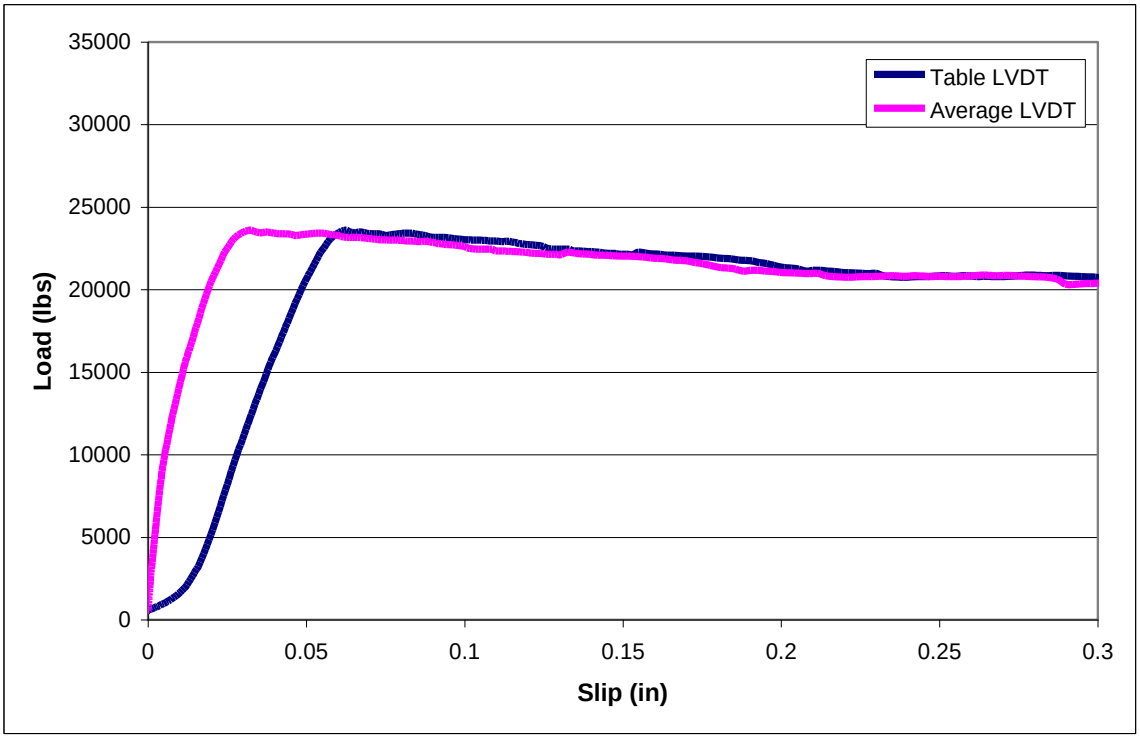

Figure C92. CJO-3A.

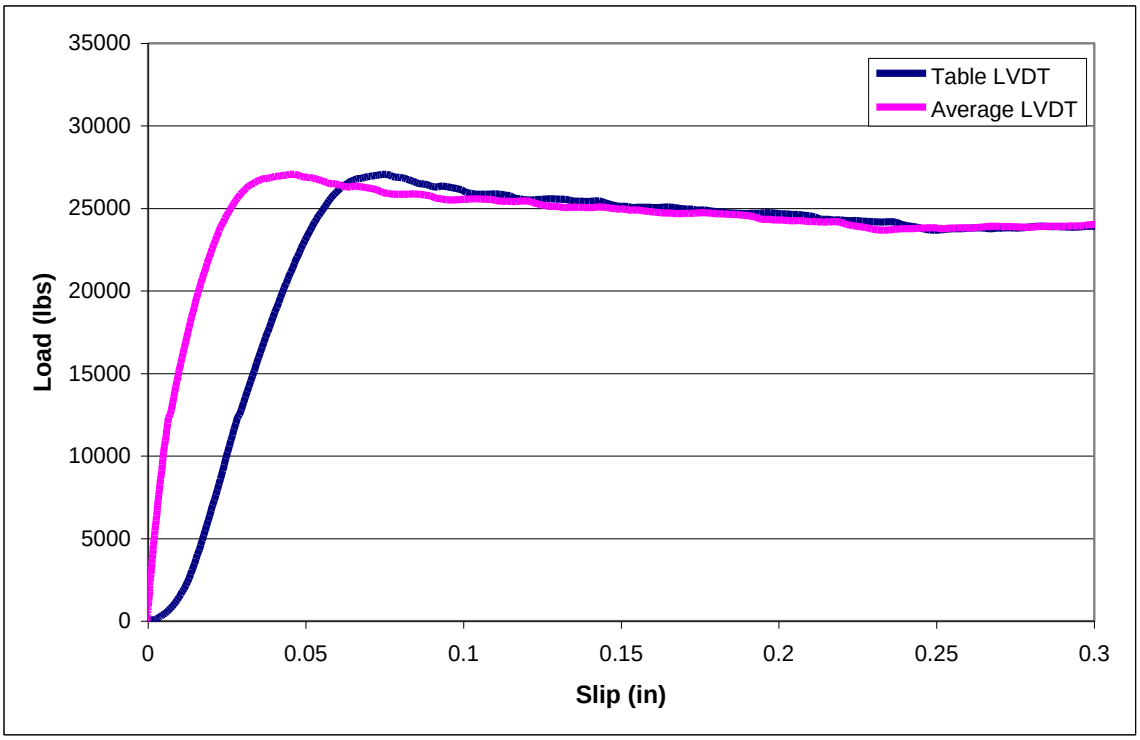

Figure C93. CJO-3B.

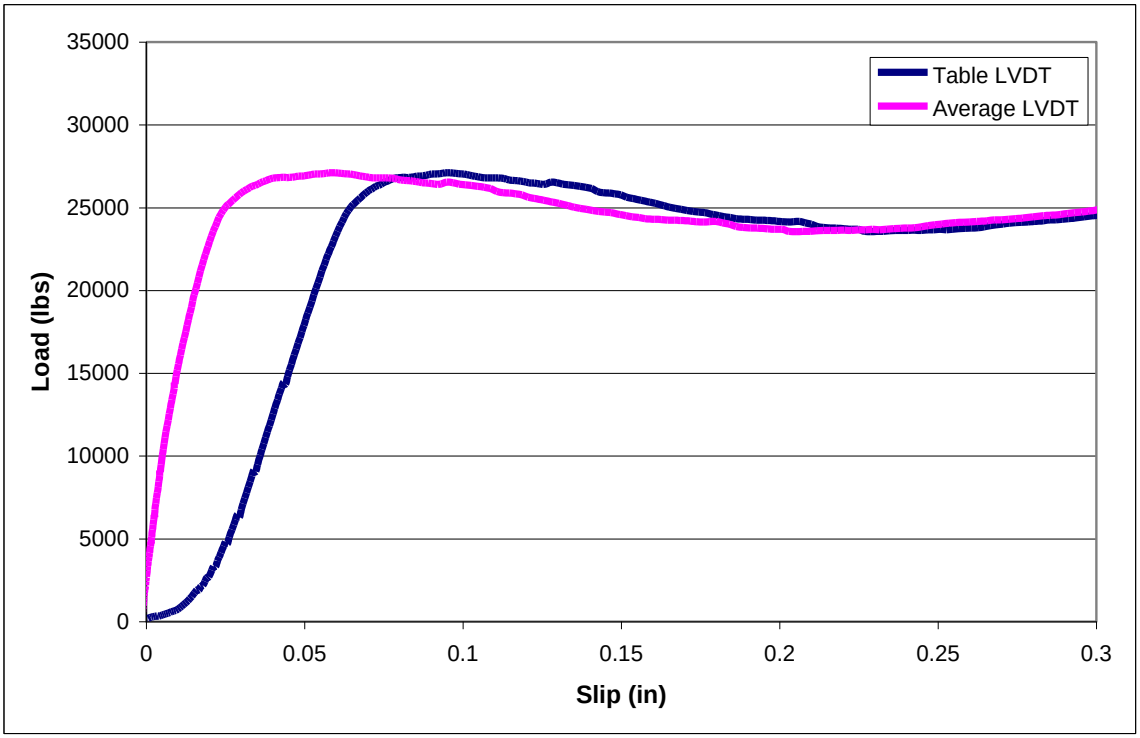

Figure C94. CJO-3C.

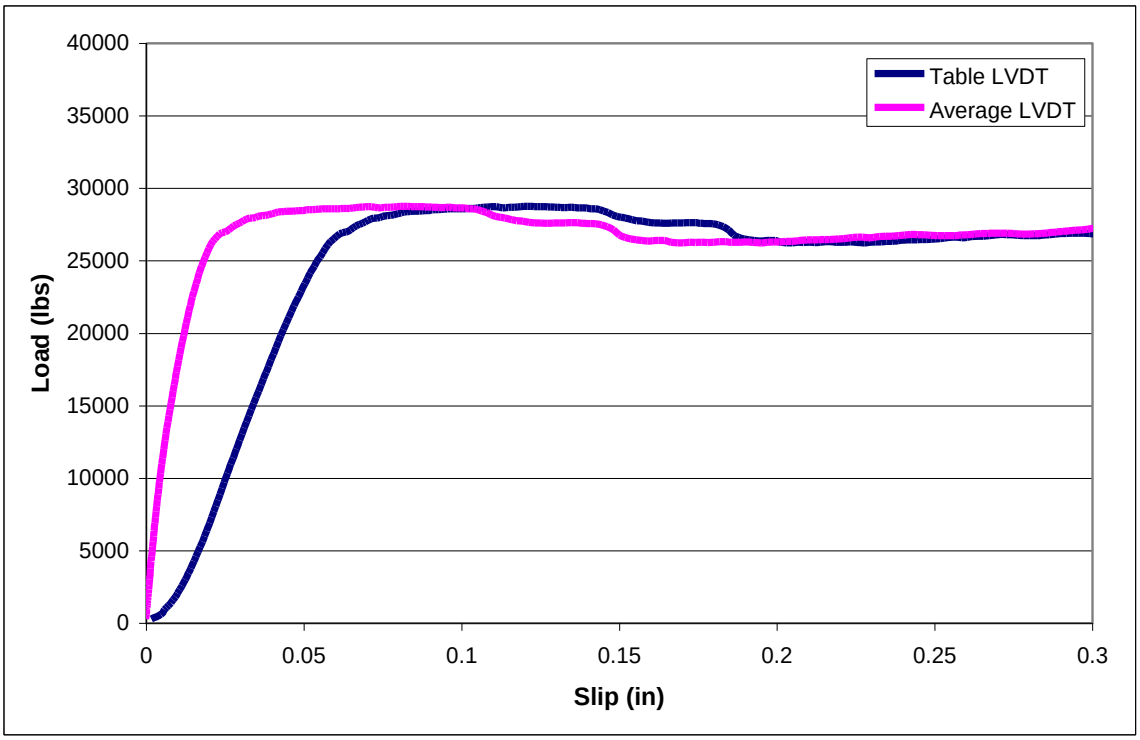

Figure C95. CJO-4A.

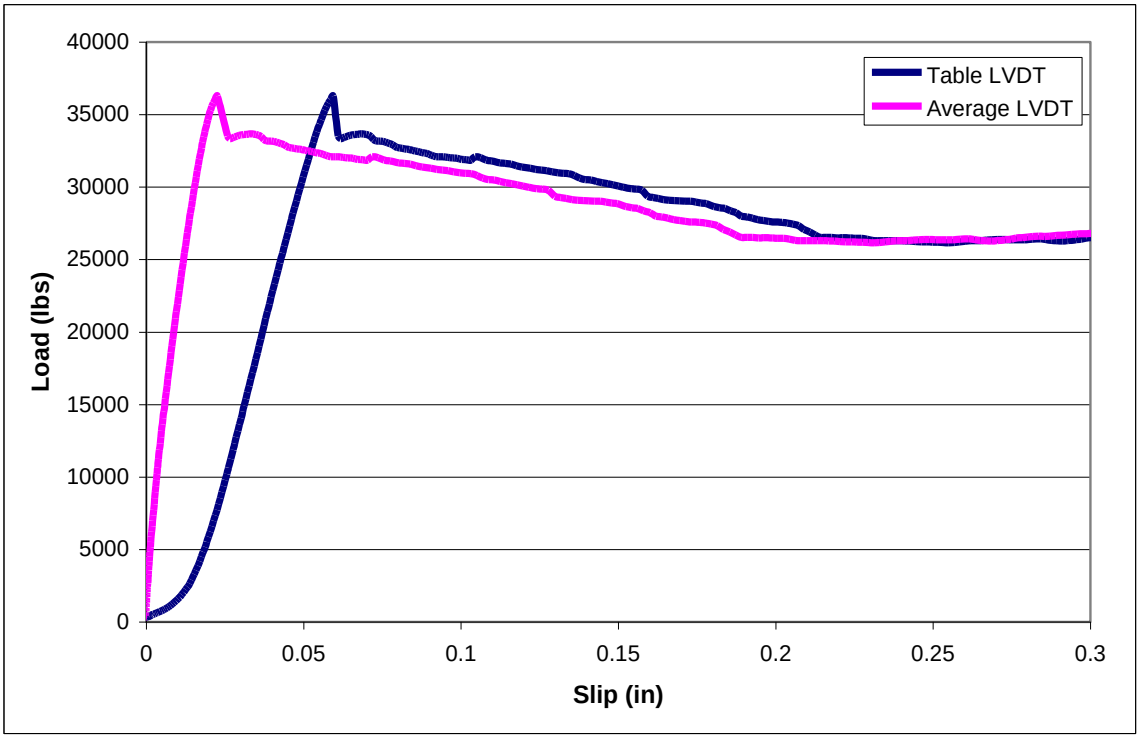

Figure C96. CJO-4B.

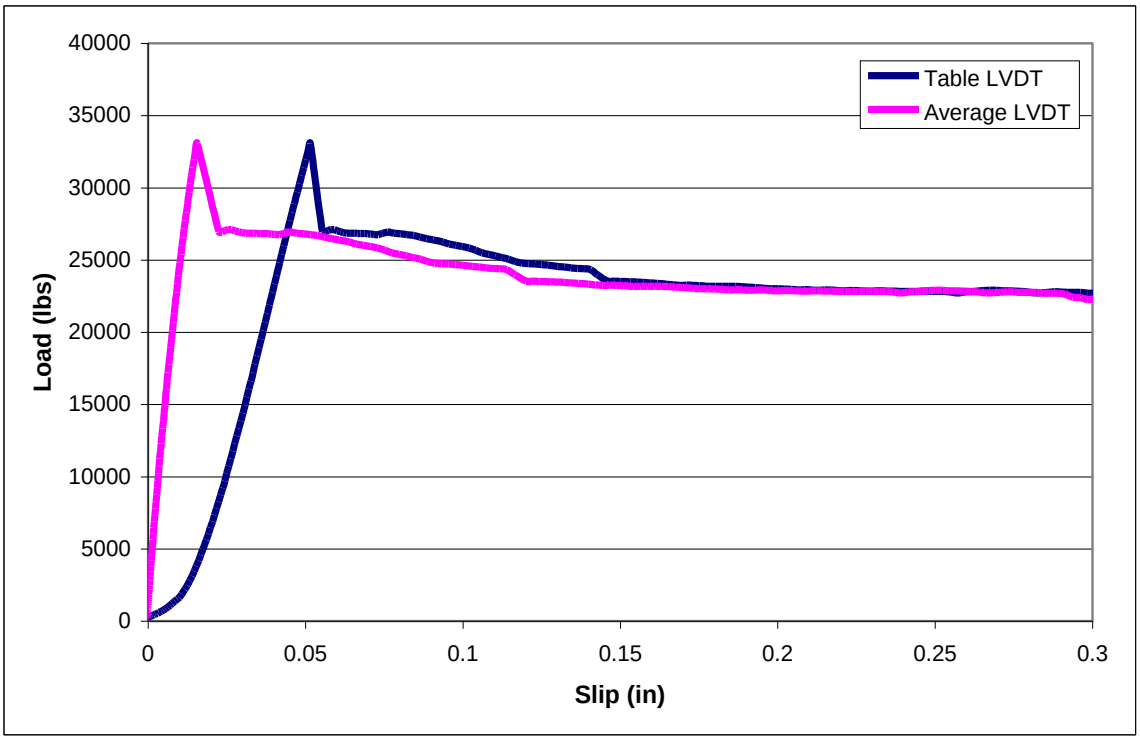

Figure C97. CJO-4C.

K-TRAN

KANSAS TRANSPORTATION RESEARCH AND NEW-DEVELOPMENT PROGRAM

AD ASTRA PER ASPERA

Kansas

Department of Transportation